A HYBRID NETWORK FLOW ALGORITHM FOR THE OPTIMAL CONTROL OF LARGE-SCALE DISTRIBUTED ENERGY SYSTEMS

by

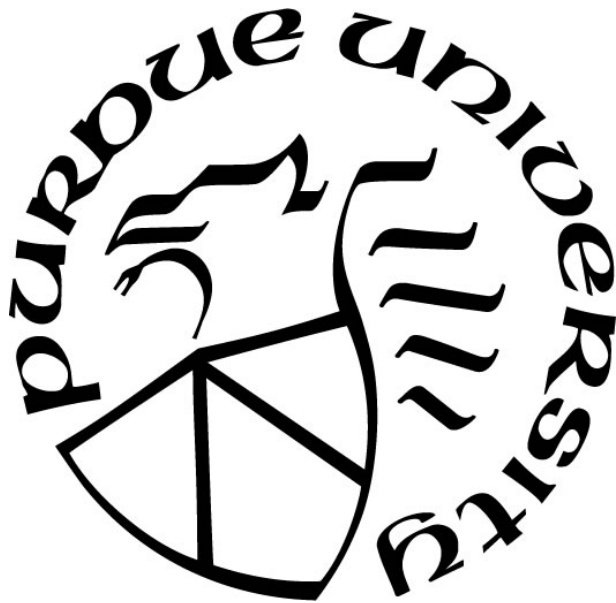**Sugirdhalakshmi Ramaraj**

A Dissertation

Submitted to the Faculty of Purdue University

In Partial Fulfillment of the Requirements for the degree of

Doctor of Philosophy

Lyles School of Civil Engineering

West Lafayette, Indiana

December 2020

THE PURDUE UNIVERSITY GRADUATE SCHOOL
STATEMENT OF COMMITTEE APPROVAL

Dr. James E. Braun, Co-Chair

School of Mechanical Engineering

Dr. William Travis Horton, Co-Chair

School of Civil Engineering

Dr. Eckhard A. Groll

School of Mechanical Engineering

Dr. Ming Qu

School of Civil Engineering

Approved by:

Dr. Dulcy M. Abraham

Dedicated to my family

ACKNOWLEDGMENTS

It is a pleasure to thank many people who made this thesis possible. Foremost, I would like to express my sincere gratitude to my advisors, Prof. James E. Braun and Prof. W. Travis Horton for providing me an opportunity to conduct my Ph.D. research under them after my masters and going above and beyond to reach my goal. Thank you for your guidance, patience, and invaluable support throughout this journey. I feel honored to have the opportunity to work with you.

I also want to extend my gratitude to Prof. Eckhard Groll and Prof. Ming Qu for serving on my advisory committee and being so understanding and supportive of my work.

The technical support provided by Purdue Physical Facilities is also greatly appreciated. Special thanks to Dan Schuster and Matthew High, for all their help in providing necessary information regarding the power plant and their insights on its operation. Dan, I am forever grateful for your support and friendship.

I appreciate all of the support and friendship that I have received from my fellow lab mates, the staff of Herrick labs and Purdue Physical Facilities. I am grateful to all my friends for making my graduate life more colorful.

Finally, I would like to thank my family, whose love and guidance is always with me in whatever I pursue. On a different note, many people have been a part of my graduate education and I am highly grateful to all of them.

TABLE OF CONTENTS

LIST OF TABLES

LIST OF FIGURES

NOMENCLATURE

Acronyms

AHU	Air Handling Unit
ATCS	Annual Total Cost Savings
CCHP	Combined Cooling Heating and Power
CDE	Carbon Dioxide Emissions
CDER	Carbon Dioxide Emission Reductions
CHP	Combined Heating and Power
COP	Coefficient of Performance
DER	Distributed Energy Resources
DES	Distributed Energy Systems
DG	Distributed Generation
DOE	Department of Energy
EA	Evolutionary Algorithm
ED	Economic Dispatch
EDM	Electric Demand Management
EESI	Environmental and Energy Study Institute
EIA	Energy Information Administration
EPA	Environmental Protection Agency
FEL	Following the Electric Load
FTL	Following the Thermal Load
GA	Genetic Algorithm
GHG	Greenhouse Gas
GRG	Generalized Reduced Gradient
HHV	Higher Heating Value
HRSG	Heat Recovery Steam Generator
HVAC	Heating Ventilation and Air Conditioning
IC	Internal Combustion
IEA	International Energy Agency

IEO	International Energy Outlook
IPM	Interior Point Method
LB	Lower Bounds
LP	Linear Programming
MILP	Mixed Integer Linear Programming
MINLP	Mixed Integer Non-Linear Programming
MIP	Mixed Integer Programming
MPC	Model Predictive Control
MT	Metric Ton
NLP	Non-Linear Programming
NWCP	Northwest Chiller Plant
OAT	Outdoor Air Temperature
OECD	Organization for Economic Cooperation and Development
OSG	On-Site Generation
PEC	Primary Energy Consumption
PES	Primary Energy Savings
PGU	Power Generation Unit
PRV	Pressure Reducing Valves
PSO	Particle Swarm Optimization
PV	Photo Voltaic
RTP	Real-Time Pricing
SOFC	Solid Oxide Fuel Cell
SP	Separation Production
SP	Switch Penalty
SQP	Sequential Quadratic Programming
ST	Short Ton
UB	Upper Bounds
TES	Thermal Energy Storage
TDM	Thermal Demand Management

Symbols

c	Cost [$]
C_p	Specific heat capacity [kJ/kg.K]
E	Electricity rate [kW]
f	Amount of fuel consumed
H	Heating rate provided [kW]
g	Inequality constraints
h	Equality constraints
h	Enthalpy [kJ/kg]
Δh	Change in enthalpy across the system [kJ/kg]
k	Multiplier
$\dot{m}$	Mass flow rate [kg/s]
P	Pressure [kPa]
P	Power consumption [kW]
$\dot{Q}$	Heat transfer rate [kW]
s	Amount of steam [kg/s]
T	Temperature [K]
TG	Turbine generator
x	Decision variable
x_s	Mass flowrate of steam (decision variable) [kg/s]
x_w	Volumetric flowrate of water (decision variable) [gpm]
η	Efficiency [%]

Subscripts/Superscripts

a	air
A	auxiliaries
AF	air flow
B	boiler
C	coal
C	chiller

co	condenser
COWP	Condenser water pump
cr	Condensate return
CT	Cooling Tower
CWP	Chilled water pump
db	dry bulb
DB	duct burner
des	design
E	electric/electricity
ev	evaporator
ex	extraction/exhaust
F	fired steam
F	fans
fw	feedwater
FWP	feed water pumps
h	heating
i	inlet
is	isentropic
L	line
m	motor
max	maximum
min	minimum
NG	natural gas
NW	Northwest Chiller Plant
o	outlet
P	pump
PRV	pressure reducing valves
pur	purchased
s	steam
S	steam
t	time (t-th hour)

t	turbine
T	temperature
TG	turbine generator
UF	unfired steam
w	water
W	Wade Plant
wb	wet bulb
15	15 psig steam line
125	125 psig steam line
600	600 psig steam line

ABSTRACT

This research focuses on developing strategies for the optimal control of large-scale Combined Cooling, Heating and Power (CCHP) systems to meet electricity, heating, and cooling demands, and evaluating the cost savings potential associated with it. Optimal control of CCHP systems involves the determination of the mode of operation and set points to satisfy the specific energy requirements for each time period. It is very complex to effectively design optimal control strategies because of the stochastic behavior of energy loads and fuel prices, varying component designs and operational limitations, startup and shutdown events and many more. Also, for large-scale systems, the problem involves a large number of decision variables, both discrete and continuous, and numerous constraints along with the nonlinear performance characteristic curves of equipment. In general, the CCHP energy dispatch problem is intrinsically difficult to solve because of the non-convex, non-differentiable, multimodal and discontinuous nature of the optimization problem along with strong coupling to multiple energy components.

This work presents a solution methodology for optimizing the operation of a campus CCHP system using a detailed network energy flow model solved by a hybrid approach combining mixed-integer linear programming (MILP) and nonlinear programming (NLP) optimization techniques. In the first step, MILP optimization is applied to a plant model that includes linear models for all components and a penalty for turning on or off the boilers and steam chillers. The MILP step determines which components need to be turned on and their respective load needed to meet the campus energy demand for the chosen time period (short, medium or long term) with one-hour resolution. Based on the solution from MILP solver as a starting point, the NLP optimization determines the actual hourly state of operation of selected components based on their nonlinear performance characteristics. The optimal energy dispatch algorithm provides operational signals associated with resource allocation ensuring that the systems meet campus electricity, heating, and cooling demands. The chief benefits of this formulation are its ability to determine the optimal mix of equipment with on/off capabilities and penalties for startup and shutdown, consideration of cost from all auxiliary equipment and its applicability to large-scale energy systems with multiple heating, cooling and power generation units resulting in improved performance.

The case-study considered in this research work is the Wade Power Plant and the Northwest Chiller Plant (NWCP) located at the main campus of Purdue University in West Lafayette, Indiana, USA. The electricity, steam, and chilled water are produced through a CCHP system to meet the campus electricity, heating and cooling demands. The hybrid approach is validated with the plant measurements and then used with the assumption of perfect load forecasts to evaluate the economic benefits of optimal control subjected to different operational conditions and fuel prices. Example cost optimizations were performed for a 24-hour period with known cooling, heating, and electricity demand of Purdue's main campus, and based on actual real-time prices (RTP) for purchasing electricity from utility. Three optimization cases were considered for analysis: MILP [no on/off switch penalty (SP)]; MILP [including on/off switch penalty (SP)] and NLP optimization. Around 3.5% cost savings is achievable with both MILP optimization cases while almost 10.7% cost savings is achieved using the hybrid MILP-NLP approach compared to the current plant operation. For the selected components from MILP optimization, NLP balances the equipment performance to operate at the state point where its efficiency is maximum while still meeting the demand. Using this hybrid approach, a high-quality global solution is determined when the linear model is feasible while still taking into account the nonlinear nature of the problem.

Simulations were extended for different seasons to examine the sensitivity of the optimization results to differences in electric, heating and cooling demand. All the optimization results suggest there are opportunities for potential cost savings across all seasons compared to the current operation of the power plant. For a large CCHP plant, this could mean significant savings for a year. The impact of choosing different time range is studied for MILP optimization because any changes in MILP outputs impact the solutions of NLP optimization. Sensitivity analysis of the optimized results to the cost of purchased electricity and natural gas were performed to illustrate the operational switch between steam and electric driven components, generation and purchasing of electricity, and usage of coal and natural gas boilers that occurs for optimal operation. Finally, a modular, generalizable, easy-to-configure optimization framework for the cost-optimal control of large-scale combined cooling, heating and power systems is developed and evaluated.

1. INTRODUCTION

1.1 Motivation

With significant economic development and population growth throughout the world, the demand for energy is increasing rapidly and will continue to rise. The International Energy Outlook (IEO) 2019 projects nearly 50% growth in worldwide energy consumption expanding from 620 quad in 2018 to 911 quad in 2050, including both OECD nations (Organization for Economic Cooperation and Development) and developing non-OECD nations as shown in Figure 1.1. The end-use fuel consumption is increasingly shifting towards electricity across all sectors and electricity generation is projected to increase around 79% between 2018 and 2050 (U.S. Energy Information Administration (EIA), IEO, 2019). Concurrently, energy production using fossil fuels along with renewable energy is also growing to meet this ever-increasing demand.

World energy consumption
quadrillion British thermal units
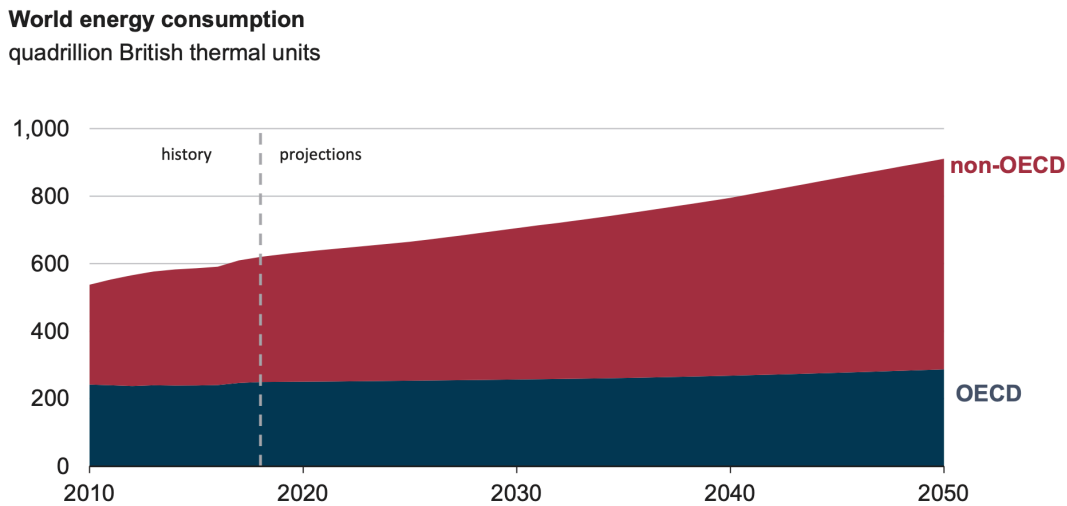
Figure 1.1. World energy consumption, 2010-2050 (U.S. EIA, IEO, 2019).

In the meantime, concerns about the future depletion of fossil fuel energy resources along with the realization of the impact of energy systems on global climate change and the growing concerns about energy security have led to initiatives to reduce our fossil fuel energy usage. Although switching to clean renewable energy generation technologies is on the rise, fossil fuels continue to dominate the world's primary energy consumption. In 2017, 81% of the energy the world consumed was oil, coal, and natural gas (International Energy Agency (IEA), 2018). A rapid

transition to alternative sources of energy and the practical challenges of abandoning traditional generation brings concerns about managing radical changes in energy production, supply, and consumption patterns. In this scenario, distributed energy systems (DES), also known as distributed generation (DG), on-site generation (OSG), district/decentralized energy, or distributed energy resource (DER) systems are a way forward to handle the ever-increasing energy demand while providing a pathway to a more sustainable future managing the reliance on fossil fuel energy. They play a critical role in increasing energy efficiency and energy independence, reducing costs and greenhouse gas emissions, and integrating increasing levels of variable renewables in the long term compared to centralized power generation. They can also support the central electric power grid in the event of a disaster. DES also enables consumers to design their energy supply to be more closely aligned with their physical needs both in terms of thermal and electrical demand. Through a combination of technological improvements, policy incentives, and consumer choices in technology and service, the role of DES is likely to become more important in the future. Properly planned and operated DES can provide consumers, as well as society, with a wide variety of benefits. With centralized generation in place for a century, proper and more DES penetration in combination with centralized generation could help in attaining continuous power production with reduced emissions and increased energy efficiency. Also, distributed generation can be optimized for buying/selling electricity from centralized power generation in the development of a future grid for resiliency, stability, and reliability in power production.

1.1.1   Combined Cooling, Heating and Power Systems

Though distributed energy systems include a variety of devices/technologies, one of the proven and most popular technologies is combined cooling, heating, and power (CCHP) systems, also known as trigeneration systems which is an extension of the combined heat and power (CHP) systems or cogeneration systems. Cogeneration generates power and makes use of the waste heat that is produced during the process for heating, while trigeneration takes a step further by also producing cooling as part of the process. In general, if the energy system delivers more than one form of energy, it is referred to as a polygeneration system. These systems have a great potential to minimize primary energy consumption in distributed energy generation systems due to their ability to recover low-grade thermal energy, resulting in higher energy efficiencies, reduced emission rates and thermal losses, and lower operating costs. Here, the by-product heat, which can

be as much as 60%-80% of the total primary energy to generate electricity, is recovered and recycled for diverse purposes. So, the overall fuel energy utilization is higher, requiring only 3/4ths of the primary energy compared to the conventional heat and power systems (U.S. Environmental Protection Agency (EPA), 2015). With a global average system efficiency of 62%, the cogeneration of heat and power is much more efficient than conventional thermal power plants (41%). In fact, state-of-the-art CHP units can reach overall energy efficiencies over 85% (IEA, 2012). Wu and Wang (2006) showed that the CCHP system could improve the overall efficiency from 59% to 88% compared with the traditional energy supply mode owing to the cascade utilization of different energy carriers. Thus, the system-wide benefits of cogeneration and trigeneration increase further when coupled with district heating and cooling. Useful heating and cooling along with the simultaneous generation of electricity not only makes it more energy efficient but also reduces greenhouse gas (GHG) emissions. CHP could reduce CO_2 emissions by 10% (950 MT/year) by 2030 compared to savings of 4% (170 MT/year) in 2015 (Kerr, IEA, 2008). CHP and CCHP systems can therefore make a meaningful contribution towards low-cost GHG emissions reductions. Another benefit of these systems is that they offer a higher level of energy security, control, and reliability by removing or mitigating reliance on centralized power grids.

CHP and CCHP plants are well established worldwide in residential, commercial, and industrial sectors for meeting desired thermal and electricity demands. Cogeneration comprises approximately 9% of the world's electricity generating capacity, which is around 330 GW (Kerr, IEA, 2008). Several countries have adopted policies to support the use of CHP/CCHP due to its more prominent advantages over separate thermal and power production. According to the U.S. Department of Energy (U.S. DOE, 2016), 'the United States has the potential for more than 240 GW of efficient CHP in industrial facilities and commercial buildings,' at over 291,000 sites, which is equivalent to about 100 large (2-3 GW) coal or nuclear power plants. That is about three times more CHP capacity than exists in the U.S. (82.7 GW for 2016). The U.S. federal government has adopted a goal of deploying 40 GW of new industrial CHP by the end of 2020 (U.S. White House, 2012), and many states offer incentives for CHP projects (U.S. EPA, 2015). Even though the situations are a little bit different around the globe, government supporting policies, favorable fiscal and tax incentives, solutions related to high capital cost, and further research and demonstration can overcome the obstacles in the worldwide implementation of CHP and CCHP technologies.

CCHP units include diverse components relating to energy conversion, recovery, and management to cater to multiple energy needs for commercial, institutional, residential, and industrial applications. Figure 1.2 shows a basic design of a CCHP system where the power generation unit (PGU) uses either fuel directly or steam from the boiler to produce electricity and waste heat is reclaimed by a heat recovery unit to provide heating/cooling to nearby buildings and facilities.
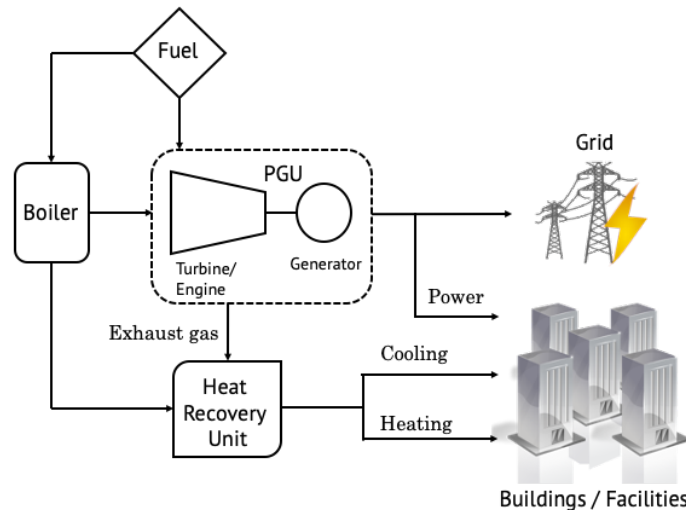
Figure 1.2. Schematic of a typical CCHP system

A typical CCHP system consists of five basic elements: prime mover, electricity generator, heat recovery system, thermally activated equipment, and the management and control system (Wu & Wang, 2006). The power generation unit (PGU) includes prime mover and electricity generator to generate electricity while the heat recovery and utilization components utilize the wasted thermal energy created as a by-product in the production of power to provide space heating, hot water, and cooling. These components are interconnected to heterogeneous subsystems with different configurations ranging from simple to complex depending on the diversity of available energy sources that meet necessary electrical and thermal demands.

Energy sources for CCHP systems are typically fossil fuels but sometimes include renewable energy sources and fuel cells. The prime moving technologies include reciprocating internal combustion engines, combustion gas turbines, boiler/steam turbines, microturbines, Stirling engines, fuel cell systems, and other renewable energy sources (U.S. EPA, 2015). Heat exchangers, auxiliary boilers, absorption heating, heat pumps, heating, ventilation and air conditioning

(HVAC) components, such as electric chillers, steam turbine chillers, absorption and adsorption chillers, cooling towers, desiccant dehumidifiers, and air handling units (AHUs), and other thermally activated technologies can be incorporated in these systems to recover waste heat for providing heating/cooling (Liu et al., 2014). Energy storage technologies, such as thermal energy storage (Parameshwaran et al., 2012), advanced batteries, and super-capacitors are used to further improve the efficiency and meet fluctuating demand profiles. While some CCHP technologies, such as internal combustion engines, gas turbines, steam turbines, and absorption cooling are commercially mature with wide availability in the market, other promising technologies including organic Rankine systems, fuel cells, and liquid desiccant cooling, are still in the research and development phase with additional work needed to demonstrate their potential and reach commercialization (Jradi & Riffat, 2014).

With a wide variety of existing trigeneration technologies and configurations, careful selection based on a good understanding of user demands and energy system conditions is required for a successful CCHP application. Upon designing a CCHP system, the components are selected based on type, efficiency, performance, and sufficient sizes, while the system configuration is characterized according to usage/demand, climate conditions, local resources, and current and future energy market scenarios (Al Moussawi et al., 2016). The two most common CCHP cycle configurations are topping cycles and bottoming cycles. The most common type is the topping cycle where fuel is first used by a prime mover to generate electricity and the waste heat from power generation is then recovered to provide useful thermal energy. The less common bottoming cycle type uses fuel to first produce useful thermal energy for an industrial process and recovers some portion of the exhausted waste heat to generate power.

For a specific design and system configuration, operation strategy is a critical factor in governing the overall performance of trigeneration systems in response to disturbances such as variations in weather or energy loads that cannot be accounted for at the design stage (Fumo et al., 2009). Conventional operational strategies include baseload operation to fulfill the constant amount of the electric and thermal load of the facility by operating the system at the maximum capacity for a predetermined period of time. Apart from this, there are two popular operation modes of CCHP systems: FEL (Following the Electric Load) and FTL (Following the Thermal Load) (Mago et al., 2009), which can also be referred to as electric demand management (EDM)

and thermal demand management (TDM). Either one of these modes can be chosen to completely satisfy thermal or electrical demand, or additional options can be used to compensate for the gap in demand. However, these different strategies may not guarantee the best performance of the system due to the inherent energy waste accompanied by the implementation of these strategies for irregular load profiles and variable fuel prices. In a general sense, it is critical to optimize the design and operation of these CCHP systems to achieve maximum benefits in terms of energy, cost, and emissions. Optimization during the design phase deals with identifying the components that need to be installed along with their optimal sizing/capacity as well as the optimal system configuration for the plant layout. Optimal operation strategies can determine the operating condition of each equipment for each timestep that optimally matches the output from a single system with the dynamic nature and non-coincidence of building energy demands. The design and operation optimization problem can be solved jointly or separately depending on the requirement. For the case study considered in this research work, the design and system configuration are already in place, so the optimization problem is reduced to determining the optimal operational strategy of the CCHP plant.

1.1.2 Optimization and Control of CCHP Systems

CCHP systems are composed of many different components and wide-ranging operational strategies are used to meet both electrical and thermal demands. It is very complex to effectively design optimal control strategies because of the stochastic behavior of energy loads and fuel prices, diverse dynamic response characteristics at various time-scales, startup, and shutdown events, operational limitations (minimum and maximum allowed loads, etc.), availability of resources, site operational changes, possibility of reselling electrical power back to the grid, fluctuation of renewable energy sources, lack of integration with existing conventional generation as well as the mutual dependency of energy components. The cooling, heating, and electrical demand often do not follow the same trends and are uncertain. However, a combination of different units must be used to satisfy demand due to the interdependency of variables for heating, cooling, and power production. The output from any unit is dependent on one or two independent decision variables or variables of other units to which they are connected. Optimal control of CCHP systems involves the determination of the mode of operation and set points to satisfy the specific energy requirements for each time period. This results in a high number of decision variables, both

continuous and discrete, especially for large-scale energy systems. While the energy flow (unit load) and setpoint decision variables are continuous, the availability (on/off staging) of the equipment are discrete variables. In general, the CCHP energy dispatch problem is intrinsically difficult to solve because of the non-convex, non-differentiable, multimodal (multiple local minima) and discontinuous nature of the optimization problem along with strong coupling to multiple energy components (electricity, heating, and cooling). Due to the nonlinear nature of equipment performance (typically nonlinear with respect to load and sometimes ambient conditions) along with continuous and discrete variables, the resulting problem is a mixed-integer nonlinear programming (MINLP) problem. Even though there are a lot of MINLP solution methodologies available, it is computationally expensive to solve these large-scale problems with high dimensionality and uncertainties. Also, the complexity of numerous constraints along with nonlinear models, makes the optimization problem hard to solve (Elsido et al., 2017). It is extremely challenging to implement optimization algorithms for the daily operation of a large-scale CCHP plant when the models are computed for a reasonable time horizon on an hourly basis.

To tackle this multi-period large-scale optimization problem, several optimization techniques have been studied over the past few decades. The optimization algorithms used in CCHP systems are generally divided into linear programming, nonlinear programming, mixed-integer, and evolutionary search. Over the years, large efforts have been made in developing algorithms to reduce calculation time and improve robustness while considering stochastic behavior for energy loads and prices. Improvement in the operation of CCHP systems can be assessed and quantified with proper performance evaluation methods and criteria. Maximizing the benefits of CCHP systems involves several different aspects: 1) thermodynamics (maximum energy efficiency, minimum fuel consumption, minimum irreversibility), 2) economics (minimum operational cost, maximum cost savings), and 3) environmental (e.g., emissions reduction). To quantify the benefits achieved by CCHP systems, different optimization algorithms have been developed for a wide range of systems. Sometimes, the analysis takes place in a broader context where tradeoffs between energy and exergy performance, emissions, or other environmental impacts, and economics are addressed (Cho et al., 2014). In this case, the optimization problem can be formulated with a single objective or multi-objective cost function depending on the decision maker's priorities. Once the problem is formulated, mathematical modeling of the equipment and system is developed. The mathematical models can be either correlation-based

(data-driven black-box approach) or physics-based (first-principle thermodynamic approach) (Bischi et al., 2014). In the correlation-based approach, the operating conditions of the equipment are defined by their performance curves which can be obtained by interpolating experimental data. This is suitable for systems with one degree of freedom. In the physics-based approach, a detailed system model is used along with equipment performance curves. The physics-based approach is mainly implemented during the design phase while the correlation-based approach is implemented during the operation phase focusing more on optimization techniques than sub-system characteristics.

Very limited research has focused on MINLP problems for long-term optimization due to the difficulties of using a comprehensive thermodynamic system model coupled with nonlinear performance curves and on/off characteristics of the equipment. Safari et al. (2018) included a steady-state thermodynamic model of a micro gas turbine, auxiliary boiler, and absorption chiller in software IPSEpro and integrated it with the MATLAB genetic algorithm (GA) toolbox to conduct short-term (24-hour period) optimization. Powell et al. (2016) developed an approach to solve a dynamic problem for charging/discharging of thermal energy storage (TES) by decomposing it into multiple static sub-problems and using MINLP optimization. The CCHP system model included a physics-based model of the gas turbine and a correlation-based model for other equipment. However, the optimum solution from this method might deviate from the global solution due to the nonconvexity of the dynamic problem. Most of the MINLP research work using thermodynamic system models has involved low dimensionality and optimization during the design and synthesis phase (Fuentes-Cortés et al., 2015), rather than application to operational control. MINLP solvers combine the usage of MILP solvers like CPLEX, GUROBI, CBC which use branch and bound and branch and cut algorithms, and NLP solvers like CONOPT which utilizes a generalized reduced gradient (GRG) method, SNOPT which uses a sequential quadratic programming (SQP) method, and IPOPT which implements an interior point method (IPM) (Gao et al., 2019). However, it becomes really cumbersome to implement MINLP solvers directly for medium or long-term horizons with an hourly resolution, because there are typically thousands of discrete and continuous variables along with nonlinear constraints for large-scale CCHP systems.

Sometimes, linear or piecewise linear approximations are utilized to model nonlinear characteristics of the system in order to reduce computational time. Assuming a constant value for

an efficiency function (e.g., constant efficiency for boilers or turbine generators, constant COP for chillers) makes the problem extremely simplified reducing the computational complexity and can be used for a medium or long-term time horizon (Rong et al., 2006). Adopting a piecewise linear approximation with an appropriate number of intervals to account for a nonlinear equipment model becomes complicated when the degrees of freedom increase by a factor of two or more. Binary variables should be considered if the components cannot operate continuously from 0% partial load, which requires a mixed-integer linear programming (MILP) formulation. MILP optimization is widely used for these types of problems to find a faster globally optimum solution, but it assumes simplistic equipment performance. On the other hand, a nonlinear programming (NLP) optimization technique takes into account the actual nonlinear characteristics of the equipment, but the optimization solution might get trapped in a poor local minimum when the problem has multiple local minima. Sometimes, there is no guarantee for the convergence of the solution. Heuristic optimization techniques like a genetic algorithm (GA), particle swarm optimization (PSO), etc. can be used for MINLP problems, but some control strategy or heuristic rules must be applied to reduce the number of variables when applied to large scale problems. Also, different solutions might be obtained in each trial since they are sensitive to parameter settings. Heuristic algorithms are most often employed when approximate solutions are sufficient and can be used as a starting point in determining a more exact solution through optimization. Compared to heuristics, deterministic optimization techniques can obtain robust solutions due to their strong mathematical foundations.

Decomposition methods, rolling horizon methods, and clustering algorithms are mainly used to overcome the high dimensionality of large-scale MILP/MINLP problems when considering a long time horizon. Decoupling or decomposition methods involve dividing and solving the problem in two or multiple steps, either in parallel or sequentially. These methods can effectively deal with nonlinear behavior of the energy systems and are easy to implement for large-scale problems. Several heuristic techniques or deterministic approaches can be combined together using this hybrid approach. The selection of typical periods with significant demand characteristics is achieved by clustering algorithms (Gao et al., 2018). Rolling horizon techniques solve the problem for short periods and then implement a feedback correction solution for the first few timesteps. This method is similar to model predictive control (MPC) and is suitable for real-time control since it requires feedback information of actual system performance. Zhu and Chow (2019)

developed a two-stage MPC strategy with combined rolling optimization and real-time adjustment for a CCHP system. The equipment design was optimized using a genetic algorithm and MILP was to be applied in the operation strategy optimization. Significant economic benefits were achieved using this strategy under various load profiles; however, no benefits were gained when the forecasting errors were above 8.8%. A similar two-stage coordinated control approach, including an economic dispatching stage and a real-time adjusting stage, was used for CCHP microgrid energy management (Luo et al., 2017) to tackle power fluctuations. A piecewise linear model was used to approximate the thermal and electrical efficiency of a micro gas turbine.

Sometimes a two-stage algorithm is used for design optimization and optimal planning where evolutionary algorithms are used for design and synthesis and operational planning is optimized using a MILP method (Guo et al., 2013 and Elsido et al., 2017). Rubio-Maya et al. (2011) implemented a sequential two-step economic optimization procedure of a polygeneration unit where the first step consisted of the synthesis and design of the polygeneration scheme based on monthly average requirements, and the second step included hourly operational analysis including energy storage systems. The optimization process for synthesis and design was based on an MINLP solved under the outer-approximation algorithm and a CONOPT module (by GAMS, 2008) and the optimized configuration resulted in an internal combustion engine as a prime mover, a lithium-bromide single-effect absorption chiller to cool the resort and a multi-effect distillation unit to provide water demand, as well a plate exchanger to accommodate heating demand. The fuel consumed in the internal combustion engine was correlated to its nominal power rate by linear expressions for full load and bi-quadratic expressions for part-load conditions. For the second step of optimizing the operation of determined system configuration and capacity, a typical NLP solved with a GRG-based algorithm was implemented and the results showed a primary energy savings ratio of about 18% and more than 850 ton per year of avoided CO_2 emissions compared to conventional practice for the tourist resort. Few studies have discussed the implementation of a two-stage algorithm only for optimal operation. Pan et al. (2018) presented a hybrid approach that combines mixed-integer linear programming and the interior point method (MILP-IPM) to solve a dynamic economic dispatch problem in power systems with complicated transmission losses. A global optimal solution from a MILP formulation without transmission losses was used as an initial point for the IPM formulation with transmission losses to improve the quality of the final dispatch results.

Detailed models for CCHP system components are complex and as such, they are typically not employed in plant-wide optimization activities due to large computation time and other associated challenges (Chandan et al., 2012). The earlier work on the CCHP optimization models may include a few but not all nonlinear characteristics of components, thermodynamic system model, mixed-integer variables to represent dispatch states (on/off) of the components, penalties for startup and shutdown, minimum technical limit of components and models for auxiliary equipment. Some assumptions and approximations are often made over these characteristics for easy implementation, but this does not accurately reflect the effect of change in operating conditions on important decision variables. Hence, the potential benefit of optimization is not completely achieved. Although previous studies have demonstrated the effectiveness of optimal control of CCHP systems in terms of energy, cost, and emissions, the results have not been widely implemented, especially for large-scale CCHP systems. The margins for improvements in the optimization of trigeneration systems still exist, which require an in-depth understanding of a plant's energetic behavior. Robustness in the optimization of trigeneration systems has more to do with 'correct and comprehensive' than with efficient modeling, such that it is more important to involve energy specialists than to experts in efficient algorithms.

Deterministic global optimization techniques such as linear, nonlinear, and mixed-integer programming can be coupled to determine more robust, best possible solutions when it is extremely difficult to find feasible solutions for large-scale CCHP problems with multiple energy networks. Even though hybrid approaches combining heuristics and deterministic techniques have been applied for optimal design, hybrid approaches combining MILP and NLP have not been implemented especially for economic optimization of large-scale distributed energy systems. Network flow models for energy systems are used to effectively illustrate the energy flow from supply to demand and across different components. A network energy flow model when combined with supervisory control improves constraint handling. The present work aims to cover the aforementioned gaps in large-scale multi-period CCHP optimization by applying a hybrid MILP-NLP approach combined with a deterministic hierarchical network energy flow model. The significance of this hybrid approach is that a high-quality global solution is determined efficiently when the linear model is feasible while still taking into account the nonlinear nature of the equipment performance curves. This solution methodology has the ability to tightly control turning on/off the components and pick the optimal mix of equipment to meet energy demand. The

framework is easy to implement for any large-scale distributed energy system with multiple units and results in improved performance taking less computational time compared to heuristic scheduling rules or other formulations.

1.2   Objectives

The main objective of this research work is to develop a modular, generalizable, easy-to-configure optimization framework for the cost-optimal control of large-scale combined cooling, heating and power systems to meet electricity, heating, and cooling demands subject to time-varying fuel prices, loads, and environmental conditions. A hybrid approach combining mixed-integer linear programming (MILP) and nonlinear programming (NLP) was chosen as the solution methodology. The optimal solution from the MILP program is used as a good initial point for solving the NLP program to reduce the total operational cost. The developed methodology must address the aforementioned issues related to the implementation of plant-wide activities, providing a more economic and easier-to-configure solution for optimal control of CCHP systems. The combined cooling, heating, and power (CCHP) plant that serves the Purdue campus was chosen as the case study with a fair amount of complexity to conduct an extensive computational simulation. The tool is validated with the plant measurements and then used with the assumption of perfect load forecasts to evaluate the economic benefits of optimal control subjected to different operational conditions and fuel prices. The effects of different (possibly future) utility rate incentives on control decisions and cost savings are investigated.

The methodology incorporates the following elements: (1) a detailed thermodynamic model that considers the linear and nonlinear characteristics of all components integrated into a multi-physical CCHP system; (2) a deterministic network energy flow model that relates the capacity and operation of the CCHP system to the building energy demands; (3) an optimization algorithm capable of handling non-convex, non-differentiable, multimodal (multiple local minima), and discontinuous functions with strong coupling between multiple energy components (electricity, heating, and cooling); (4) an energy dispatch algorithm that employs a hybrid MILP and NLP approach to provide control signals to the primary energy consuming and producing components (boilers, turbine generators, chillers, etc.) using an outer supervisory control loop based on the energy (thermal and electric) demand and to an inner layer of auxiliary components (pumps, fans,

cooling tower and other auxiliaries). The chief benefits of this formulation are its ability to handle the complexities of MINLP problem, determine the optimal mix of equipment with on/off capabilities and penalties for startup and shutdown, consideration of costs from all auxiliary equipment, and applicability to large-scale energy systems with multiple heating, cooling, and power generation units resulting in improved performance.

1.3   Approach

To achieve the objectives mentioned in section 1.2, the following tasks were executed.

1. Literature review: A comprehensive literature review was conducted to determine the current state of the optimization of CCHP systems. Several optimization techniques used to determine optimal operational strategies for CHP and CCHP systems such as linear and nonlinear programming, mixed-integer and evolutionary search, and other decomposition methods were investigated. This material provided the framework for this research work.

2. Combined cooling, heating, and power system modeling: The case study selected for optimization is the Wade Power Plant at the Purdue University-Main Campus. Each component of the plant is represented as a set of mathematical expressions with its parameters, input and output variables, and expressed in functional (input-output) form for both linear and nonlinear functions. The parameters of the components are tuned according to equipment performance data. Then, these components are interconnected according to their physical arrangement in the power plant. The developed component models and the system behavior is validated against the actual performance of the plant.

3. Energy dispatch algorithm: Based on the energy flows across components, a deterministic network flow model is developed that connects the supply to the demand. Mass and energy conservation are applied to develop an energy dispatch algorithm using a network model. The demand drives the activation of individual components throughout the network.

4. Hierarchical paradigm: The separate components for heating, cooling, and electricity production are constructed in a hierarchy that includes controllers for outer and inner layers of components. Depending on the demand, price signals, and other constraints, the outer supervisory control layer determines which components should be operating and their operational load. Depending on the results of this outer layer, the inner layer of component

controllers activates other auxiliary equipment associated with the major components in the CCHP system.

5. Optimization: The objective function, constraints, and bounds are developed and an optimization method capable of handling non-convex / non-differentiable functions and discontinuous design spaces is incorporated. The optimization involves both discrete binary (0 or 1) variables (on/off states for each component) and continuous variables (load level of each component). The optimization routine is applied on an hourly basis because both energy load and prices are time dependent. A hybrid approach combining mixed-integer linear programming (MILP) and nonlinear programming (NLP) is implemented with the energy dispatch algorithm to find the minimum operating cost of the CCHP plant. In the first step, MILP is applied to the optimization model which includes the linear model of all components and the penalty for turning on or off a few units. MILP determines which components need to be turned on and their respective load needed to meet the campus energy demand for the chosen time period. Based on the solution from MILP as a starting point, NLP determines the actual hourly state of operation of each component including the nonlinear performance characteristics of the components. The entire model is coded in MATLAB (R2019b) and optimized using MATLAB's MILP and NLP optimization toolbox. The optimal results from the MILP and NLP approach are compared with the conventional operational strategy (plant data) on a daily basis for different seasons in order to understand the optimal control characteristics and its economic benefits.

6. Sensitivity analysis: The sensitivity of the control responses and cost savings to variability in energy loads (seasonal), operational conditions, time period (short, medium, and long term), and fuel prices are studied through simulation.

1.4 Main Contributions of the Work

In relation to previous work, this research incorporates a more detailed optimization model for CCHP systems that uses a network energy flow model both with linear and nonlinear programming techniques. For this purpose, a hybrid approach combining MILP and NLP is implemented along with an energy dispatch algorithm employed in a hierarchical paradigm for the optimal control of components in the plant. This combination of tools has not been previously employed especially for this complex and large-scale application and is believed to be more

scalable as a general framework for optimizing the control of any CHP and CCHP systems. In addition, this work provides a much more extensive evaluation of the cost savings benefits and optimal control characteristics for CCHP systems than has been previously presented in the literature. Specific contributions of this work include the following:

- Previous studies used models that do not accurately capture the thermodynamic behavior of the system and did not include auxiliary components modeling in the analysis. In this work, the optimization model includes a detailed thermodynamic model for all the components including the mass and energy balance constraints across various energy levels. The models for auxiliary components including fans, pumps, cooling tower, and other auxiliaries assisting the major components in operation is developed and implemented within a hierarchical paradigm. The cost contributions from auxiliary equipment also play a major part in the selection of equipment.

- The network energy flow modeling approach was previously applied only for linear programming solutions to CHP and CCHP optimization problems. Here, an energy dispatch algorithm is formulated using the network energy flow model including the hierarchical class of all components with both linear and nonlinear programming solutions. This optimal control problem for CCHP systems deals with a non-convex cost function and discrete control variables for different modes of operation. This work explores the implementation of a hybrid approach combining MILP and NLP optimization techniques with the network energy flow model to address this difficult optimal control problem. The significance of this hybrid approach is that a high-quality global solution is determined efficiently when the linear model is feasible while still taking into account the nonlinear nature of the problem taking less computational time compared to other techniques. This solution methodology has the ability to tightly control turning on/off the components and pick the optimal mix of equipment to meet the energy demand. The framework is easy to implement for any large-scale distributed energy system with multiple units and results in improved performance over heuristic scheduling rules or other formulations.

- An extensive simulation-evaluation of the proposed optimization framework is carried out for minimizing the operational cost of the daily operation of a large CCHP plant. Optimal performance results are compared with the plant operational strategy and the benefits are

evaluated. Also, the sensitivity of the results to fuel prices is examined to understand how to plan for the advanced purchases of base electricity and hedging of natural gas.

- Finally, the optimization tool can be implemented for recommending the daily operation of the power plant, and the cost and energy savings can be directly estimated and provided as feedback to operators and plant managers. This tool is modular and generalizable to different types of systems so that it can be easily modified for different architectures or configurations and could be implemented for any CHP or CCHP system in the future.

1.5   Organization of the Document

The remainder of the document is organized as follows. Chapter 2 presents a review of research on various optimization techniques used for the control of CCHP systems. Chapter 3 introduces the case study along with detailed mathematical models of each equipment at the Wade Power Plant and the Northwest Chiller Plant (NWCP) and their assembly in the power plant. Chapter 4 presents the formulation and implementation of the energy dispatch algorithm using the network energy flow model and solved by a hybrid optimization approach which uses the optimal solution from mixed-integer linear programming (MILP) as a starting point for solving the nonlinear programming (NLP) formulation to reduce the total operational cost. The objective function and constraints are included in this section. In Chapter 5, the optimization results for a 24-hour period for different seasons are presented. Also, the sensitivity analysis of the control responses and cost savings to variability in time period, energy loads, operational conditions, and fuel prices are analyzed. Finally, a summary of research contributions and some recommendations are presented in Chapter 6.

2. LITERATURE REVIEW

The benefits of cogeneration and trigeneration systems have been studied for decades, but optimized control systems can help in realizing the full potential of these systems in terms of energy and cost savings and emissions reduction, regardless of the application and technologies employed. Several papers have been published on optimizing the performance of CHP and CCHP systems based on energetic, economic, and environmental analysis. The performance of these systems is mainly dependent on the plant design and operational strategy used to improve energy efficiency and reduce overall cost and greenhouse gas emissions. Even though there are many optimization procedures for CCHP component design and system configuration, only optimization techniques considered for use as part of operational strategies for CCHP systems are discussed in the following literature review. The optimization algorithms used in CCHP systems are generally divided into linear programming, nonlinear programming, mixed-integer, and evolutionary search. Different operation strategies and optimization techniques are discussed according to the formulation of the optimization problem based on chosen performance metrics (primary energy consumption, operational cost, and CO_2 emissions reduction), either separate or combined analysis.

In order to optimize system performance, a mathematical model is constructed with an objective function, constraints, and boundary conditions. Operation strategies may differ depending on the different definitions of 'optimal' varying from simple economic interests to environmental criteria. Most of the optimization problems include economic dispatch (ED) that minimizes the cost of supplying energy demand subject to operational constraints. While scheduling is addressed as a mixed-integer programming problem, an economic dispatch problem is settled mainly as a linear or nonlinear problem. Incorporation of environmental considerations along with cost and energy savings poses a multi-objective optimization problem. Generally, optimization problems for CCHP systems can be stated as linear programming, nonlinear programming, mixed-integer programming or multi-objective programming problems. Classical solution methods for these optimization problems include the simplex method, dynamic programming, Lagrangian relaxation, interior point method (IPM), sequential quadratic programming (SQP), Newton's method, and the reduced gradient method (Salgado and Pedrero,

2008). Some of the artificial intelligence methods to optimize CCHP system include branch-and-bound algorithms, genetic algorithms (GA), evolutionary programming, and particle swarm optimization (PSO) algorithms (Wang et al., 2010). Optimization can be performed using many algorithms, some of which are mentioned below. The rest of this section presents an overview of the research on optimization of CCHP systems and some of its practical implications.

2.1   Linear Programming

Linear programming techniques have been extensively used and are easily employed for CCHP system optimization problems. In general, the cost-efficient operation of a CHP system can be formulated as a linear programming (LP) problem over a long-term optimization period by decomposition into thousands of hourly models and then solving the problem of minimizing the total operational costs (Lahdelma and Hakonen, 2003). For example, Gustafsson and Karlsson (1991) used a linear programming model for finding the best combination of electricity production, electricity purchase, and heat production in a district heating system in Malmo, Sweden. An optimal solution for this model was characterized by the lowest possible operating cost for one year depending on the high and low-price conditions in the electricity grid for several time segments. A basic linear cost model with the constraints on the total capacities and energy balance on meeting demand is solved using the simplex method and branch and bound algorithm. The results suggested that it is cheaper to buy the electricity than to produce it in the municipal CHP plant during low price conditions in the electricity grid. However, the model doesn't include a clear description of the system configuration or the performance of components in the CHP system.

Rong and Lahdelma (2005) used a tri-commodity simplex algorithm for optimizing the cost-efficient operation of a trigeneration system. It includes a linear programming (LP) model with a joint characteristic for energy components to minimize simultaneously the production and purchase costs, as well as CO_2 emissions costs. The power plant consists of one boiler which can operate with two fuels simultaneously and a backpressure turbine from which medium and low-pressure steam can be extracted. The constraints in the model include energy balances for the three energy products and the extreme points of the operating region of the plant. The computational speed of the tri-commodity simplex algorithm was compared with an LP2 simplex code and the

former was 36-58 (average 45.6) times faster than the latter. The operational strategy and the results regarding minimum cost values are not elaborated.

Rong et al. (2006) formulated an LP problem for long-term planning by decomposing it into thousands of hourly models and solved it using the extended power simplex algorithm. This includes an hourly multi-site CHP planning problem with multiple heat balances as an LP model while the sub-problem for each site is tied together by the global power balance constraint. This problem is an extension of (Lahdelma and Hakonen, 2003) and extended the power simplex algorithm proved to be 29 to 85 times faster than a simplex code for large multi-site CHP models.

Lozano et al. (2008) incorporated thermo-economic analysis to determine and evaluate an optimal operational strategy as a function of the demand for energy services and the prices of the resources consumed, using a linear programming model. The trigeneration module consisted of a natural gas reciprocating engine, an auxiliary boiler, a single-effect absorption chiller, and an electric-driven chiller. A constant efficiency was assumed for all the components. The operating strategies include the possibilities of selling the electricity to market and wasting the cogenerated heat. Nine different operation modes were considered with the combinations of purchased electricity, sold electricity, auxiliary heat, and waste heat. The energy flows that correspond to the operation with minimum variable cost differed for every operating mode and the economic impact of the changes in demand or operational condition of the equipment are evaluated.

Piacentino and Cardona (2008) developed a MATLAB optimization tool, EABOT (Energy Analysis-Based Optimization of Trigeneration plants), including an in-depth energetic analysis using a linear-programming interior point method (a variant of Mehrotra's predictor-corrector method) for the synthesis, design, and operation of a CCHP system including thermal energy storage. They used the tool to perform multi-objective optimizations including economical and energo-environmental analyses for two large buildings in the civil sector and derived conclusions about the optimal number of days to be used for the optimization.

Assumptions such as neglecting efficiency drops at part load operation (constant efficiency) and not introducing binary variables for the on/off states were made for modeling of the system component dynamics to make the problem linear in order to avoid large computational time and other associated challenges. The CCHP equipment are assumed to operate continually between

0% and 100% of their rated capacity. The linear programming approach solves many diverse combination problems because of its flexibility. However, the nonlinear characteristics of the equipment and system cannot be ignored completely.

2.2 Nonlinear programming

In nonlinear programming problems, either the objective function is nonlinear or the constraints or both considering the nonlinear characteristics of the equipment models. Chapa and Galaz (2004) formulated an economic dispatch problem for CHP systems and used a Sequential Quadratic Programming (SQP) algorithm with a Lagrangian relaxation technique to solve a nonlinear constrained optimization problem. Part-load relations between energy production and fuel consumption were included as convex quadratic input-output relations in the model to find the minimum operation cost. The system included a conventional power unit, co-generation units, and auxiliary boilers with the consideration for buying and selling power to the utility electric grid. The results showed that the proposed algorithm was more effective and gave a lower operating cost by 4% than the standard SQP inside the feasible region of CHP units.

Dieu and Ongsakul (2009) presented an augmented Lagrange-Hopfield network for the CHP economic dispatch problem. In the augmented Lagrange-Hopfield network, the energy function was augmented by Hopfield terms from the Hopfield neural network and penalty factors from the augmented Lagrangian function to damp out oscillation of the Hopfield network during the convergence process, leading to faster convergence. They consider the same system as Chapa and Galaz (2004) with a conventional power unit, co-generation units, and heating units with a varied number of units for different cases considered. The performance of the augmented Lagrange–Hopfield network was compared with other algorithms such as Lagrangian relaxation, a genetic algorithm, an ant colony search algorithm, evolutionary programming, an improved genetic algorithm with multiplier updating, and a harmony search algorithm. The augmented Lagrange–Hopfield network resulted in lower total cost and faster computational time for all the cases considered, especially for large-scale combined heat and power economic dispatch problems.

Hashemi (2009) developed a model for offline determination of nonlinear techno-economic optimal operation of cogeneration systems (TOOCS). The system includes a combined heating power (CHP) module, auxiliary boiler, absorption chiller, heat storage unit, and utility grid catering

to electrical, thermal, and cooling needs. The CHP module meets the electrical load of the buildings and the excess electricity produced is sold back to the grid. The total economic benefit of this system was maximized during total daily operation time with the effective use of a thermal storage tank and an absorption chiller. However, there was no benchmark for comparing the optimum results.

Chandan et al. (2012) adopted reduced order thermo-economic models of CCHP components integrated with nonlinear programming for a CCHP plant at the University of California, Irvine, which includes thermal energy storage capabilities. The CCHP system includes seven electric chillers, a thermal energy storage tank, a gas turbine, a heat recovery steam generator, and purchase of electricity from the utility grid. The nonlinear model incorporates a supervisory control layer using a system engineering approach to determine the optimal plant operation parameters or set points for control of the CCHP system. The look-ahead optimization problem used forecasted electric and thermal demands and the results showed 8.5% improvement compared to rule-based strategy in terms of operating cost. The nonlinear model included the part-load characteristics of the equipment but did not include on/off control of each component. Also, the determination of optimal solution was highly sensitive to the choice of initial conditions and could result in multiple local minima or the optimization solution might get trapped in a poor local minimum. NLP could be used with a multi-start option to find the global optimum; however, this involves huge computational time. Sometimes, there is no guarantee for the convergence of the solution for large scale problems.

2.3   Mixed Integer Programming

Due to the on-off characteristics of the components, mixed integer programming is widely used with linear or nonlinear programming. Both discrete and continuous variables can be included in these optimization techniques. While binary variables are used to represent the staging of equipment (i.e., on/off), continuous variables are used to represent the operational or capacity conditions (i.e., how much). If the objectives and constraints are linear, then the problem can be solved using Mixed Integer Linear Programming (MILP) optimization. Either the objectives or constraints or both are nonlinear, then the problem can be formulated and solved using Mixed Integer Nonlinear Programming (MINLP) optimization.

2.3.1 Mixed Integer Linear Programming (MILP)

MILP optimization is widely used for CCHP problems to find a fast globally optimum solution. Branch and bound algorithms are the most effective techniques used for MILP optimization. There are a lot of commercially available solvers such as CPLEX, GUROBI, CBC, Xpress and MATLAB which use branch and bound and branch and cut algorithms to solve MILP problems. Thorin et al. (2005) developed a long time-horizon optimization tool for cogeneration systems based on mixed integer linear programming (MILP) and Lagrangian relaxation. The model takes into account the possibility to buy and sell electric power at a spot market and has been tested on a demonstration system based on an existing CHP system in Berlin, Germany which includes extraction condensing steam turbines, backpressure turbines, gas turbines, and boilers fueled with either coal, oil or gas. The fuel consumption of the turbines is approximated by linear functions of electric power and thermal power produced and a constant efficiency is assumed for boilers. The results showed that with a high heat demand, most of the turbines run at their maximum capacity to fulfill the heat demand while low heat demand affords many possible combinations to run the plant with generators of the same capacity.

Lozano et al. (2010) developed an optimization model using MILP to determine the preliminary design of CCHP systems with thermal storage, thereby minimizing the total annual cost of the plant. The application of the model was demonstrated by a case study for a set of buildings with 5000 apartments located in Zaragoza (Spain). The system is made up of cogeneration modules, consisting of natural gas engines and heat recovery equipment, auxiliary boilers, vapor compression refrigerators, single-effect absorption refrigerators, cooling towers, and thermal storage. The trigeneration system economics with and without thermal storage were compared with the conventional energy supply system. Although there was a significant increase in invested capital for the trigeneration system without thermal storage (9,380,000 €) and with thermal storage (7,801,000 €), considerable annual profits in energetic turnover of 2,404,000 €/yr and 2,536,000 €/yr were estimated for the trigeneration systems without and with thermal storage, respectively.

Even though MILP optimization is widely implemented for these types of problems, it assumes over optimistic equipment performance. Some drawbacks include the impossibility of taking into account nonlinear effects of subsystems; considering all the time periods at once; the

risk of high dimensionality of the problem (Urbanucci, 2018). Adopting a piecewise linear approximation with an appropriate number of intervals to account for nonlinear equipment models creates its own optimization problem and becomes complicated when the degrees of freedom increase to two or more.

2.3.2   Mixed Integer Nonlinear Programming (MINLP)

Very limited research has focused on MINLP problems for long time-horizon optimization due to the difficulties of using a comprehensive thermodynamic system model coupled with nonlinear performance curves and on/off characteristics of the equipment. High dimensionality and uncertainties make the problem even more complicated and computationally expensive to solve. Powell et al. (2016) developed an approach to solve the dynamic problem for charging/discharging of thermal energy storage (TES) by decomposition into multiple static sub-problems and solutions using MINLP optimization. The CCHP system model included a physics-based model of the gas turbine and a correlation-based model of other equipment. However, the optimum solution from this method might deviate from the global solution due to the nonconvexity of the dynamic problem.

Li et al. (2008) carried out a sensitivity analysis of energy demands of a hotel and hospital to study its influence on the performance of a CCHP system using MINLP to reflect average, uncertainty bounds, and historical peaks in demand profiles. The system configuration includes a gas turbine, heat exchanger, absorption refrigerator, gas boiler, and electrical refrigerator. Electricity is purchased from the utility in case of high electrical demand. A constant efficiency is assumed for the turbine, boiler, and heat exchanger and a constant coefficient of performance is assumed for the chillers. The mixed-integer nonlinear model was solved with the barrier method combined with the branch and bound algorithm. The optimization results showed that the gas turbine's capacity is not sensitive to uncertainty and historical peaks of energy demands while the heat exchanger and absorption refrigerator are sensitive. Also, uncertainty and historical peaks of energy demands have only a little influence on the annual cost savings and economic feasibility depends mainly on the average energy demands.

Most of the MINLP research work using thermodynamic system modeling involves low dimensionality and optimization during the design and synthesis phase (Fuentes-Cortés et al., 2015), rather than operational control. MINLP solvers include CPLEX, GUROBI, CBC that use branch and bound and branch and cut algorithms, NLP solvers like CONOPT utilize the generalized reduced gradient method, SNOPT uses a sequential quadratic programming method and IPOPT implements the interior point method (Gao et al., 2019). Even though there are a lot of MINLP solution methodologies available, it is cumbersome to implement MINLP solvers directly for medium or long-term horizon dynamic problems with hourly resolution, because there are thousands of discrete and continuous variables. Also, the complexity of numerous constraints along with nonlinear characteristics in the thermodynamic model, makes the optimization model hard to converge (Elsido et al., 2017). It is extremely challenging to implement these algorithms for the daily operation of a power plant when the simulations are computed for a reasonable time horizon on an hourly basis.

2.4   Evolutionary Algorithms

Evolutionary algorithms (EA) are generic population-based metaheuristic optimization algorithms. They are most often employed when approximate solutions are sufficient and exact solutions are necessarily computationally expensive. Particle swarm optimization (PSO) and genetic algorithms (GA) are the most popular EAs and have been applied for both system design and control of CCHP systems.

2.4.1   Particle Swarm Optimization

For Particle Swarm Optimization (PSO), potential candidate solutions fly through the problem search-space by following their own current optimum position as well as guided by the entire swarm's best-known position. Wang et al. (2010) employed a PSO algorithm to simultaneously measure the energetic, economic, and environmental benefits of a CCHP system in comparison to a conventional Separation Production (SP) system where heating is provided by boilers, cooling by electric chillers and electricity from the grid. The system includes a natural gas power generation unit, auxiliary boiler, hybrid cooling system with electrical chiller and absorption chiller, cold/heat storage, fans, and distribution pumps. The analysis in this paper is based on the

operation strategy following the electrical demand since the excess electricity from the CCHP system is not allowed to be sold back to the outside grid while the excess heat produced can be stored in the heat storage tank. The power generation unit thermal efficiency varies with the load factor nonlinearly for the estimation of fuel energy consumption. The capacity of the power generation unit (PGU), the capacity of heat storage tank, the on-off coefficient of the PGU, and the ratio of electric cooling to cooling load were optimized in considering both design and operation of the CCHP system. The optimal results show that the CCHP system saves 12.2% of energy and 11.2% of cost and reduces CO_2 emissions by 25.9% compared to the conventional SP system. Also, the results from the PSO algorithm are compared with a genetic algorithm (GA) and PSO algorithm's computation time (PSO - 24 min and GA - 35 min) and the optimum primary energy savings ratio (PSO - 16.43% and GA - 16.26%) are somewhat better than the GA.

Tichi et al. (2010) examined the effects of current and future energy price policies on the optimal configuration of CHP and CCHP systems in Iran, under the conditions of selling and not-selling electricity to the utility. A PSO algorithm was used for minimizing the cost function for owning and operating various CHP and CCHP systems in an industrial dairy unit. The CCHP system in this study consists of a prime mover, heat exchanger, supplementary boiler, absorption chiller, and electric chiller. Different prime movers were considered, and a reciprocating engine was determined as the best choice with the capital recovery periods for the best case for subsidized and unsubsidized energy prices are 4.9 and 1.3 years, respectively. Also, from an economic point of view, when it is allowed to sell electricity to the utility, it is better to choose a prime mover with higher capacity for both CHP and CCHP systems. It was concluded that promoting the policy of selling electricity to the utility as well as eliminating subsidies are prerequisites for widespread utilization of CHP and CCHP systems in Iran.

Liu et al. (2012) presented an operation strategy, based on the variation in electric cooling to total cooling load ratio, for a CCHP system with hybrid chillers, consisting of a combined electric and absorption chiller, power generation unit with unlimited and limited capacity, heat recovery system and auxiliary boiler. An enumeration algorithm was adopted to determine the optimal value of PGU capacity which was found to be 96 kW considering the whole year's thermal and electrical demand. Test results showed that, with the proposed operation strategy and corresponding optimal PGU capacity, the CCHP system performed much better than the

conventional SP system with primary energy savings of 8%, total cost savings of 37%, and carbon dioxide emission reduction of 25%. Also, the optimized results from the enumeration algorithm are better in terms of total cost savings than the results from following the thermal load by 7% and following the electric load strategies by 33%.

2.4.2 Genetic Algorithms

Genetic Algorithms (GA) are a particular class of evolutionary algorithms for determining exact or approximate solutions to optimization and search problems. The most noteworthy features of evolutionary algorithm are that they do not rely on derivatives of the objective function to be solved and simulate the mechanisms of biological evolution over a number of iterations to find the global optimum or near-optimal. An evolutionary GA was used to maximize primary energy savings (PES), annual total cost savings (ATCS), and carbon dioxide emission reductions (CDER) of a CCHP system for a hotel building in Beijing, China (Wang et al., 2010). The CCHP system includes a natural gas driven PGU, a waste recovery system, a back-up boiler, an electric chiller, and an absorption chiller. The CCHP system operates following thermal demand where excess electricity is purchased from the grid. The capacity and operation strategy of the CCHP system was optimized based on energy flow to evaluate the performance of CCHP system. With the optimal PGU capacity of 525 kW and the 53% of cooling load provided by electric chillers, the CCHP system outperforms the separation production (SP) system by 18.40% in integrated performance (PES, ATCS, and CDER). Also, based on the electricity price sensitivity analysis, the ratio of electric cooling to cool load was fitted into a curve as a function of cost of electricity to guide the operation strategy. The PES, ATCS, and CDER were weighted equally to evaluate the integrated performances of the CCHP system in comparison to a SP system and GA was used to provide optimization for sixteen hypothetical buildings with various energy demands (Wang et al., 2014). The primary energy consumptions of the CCHP system following electric demand management (EDM) and thermal demand management (TDM) were analyzed. The average performances (PES, ATCS, CDER, and integrated performance of the CCHP systems) of the CCHP system for all of the scenario buildings in EDM mode are 5.4%, 4.3%, 25.3%, and 11.7% better while the corresponding performances in TDM mode are 6.2%, 1.8%, 20.8%, and 9.6% better than the SP system. It can be found that the performance in EDM mode is better than in TDM mode except for the PES. The CCHP systems produce excess electricity in TDM mode or

excess heat in EDM mode. The excess ratio (ratio of excess product to primary energy consumption) in EDM mode of scenarios having a lower ratio of heat to electricity are much larger than in TDM mode, which does not lead to primary energy savings.

Almasi et al. (2011) used GA to optimally find the design parameters (same as Wang et al., 2010 for the same set of CCHP components) of the 120 MW Mashar gas turbine CHP plant in Iran using a thermo-economic approach (minimizing the total operating cost which is related to fuel expense, capital investment and maintenance expenses, and the corresponding cost for exergy destruction). The results of the thermodynamic simulation were compared with the actual properties of the power plant and temperature profiles agreed within 10%, on average. Also, the variation of decision variables and exergy destruction were studied for different fuel costs. By increasing the fuel cost, the values of design parameters increased leading to high capital cost of components. Higher efficiency of components leads to less exergy destruction and saves fuel consumption. The total exergetic efficiency of the plant was 36.08% with the combustion chamber having the lowest value of all the components due to high irreversibility.

Ebrahimi et al. (2012) optimized the overall efficiency of a CCHP cycle operated on a micro-steam turbine using a genetic algorithm. The heating and cooling systems include a steam and air heat exchanger and a steam ejector condenser. A constant efficiency was assumed for all components. The exergy analysis revealed that the biggest exergy destruction takes place in the steam generator for both summer and winter seasons. The optimization results show that the maximum of the overall efficiency is 25% for summer and 62% for winter and the corresponding fuel energy savings ratios are 69% and 25%, respectively.

Compared to other methods, GA needs no initial information and searches the global optimization solution. GA operates in parallel from multi-points, searches heuristically in the solution area, overcomes the search blindness, and accelerates the search speed. If the initial values are selected appropriately, the search speed will be even faster. However, it is unlikely to obtain satisfactory answers from GA when the number of variables increases as the population size doubles with variables. A GA nonlinear constraint algorithm takes a large number of iterations for constraint satisfaction. Also, a GA has no guarantees regarding the quality of its solutions.

Heuristic optimization techniques like genetic algorithms (GA), particle swarm optimization (PSO), etc. can be used for MINLP problems, but some control strategy or heuristic rules must be applied to reduce the number of variables and constraints when applied to large scale problems. Also, different solutions might be obtained in each trial since they are sensitive to parameter settings. Heuristic algorithms are most often employed when approximate solutions are sufficient and can be used as a baseline to achieve exact solutions.

2.5   Decomposition Methods

Decoupling or decomposition methods involve dividing and solving the problem in two or multiple steps, either in parallel or sequentially. These methods can effectively deal with the nonlinear behavior of energy systems and are relatively easy to implement for large-scale problems. Several heuristic techniques or deterministic approaches can be combined together using this hybrid approach. Sometimes two-stage algorithms are used for design optimization and optimal planning where evolutionary algorithms are used for design and synthesis and operational planning is optimized with a MILP method that uses branch and bound or branch and cut algorithms.

Guo et al. (2013) used a two-stage optimal planning and design method for a combined CCHP microgrid system in a hospital to minimize the total net present cost and carbon dioxide emissions. For the first stage, a multi-objective GA based on a non-dominated sorting genetic algorithm-II (NSGA-II) was applied to solve the optimal design problem including the optimization of equipment type and capacity. For the second stage, mixed-integer linear programming (MILP) algorithm was used to solve the optimal dispatch problem. The resulting CCHP microgrid system was comprised of a boiler, absorption chiller, electric chiller, photovoltaic (PV) array, ice storage air conditioning system, thermal storage to store excess heat energy and natural gas fired PGU. Electricity purchased from the grid was used to meet excess electrical demand. The optimal results show that the maximum capacity of the PV to be installed is 60 KW for the given size of the hospital. Also, as the number of PGU increases, the net present cost increases while the carbon dioxide emission reduces due to the lower emission of PGU compared to the grid.

Elsido et al. (2017) solved an upper level, synthesis and design MINLP problem by means of two different evolutionary algorithms and discrete variable relaxation, while, at the lower level, the multi-period operational problem was handled by a MILP method for the optimization of CHP units with heat storage.

Rubio-Maya et al. (2011) implemented a sequential two-step economic optimization procedure for a polygeneration unit where the first step consisted of the synthesis and design of the polygeneration scheme based on monthly average requirements, and the second step included an hourly operational analysis that included the energy storage systems. The optimization process for synthesis and design was based on MINLP (Mixed Integer Non-Linear Programming) solved under the outer-approximation algorithm and a CONOPT module (by GAMS, 2008) was used to optimize the operation of the plant. For the first step, the optimized configuration was an internal combustion engine as prime mover, a lithium-bromide single-effect absorption chiller to cool the resort, and a multi-effect distillation unit to provide water demand, as well a plate exchanger to accommodate heating demand. The fuel consumed in the internal combustion engine was correlated to its nominal power rate by linear expressions for full load and by quadratic expressions for part load conditions. For the second step of optimizing the operation of the determined system configuration and capacity, a typical NLP solved with a GRG-based algorithm was implemented and the results showed that a primary energy savings ratio of about 18% and more than 850 ton per year of avoided CO_2 emissions compared to conventional practice for a tourist resort.

2.6 Multi-Objective Optimization

Mostly, trigeneration optimization is based on economic criteria. However, in some cases, there is interest in trading off costs with energy savings and environmental benefits. Environmental economic dispatch could be treated as a single objective optimization problem by treating gas emissions as a constraint with a permissible limit or by expressing pollution damage costs due to the emissions (Ahmadi and Dincer, 2010), or by using weighted sum methods (Bracco et al. 2013). The use of a single-objective function with a weighted combination of several objectives does not provide a clear optimal solution because of the trade-offs in interrelated objectives of different quantities, thereby making the objective function lose its significance (Deb, 2001). However, multi-objective techniques provide a set of several non-dominated optimal solutions, also known

as a Pareto optimal set. For such solutions, there is a trade-off between the optimal solutions of different objective functions, depending on which the user can choose the solution he needs.

Kavvadias and Maroulis (2010) used a multi-objective evolutionary algorithm (genetic algorithm) for economical, energetic, and environmental performance of a trigeneration system in a 300-bed hospital. The system includes a natural gas reciprocating engine, absorption chiller, auxiliary boiler, and electric chiller. The CHP efficiency is represented as a linear function of capacity factor, which is the ratio of the actual energy produced to its nominal power. Both construction (equipment sizes) and discrete operational (pricing tariff schemes and operational strategy) variables were optimized based on realistic conditions under fluctuating energy prices to maximize economic, energetic or environmental objective criteria (net present value of the investment, primary energy savings ratio, emission reduction ratio). The optimum pareto results show three clusters of solutions with a trade-off between economic, energetic, and environmental indices. Economic optimal solutions were preferred when a peak shaving strategy is used in summer and heat following strategies are used in winter. Energetic optimal solutions perform better when the system operates with a heat following strategy in summer and an electricity following strategy in the winter.

Wu et al. (2012) determined optimal operation strategies for a micro-CCHP system using objective functions for energy savings ratio and cost savings ratio. Operation strategies under various load conditions were analyzed using a mixed-integer nonlinear programming model. The micro-CCHP system included a gas engine, adsorption chiller, gas boiler, heat pump, and electric chiller with an allowance to purchase electricity from the grid. For energy savings optimization, the optimal operation strategy changes with load conditions while for cost savings optimization, the optimal operation strategy not only changes with load conditions but also changes with energy prices. A Micro-CCHP system was found to be superior to a conventional separated system when the heating load was over 12 kW in CHP mode or over 21 kW in CCHP mode. Both in energy savings optimization and cost savings optimization, increasing the electric load improved system performance when the part load ratio of the gas engine was relatively low. Also, when the energy price ratio reached 0.45, it was economical to use the conventional separated system.

Shi et al. (2013) developed a multi-objective model for a CHP economic dispatch problem, where the competing fuel cost and environmental impact objectives were simultaneously optimized. The model includes a multi-objective line-up competition algorithm to handle nonlinear constraints, diversity-preserving mechanisms to produce well-distributed pareto-optimal solutions, and a fuzzy decision-making process to extract the best compromise for a non-dominated solution from the Pareto-optimal set. The system consists of conventional thermal generators (power-only units), CHP units, and heat-only units to serve the power and heat demand. The results obtained by the proposed approach were compared with different evolutionary algorithms (bee colony optimization; evolutionary programming; particle swarm optimization; real-coded genetic algorithm) and the proposed method resulted in the lowest fuel cost, 10,104.38 $/h, which is about 212.62 $/h less than the best solution from evolutionary algorithms, (10,317 $/h) and about 2.1% energy savings. In the multi-objective techniques, pareto-optimal solutions were be obtained by varying the weights between different criteria. However, there is no rational basis for determining adequate weights and the objective function so formed may lose significance due to combining incommensurable objectives. In addition, the process is time consuming and sometimes, not all solutions are generated, and important solutions can be overlooked in this method. In general, a multi-objective problem usually does not have a unique solution, as compared with a single objective problem.

2.7   Network Energy Flow Models

Network flow models are commonly used to help in setting up linear programs. The advantage of using a network flow model for energy system problems is to effectively illustrate the energy flow from supply to demand. This facilitates setting up an objective function and constraints and provides for easy interpretation of the results. Cho et al. (2008) developed an energy dispatch algorithm using linear programming with network flow models to provide operational/control signals for the optimal operation of the CCHP equipment in order to minimize the energy costs. Also, the algorithm provided optimal solutions for decisions regarding generating power locally or buying power from the grid. The micro-CCHP facility included a 15-kW natural gas internal combustion (IC) engine, 10-ton absorption chiller, heat exchanger, and boiler. The optimal results show that the IC engine was not operated at low electrical demand due to lesser

efficiency. Also, the optimal energy cost was lower than the baseline case (importing electricity from grid and auxiliary boiler) for all demand scenarios throughout the day.

Cho et al. (2009) extended this energy dispatch algorithm to minimize the operational cost, primary energy consumption (PEC), and carbon dioxide emissions (CDE) of CCHP systems for cities with different climate conditions: Columbus, Minneapolis, San Francisco, Boston, and Miami. Here the objective function to minimize the total operational cost of running the CCHP system was modified using conversion factors to minimize the amount of primary energy consumption and CO_2 emissions satisfying the total energy demand. The CCHP system is connected to the electrical grid so that electricity can be purchased from the grid when the electrical demand is high and excess electricity from the CCHP system can be sold back. The results show that optimizing one objective reduces or increases the other two objectives. For the cities considered, the site energy consumption is higher when compared to the reference case of using a vapor compression cycle for cooling, natural gas for heating, and electricity from the grid. The reduction in emissions strongly depended on the site energy consumption and the mix of electricity from various fuel sources for different locations. The results suggest that the implementation of CCHP systems should be considered only when the energy savings and reduction of emissions are guaranteed.

The algorithm from Cho et al. (2009) was used along with supervisory feed-forward control for real-time CHP operation with electric and thermal energy storages using short-term load prediction for a small office building model in Chicago (Cho et al., 2010). The results indicate that CCHP systems with an energy dispatch algorithm have the potential to realize savings in operational cost, primary energy consumption (PEC), and carbon dioxide emission (CDE) with respect to a conventional system. CCHP operation with electrical energy storage and thermal energy storage resulted in significant cost savings on a winter day of 11% and on a summer day of 4% compared with a conventional system. The single-year simulation results show that the CCHP system with energy storage could reduce PEC by up to 7.6% and CDE by up to 10.3% compared with those of the reference conventional system.

Hu and Cho (2014) presented a stochastic multi-objective optimization model with an energy dispatch algorithm using linear programming to optimize the CCHP operation strategy for

different climate conditions based on operational cost, primary energy consumption, and CO_2 emissions. To assist the multi-objective decision analysis, an incentive model for PEC, and CDE reduction is used to evaluate the pareto operation decisions derived from the stochastic model. The analysis results showed that increasing the PEC incentive decreases PEC and increases operational cost and increasing the CDE incentive decreases CDE.

2.8 Chapter Summary

Previous research efforts on optimization of CHP and CCHP systems have demonstrated the superior performance of optimal control compared to conventional strategies or other rule-based techniques. However, the results have not been widely implemented. From the reviewed work, a few observations can be made.

- The components of cogeneration and trigeneration systems are often represented as black boxes considering the type of energy delivered and modeled either by assuming constant efficiency in most cases to simplify the analysis and calculation or by characterizing their part load behavior using empirical relations in a few cases. Most equipment behavior is nonlinear and accurate prediction should consider variable efficiency as a function of load and/or ambient conditions.

- The absence of variables involving the thermodynamic state of working fluids simplifies design optimization. However, these models do not accurately characterize the effect of change in operating conditions on the important decision variables.

- The minimum technical limit of CCHP system operation has not been considered in previous work. The CCHP equipment can operate anywhere between 0% and 100% of its rated capacity, and the ramping rate for load adjustment has not been included.

- In most of the work, auxiliary components such as pumps, fans, and other auxiliaries have not been considered or described.

- There has been very limited sensitivity analysis of CCHP systems that have studied the influence of the change of parameters on optimization results.

Detailed models for CCHP system components are complex and as such, they are typically not employed in plant-wide optimization activities due to the large computation time, nonlinear characteristics of components, thermodynamic constraints, mixed-integer variables to represent dispatch states (on/off) of the components, and other associated challenges (Chandan et al., 2012). Although many approaches have been developed, extensive evaluations of the proposed control methodologies in terms of performance and computational requirements are still missing, especially for large scale implementation. A network flow model with a detailed thermodynamic behavior of all components can accurately characterize energy flows throughout the system. However, network flow algorithms have been applied mostly in combination with linear programming where component nonlinearities are not captured. To the author's knowledge, a practical and hybrid approach combining mixed-integer linear programming (MILP) and nonlinear programming (NLP) has not been implemented for large-scale CCHP systems. Also including network energy flow models with this hybrid approach can be useful for handling linear and nonlinear constraints. A global optimal solution from a MILP formulation can be used as an initial point for a NILP formulation to improve the quality of the final results. This thesis is focused on the adaptation and application of a hybrid NILP-NLP approach for large-scale multi-period CCHP optimization.

3. DESCRIPTION AND MODELING OF THE CCHP PLANT

3.1 Case Study Description

The case-study considered in this research work is the Wade Power Plant and the Northwest Chiller Plant (NWCP) located at the main campus of Purdue University in West Lafayette, Indiana, USA. The Wade Utility Plant was designed and constructed from 1960 to 1962 and serves the electrical and thermal demands of more than 150 buildings at the Purdue campus. The Wade power plant produces electricity, steam, and chilled water through a Combined Cooling, Heating, and Power (CCHP) or trigeneration system to meet the campus electricity, heating, and cooling demands. The steam generated from the utility boilers along with the CHP facility is used for campus heating, power generation, chilled water production, and in-plant auxiliary component usage. The steam, which is distributed through a steam tunnel system, one set of two lines at 125 psig (963.2 kPa) and another two lines at 15 psig (204.8 kPa), is the primary heating source for 13.5 million gross square feet of Purdue campus buildings. The electricity generated using steam turbine generators provides 30-60% of the electricity required to meet campus needs, and in-plant usage; while the remainder of electricity is purchased from the local electric utility, which includes a real-time pricing (RTP) component. The power plant has one diesel engine driven generator for emergency purposes. Purdue generates the chilled water required for cooling using both electric and steam chillers from the Wade power plant and only electric chillers from the Northwest Chiller Plant (NWCP). Chilled water generated using these chillers is delivered through a closed water circulation loop to campus to meet the time-varying cooling demand. Apart from the major components, there are other auxiliary equipment such as boiler fans, feedwater pumps, chilled water pumps, cooling tower fans, condenser water pumps, and other auxiliaries that are activated depending on the major components to which they are linked to. Purdue's environmental footprint has significantly been reduced as a result of the increased efficiencies of trigeneration. Figure 3.1 shows a simple schematic of the Wade power plant providing heating, cooling, and electricity to the Purdue campus.
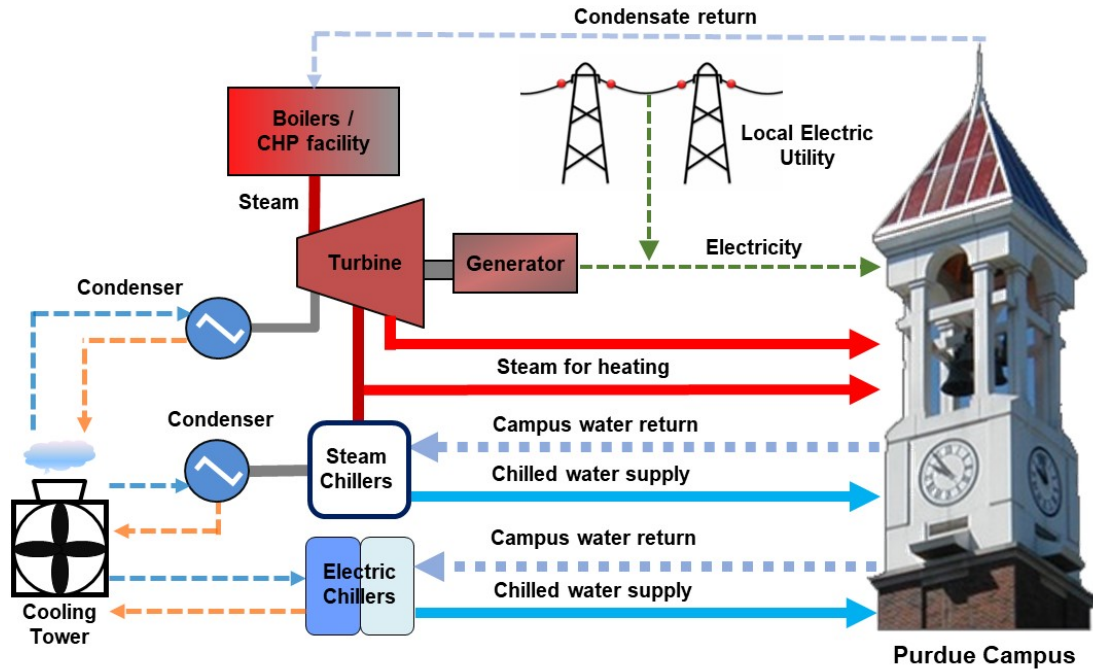
Figure 3.1. Wade power plant operational schematic

3.2   Energy Flow in the CCHP System

The CCHP system contains separate components for heating, cooling, and electricity production. The thermal and electrical demand of the entire Purdue campus is met by the combination of all components in the plant. The CCHP system contains components that are operated using steam, electricity, or both as the input. Table 3.1 lists all the CCHP components both in Wade power plant and Northwest Chiller Plant (NWCP) that are included in the modeling. The description of each component is given in section 3.3.

Table 3.1. CCHP components

Component Name	Nos.	Fuel or Driven by	Location
Boilers	4	Natural Gas / Coal	Wade
CHP facility	1	Natural Gas	Wade
Turbine Generators	2	Steam	Wade
Chillers	13	Steam / Electricity	Wade / NWCP
Cooling tower cells/fans	18	Electricity	Wade / NWCP
Condenser Water Pumps	12	Electricity	Wade / NWCP
Chilled Water Pumps	13	Steam / Electricity	Wade / NWCP
Boiler Feed Water Pumps	7	Steam / Electricity	Wade
Boiler Fans	7	Steam / Electricity	Wade
Pressure reducing valves	2	Steam	Wade
Feedwater Heater	1	Steam	Wade
Deaerator	1	Steam	Wade
Auxiliaries		Steam / Electricity	Wade

The following section describes energy flow in the CCHP system including steam, chilled water, and electricity. Figure 3.2 shows the steam flow across various components in the Wade CCHP system. Superheated steam is generated at 600 psig (4238.2 kPa) by four boilers (three water-tube natural gas boilers - B1, B2, B3 and one circulating fluidized bed coal boiler - B4) and a CHP facility (fired and unfired steam); and sent through a common 600 psig steam line. There are two steam-driven turbine generators (a 30 MW extraction/condensing turbine - TG1 and a 10 MW extraction/backpressure turbine - TG2) that utilize the 600 psig steam to generate electricity. In the extraction/condensing turbine (TG1), some portion of the steam is extracted at 125 psig (963.2 kPa) to meet campus steam demand and to run steam chillers and other auxiliaries while the remaining steam is condensed. In the extraction/backpressure turbine (TG2), one portion of the steam is extracted at 125 psig (963.2 kPa) while the other is exhausted at 15 psig (204.8 kPa). There are four steam-driven feedwater pumps (4-FWPs), three steam-driven chilled water pumps (3-CWPs), a fan of coal boiler B4 (F-B4), and a fan of natural gas boiler B2 (F-B2) which are driven by 600 psig steam and they output steam at 125 psig except for the fan of natural gas boiler B2 (F-B2) that outputs steam at 15 psig. The extracted 125 psig steam is utilized by steam turbines that drive three centrifugal chillers (SC1, SC2, and SC3), fans of a natural gas boiler B1 (F-B1),

and coal boiler B4 (F-B4). The steam from the fans is extracted at 15 psig while the steam from the chiller turbines is condensed. Some portion of the steam is extracted from 125 psig and 15 psig steam lines and sent to Purdue campus through campus 125 psig (125#) and 15 psig (15#) steam tunnel lines respectively to meet the campus heating demand. There are pressure reducing valves in both the 600 psig steam line (PRV1) and the 125 psig steam line (PRV2) that bypass other components and are used to reduce steam pressure to meet the heating requirements when the demand is high. Also, there are some steam auxiliary equipment A1, A2, and A3 that utilize 600 psig, 125 psig, and 15 psig steam respectively, and their output steam is condensed. The condensate from campus and the various plant components is collected in the condensate tank. The makeup water is added to compensate for any losses and some amount of 15 psig steam is mixed in the deaerator (DA) to bring the water to the required feedwater temperature. The water is then fed to the boilers and CHP facility using the seven feedwater pumps to repeat this cycle.
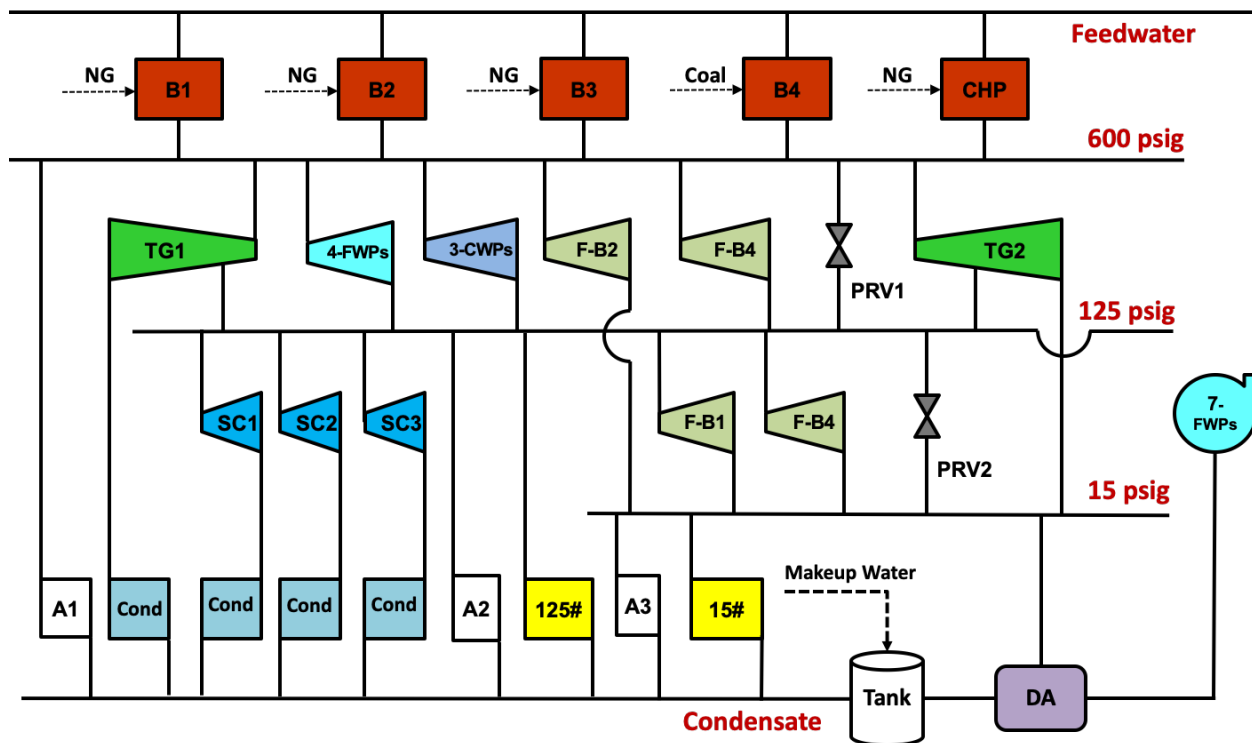
B – Boiler; CHP – CHP facility; NG–Natural Gas; TG – Turbine Generator;
4-FWPs – Four steam-driven Feed Water Pumps; 3-CWPs – Three steam-driven Chilled Water Pumps;
F-B – Steam-driven Fan of the respective boiler; PRV – Pressure Reducing Valve;
SC– Steam Chiller; A – Steam-driven Auxiliaries; Cond – Condenser; DA – Deaerator;
125# – 125 psig campus steam line; 15# – 15 psig campus steam line.

Figure 3.2. Wade power plant steam-driven components and steam flows

Purdue generates the chilled water required for cooling using both electric and steam chillers from two locations on campus: Wade power plant and Northwest Chiller Plant (NWCP). Wade power plant has three steam-driven centrifugal chillers and four electric chillers. NWCP plant has six two-stage electric compressor chillers. Figure 3.3 shows a simplified schematic of the chilled water flow across components in the loop. The chilled water is circulated through 37 km of underground piping using chilled water pumps to air handling unit coils of each building and then is returned to the chiller locations to be chilled again for redistribution using the chilled water loop. In the condenser water loop, chillers reject heat to the water that is circulated through the cooling towers and stored in the cold well. From there, the water is pumped again to the chillers by the condenser water pumps.
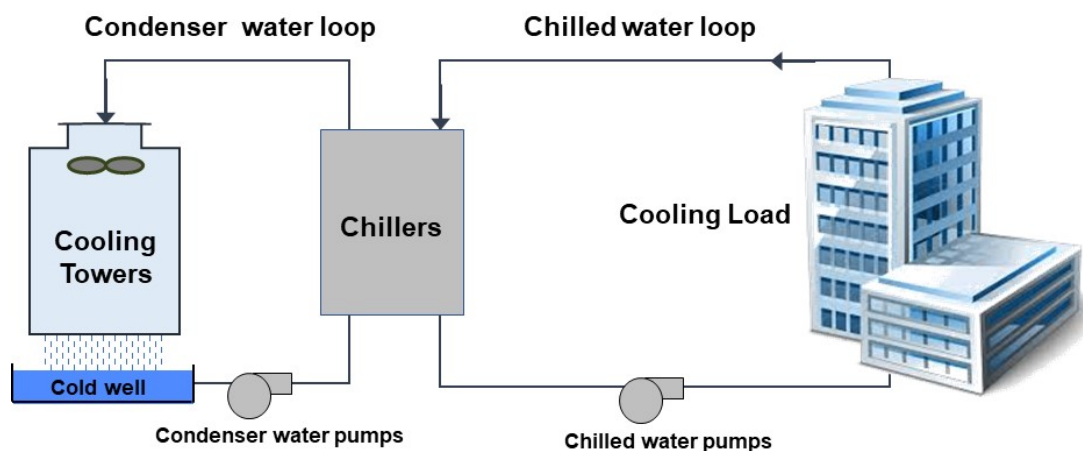
Figure 3.3. Simplified schematic of chilled water flow

The electricity generated using the two turbine generators and the remainder purchased from the local electric utility is used to meet the campus electricity demand and to operate the other components within the power plant, such as the four electric chillers at Wade power plant and six electric chillers at NWCP, boiler feedwater pumps, boiler fans, chilled water pumps, cooling tower fans, condenser water pumps, and other auxiliaries. The operation of pumps, fans, and other auxiliaries depends on the state of the primary equipment being equipped to meet campus energy demands.

3.3   Plant Component Modeling

This section describes the mathematical models of plant equipment including major and auxiliary components used to achieve the production of steam, chilled water, and electricity. Boilers, chillers, and turbine generators are the major components that are used for producing steam, chilled water, and electricity. However, there are other auxiliary components such as pumps (boiler feedwater pumps, chilled water pumps, condenser water pumps, etc.), fans (boiler fans and cooling tower fans), and other equipment that are operated along with the major components to accomplish campus energy demands. Each plant component model has a set of parameters, inputs, and output variables. The models are mostly empirical or semi-empirical and linear or nonlinear with respect to inputs. In this study, the model parameters were mostly determined from plant performance data, but very few from equipment's manufacturer data. The model equations are then interconnected according to their arrangement in the physical plant and incorporated into the optimization framework. The entire model is developed using MATLAB (R2019b). In the following sections, the variables will be represented as x to indicate that they are the decision variables to be optimized. A detailed description of decision variables is explained in Chapter 4.

3.3.1   Boilers

Boilers are an essential part of the CCHP system for steam generation. The Wade plant has four boilers: three water-tube natural gas boilers (B1, B2, and B3) and one circulating fluidized bed coal boiler (B4). Feedwater from the condensate tank and deaerator is pumped into the boilers at 600 psig / 250 °F using feedwater pumps. Boiler #1 (B1) has a feedwater heater that uses 125 psig steam, so its inlet feedwater temperature is approximately 350°F. Superheated steam is generated approximately at 600 psig / 800 °F to primarily serve the turbine generators, few pumps, fans, and sometimes the pressure reducing valves and other auxiliaries. Table 3.2 gives the specifications of each boiler.

Table 3.2. Boiler specifications

Units	Boiler #1 (B1)	Boiler #2 (B2)	Boiler #3 (B3)	Boiler #4 (B4)
Primary Fuel	Natural Gas	Natural Gas	Natural Gas	Coal
Type	Water-tube	Water-tube	Water-tube	Circulating fluidized bed
Rated Capacity, klb/h (kg/s)	215 (27.09)	200 (25.20)	200 (25.20)	200 (25.20)
Operating Range, klb/h (kg/s)	65-195 (8.19-24.57)	30-190 (3.78-23.94)	70-190 (8.82-23.94)	75-195 (9.45-24.57)
Steam pressure, psig (kPa)	600 (4238.21)	600 (4238.21)	600 (4238.21)	600 (4238.21)
Steam temperature, °F (K)	810 (705.37)	750 (672.04)	750 (672.04)	810 (705.37)
Feedwater temperature, °F (K)	350 (449.82)	250 (394.26)	250 (394.26)	250 (394.26)
HHV of fuel	1010 (Btu/ft³)	1010 (Btu/ft³)	1010 (Btu/ft³)	26051 (kJ/kg)

The steam pressure ($P_{s,B}$), steam temperature ($T_{s,B}$) and feedwater temperature ($T_{fw,B}$) are given as input to the boiler model from the plant operational specifications to determine the enthalpy of steam ($h_{s,B}$) and feedwater ($h_{fw,B}$). The mass flow rate of steam through the boiler ($x_{s,B}$) is determined by the campus heating demand and the demand from the equipment that is hooked to. The actual fuel consumption (f) to produce steam is calculated using Eq.3.1 for the natural gas boiler and Eq.3.2 for the coal boiler.

$$f_{NG} = \frac{x_{s,B} * (h_{s,B} - h_{fw,B})}{\eta_B}$$
(3.1)

$$f_C = \frac{x_{s,B} * (h_{s,B} - h_{fw,B})}{\eta_B * HHV}$$
(3.2)

where,

f_{NG} - amount of natural gas consumed [kJ/s]

f_C - amount of coal consumed [kg/s]

$x_{s,B}$ - mass flow rate of steam produced in boilers (decision variable) [kg/s]

HHV - higher heating value of coal [kJ/kg]

η_B - efficiency of boiler [-]

The boiler's nominal thermal efficiency changes due to loading. So, a quadratic efficiency curve solely as a function of boiler load $(x_{s,B})$ is used to accurately represent the performance of the boiler as shown in Eq.3.3.

$$\eta_B = C1 * x_{s,B}^2 + C2 * x_{s,B} + C3 \tag{3.3}$$

The coefficients $(C1, C2, C3)$ of this equation are estimated for each boiler by regression of the boiler's actual performance data and the R-squared values are listed in Table 3.3. Figure 3.4 shows the performance efficiency curve of the boilers as a function of the steam load. It can be observed that the correlation provides a close fit of the performance data and the R-squared values are greater than 95%.

Table 3.3. Coefficients of boiler efficiency curve

Boilers	$C1$	$C2$	$C3$	Data points	R-squared
B1	-0.0531	2.2597	57.158	74	0.9524
B2	-0.1184	4.0242	54.159	62	0.9502
B3	-0.0544	2.0770	64.957	56	0.9524
B4	-0.0994	3.6202	51.379	59	0.9504
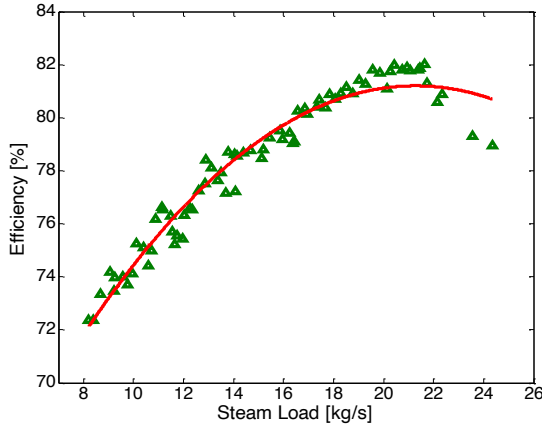
(a) Boiler #1 (B1)
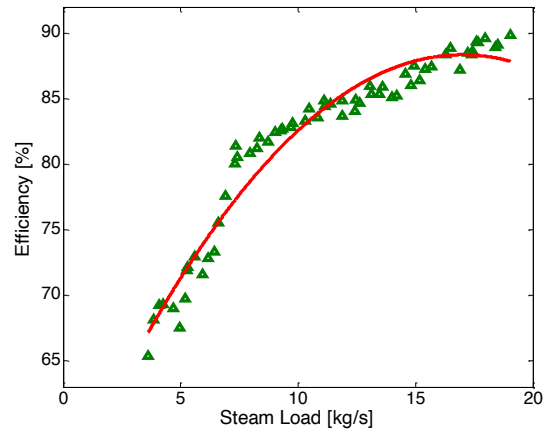
(b) Boiler #2 (B2)
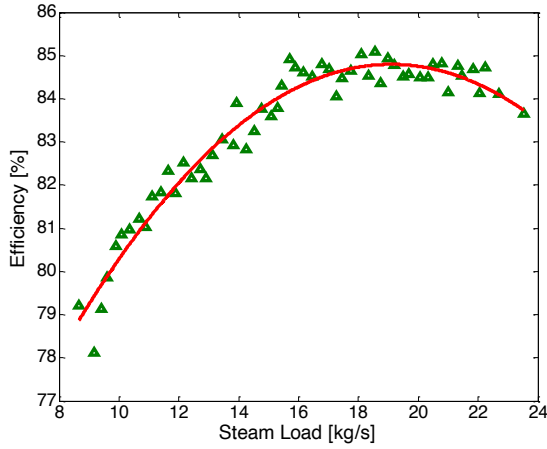
(c) Boiler #3 (B3)
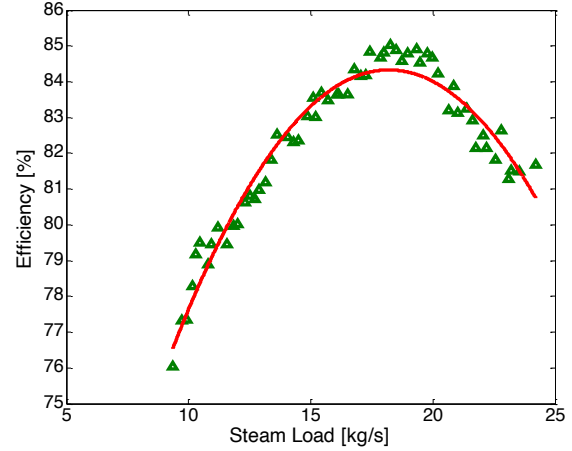
(d) Boiler #4 (B4)

Figure 3.4. Performance curves of the boilers

These quadratic efficiency curves are used only for nonlinear models. However, for linear modeling of the CCHP plant, a constant efficiency is assumed for each of the boilers and given as an input to the boiler model in the place of Eq.3.3. This value depends on the average nominal boiler efficiency between 60% to 80% of the steam load for each boiler based on the boiler's performance data as shown in Figure 3.4. The nominal boiler efficiencies used for the linear modeling of the boilers are listed in Table 3.4.

Table 3.4. Boiler nominal efficiency for linear models

Boilers	$B1$	$B2$	$B3$	$B4$
Efficiency [%]	81	85	84.5	83

The set of mathematical expressions can be grouped and expressed in functional (input-output) form for nonlinear models of natural gas (NG) and coal (C) boiler using Eq.3.4 and Eq.3.5 respectively:

$$[f_{NG}] = NGBoiler(P_{s,B}, T_{s,B}, T_{fw,B}, x_{s,B})_{NG} \tag{3.4}$$

$$[f_C] = CoalBoiler(P_{s,B}, T_{s,B}, T_{fw,B}, x_{s,B}, HHV)_C \tag{3.5}$$

Similarly, Eq.3.6 and Eq.3.7 are used for the linear model of natural gas (NG) and coal (C) boiler respectively, including the boiler efficiency as input:

$$[f_{NG}] = NGBoiler(P_{s,B}, T_{s,B}, T_{fw,B}, x_{s,B}, \eta_B)_{NG} \tag{3.6}$$

$$[f_C] = CoalBoiler(P_{s,B}, T_{s,B}, T_{fw,B}, x_{s,B}, HHV, \eta_B)_C \tag{3.7}$$

3.3.2 CHP Facility

The Combined Heat and Power (CHP) facility includes a combustion turbine to generate electricity and the exhausted waste heat from power generation is reclaimed using a heat recovery steam generator (HRSG) to produce additional steam. The combustion turbine-based CHP system generates approximately 15.5 MW of power and is sent directly to the utility grid. This electricity is not used by the Wade plant. Only the steam generated using HRSG is used by the Wade plant. The CHP system delivers 150,000 lb/h (18.9 kg/s) steam at 600 psig / 775 °F which is combined with the steam from other boilers and sent through a common 600 psig steam line to serve the steam turbine generators and other auxiliaries. Feedwater from the condensate tank is pumped into the heat recovery steam generator (HRSG) at 600 psig / 250 °F using feedwater pumps. The exhaust gas from the combustion turbine is directly used to produce unfired steam while an additional duct burner is used to produce fired steam. The CHP facility will supply 49,000 lb/h

(6.17 kg/s) unfired steam throughout the year and an optional 101,000 lb/h (12.73 kg/s) fired steam depending on the steam demand.

Enthalpy of unfired steam ($h_{s,UF}$) is determined from the outlet steam pressure ($P_{s,UF}$) and steam temperature ($T_{s,UF}$). The natural gas fuel consumed by the CHP facility ($f_{NG,UF}$) to produce 49,000 lb/h unfired steam ($x_{s,UF}$) using the exhaust gas from combustion turbine includes a multiplier (k) and is calculated as follows:

$$f_{NG,UF} = k * x_{s,UF} \tag{3.8}$$

The duct burner is used to produce optional fired steam through HRSG depending on the steam demand. The steam pressure ($P_{s,F}$), steam temperature ($T_{s,F}$) and feedwater temperature ($T_{fw,F}$) are given as input to the HRSG model from the plant operational specifications to determine the enthalpy of fired steam ($h_{s,F}$) and feedwater ($h_{fw,F}$). The mass flow rate of fired steam through the HRSG ($x_{s,F}$) is determined by the campus heating demand and the demand from the equipment that is hooked to 600 psig steam line. The actual fuel consumption ($f_{NG,F}$) to produce fired steam is calculated as:

$$f_{NG,F} = \frac{x_{s,F} * (h_{s,F} - h_{fw,F})}{\eta_{DB}} \tag{3.9}$$

where,

$f_{NG,F}$ - amount of natural gas consumed [kJ/s]

$x_{s,F}$ - amount of fired steam produced through HRSG (decision variable) [kg/s]

η_{DB} - efficiency of duct burner [91% - from manufacturer's data]

The set of mathematical expressions can be grouped and expressed in functional (input-output) form for both linear and nonlinear model of unfired (UF) and fired (F) steam from the CHP facility as:

$$[f_{NG,UF}] = Unfired(P_{s,UF}, T_{s,UF}, k, x_{s,UF})_{UF} \tag{3.10}$$

$$[f_{NG,F}] = Fired(P_{s,F}, T_{s,F}, T_{fw,F}, x_{s,F}, \eta_{DB})_F \tag{3.11}$$

The CHP facility is currently under construction and it is not employed in the plant operation. It will be used along with the boilers for steam generation in the future. The CHP facility is incorporated in the plant model, but the values were set to zero during optimization. The options can be turned on when under operation.

3.3.3 Turbine Generators

There are two steam-driven turbine generators (TG): TG1 is a 30 MW extraction/condensing turbine and TG2 is a 10 MW extraction/backpressure turbine. Both the turbines use 600 psig steam from boilers and the CHP facility to generate electricity. In the extraction/condensing turbine (TG1), some portion of the steam is extracted at 125 psig while the remaining steam is condensed at vacuum pressure. In the extraction/backpressure turbine (TG2), one portion of the steam is extracted at 125 psig while the rest is exhausted at 15 psig. The extracted steam at 125 psig and 15 psig are used for campus heating and other in-plant auxiliaries. Table 3.5 gives the specifications of each turbine generator.

Table 3.5. Steam turbine generator specifications

Turbine Generator Units	Turbine Generator #1 (TG1)	Turbine Generator #2 (TG2)
Type of turbine	Extraction/condensing	Extraction/backpressure
Rated output (MW)	30	10
Rated speed (RPM)	3600	3600
Inlet steam pressure, psig (kPa)	600 (4238.21)	600 (4238.21)
Inlet steam temperature, $^{\circ}$F (K)	810 (705.37)	825 (713.71)
Inlet steam flow, klb/h (kg/s)	250 (31.5)	265 (33.4)
1st Extraction steam pressure, psig (kPa)	125 (963.2)	125 (963.2)
1st Extraction steam flow, klb/h (kg/s)	200 (25.2)	250 (31.5)
2nd Extraction/Exhaust steam pressure, psig (kPa)	-13.5 (8.48)	15 (204.77)
2nd Extraction/Exhaust steam flow, klb/h (kg/s)	250 (31.5)	40 (5.04)
Condenser water flow, gpm (lt/s)	24,660 (1555.8)	-
Condenser water entering temp., $^{\circ}$F (K)	85 (302.59)	-
Condenser water leaving temp., $^{\circ}$F (K)	105 (313.71)	-

The 600 psig steam from all the four boilers and CHP facility is collected and mixed in the 600 psig steam line and is sent to the turbine generators and other components connected to the 600 psig steam line. The 600 psig inlet steam pressure (P_{600}) and temperature (T_{600}), 1st level 125 psig extraction pressure $(P_{ex1,TG})$ and exhaust or 2nd level extraction pressure $(P_{ex2,TG})$ are inputs to the turbine generator model from the plant operational specifications. The mass flow rate of steam across each stage of the turbine generator level 125 psig extraction pressure $(P_{ex1,TG})$ and exhaust or 2nd level extraction pressure $(x_{s,TG})$ is determined by the campus heating demand, campus electricity demand and the steam demand from the equipment that it is connected to. Figure 3.5 represents the flow of steam across two stages of turbine generator 1 (TG1) and 2 (TG2), respectively.
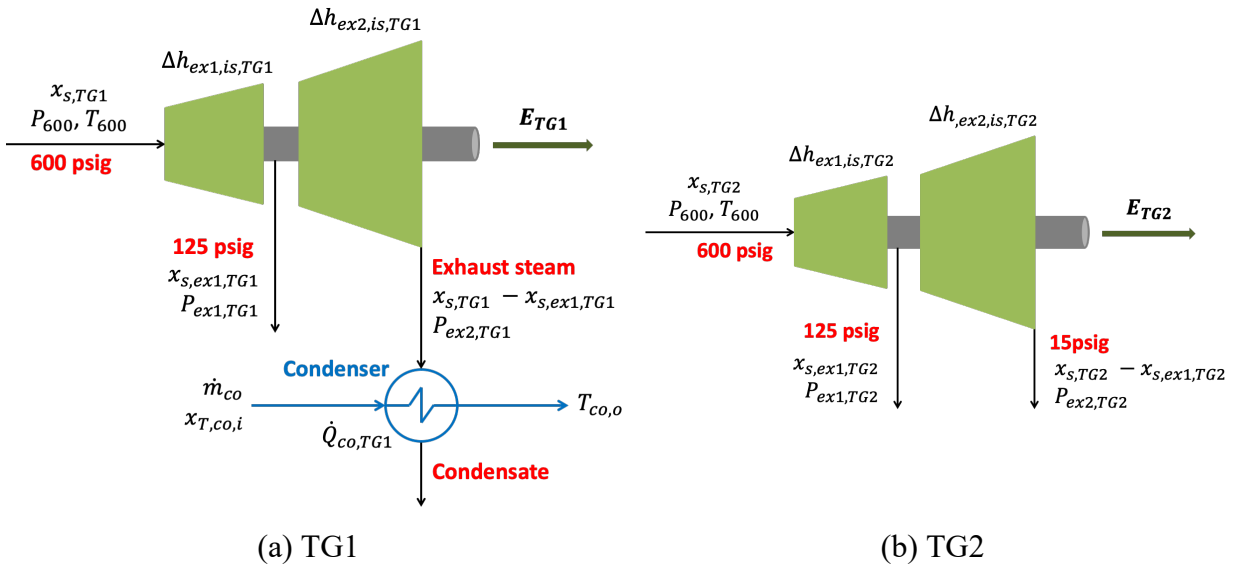
Figure 3.5. Operation and steam flow across stages of turbine generators

The amount of electricity generated for each turbine generator $(E_{TG} \ [kW])$ is given by equations (3.12) and (3.13):

$$E_{TG1} = \eta_{TG1}[x_{s,TG1} * \Delta h_{ex1,is,TG1} + (x_{s,TG1} - x_{s,ex1,TG1}) * \Delta h_{ex2,is,TG1}] \qquad (3.12)$$

$$E_{TG2} = \eta_{TG2}[x_{s,TG2} * \Delta h_{ex1,is,TG2} + (x_{s,TG2} - x_{s,ex1,TG2}) * \Delta h_{ex2,is,TG2}] \qquad (3.13)$$

where,

$x_{s,TG}$ – Input throttle steam to the turbine generator (decision variable) [kg/s]

$x_{s,ex1,TG}$ – Amount of steam extracted after the 1st stage (decision variable) [kg/s]

$\Delta h_{ex,is,TG}$ – Isentropic expansion work of turbine generator across each stage (1st or 2nd) [kJ/kg]

η_{TG} – Isentropic turbine generator efficiency [-]

The turbine generator efficiency (η_{TG}) changes due to loading and the amount of steam extracted across each stage. So, a quadratic efficiency curve solely as a function of inlet throttle steam ($x_{s,TG}$) and 1st level extraction steam ($x_{s,ex1,TG}$) is used to represent the performance of turbine generator.

$$\eta_{TG} = C1 + C2 * x_{s,TG} + C3 * x_{s,ex1,TG} + C4 * x_{s,TG}^2 + C5 * x_{s,TG} * x_{s,ex1,TG} + C6 * x_{s,ex1,TG}^2 \quad (3.14)$$

The coefficients ($C1,..,C6$) of this equation are estimated for each turbine generator by regression of its actual performance data and the R-squared values are listed in Table 3.6. Figure 3.6 shows the isentropic efficiency curve of the turbine generators (TG1 and TG2) as a function of 600 psig inlet steam load and the amount of 125 psig steam extracted. The curves represent correlation fit and the points represent performance data. It can be observed that the correlation provides a close fit of the performance data. Also, it can be noted that the efficiency of TG2 is significantly lower than that of TG1. This could affect the amount of electricity and steam produced from the turbine generators to meet demand during optimization.

Table 3.6. Coefficients of turbine generator efficiency curve

Turbine Generator	$C1$	$C2$	$C3$	$C4$	$C5$	$C6$	Data points	R-squared
TG1	0.1711	0.04142	-0.02838	-0.0007353	0.001026	-0.0004814	62	0.9707
TG2	-0.06704	0.0656	-0.02615	-0.001153	0.0004277	0.0001787	69	0.9573
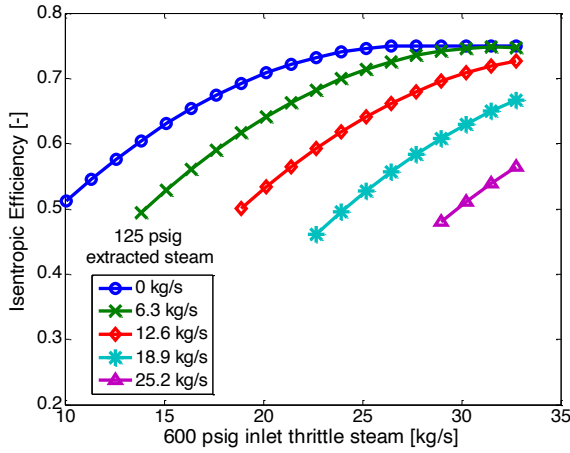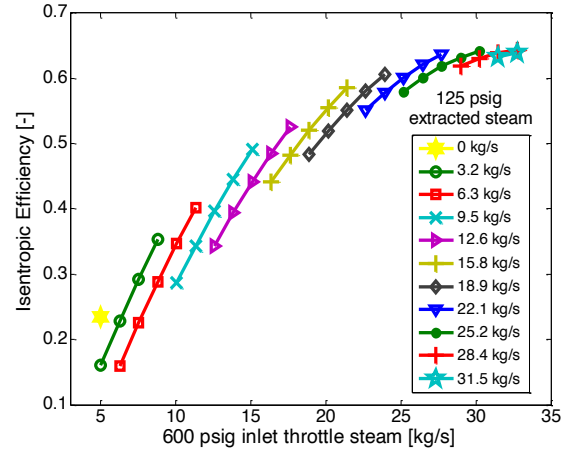
|(a) TG1|(b) TG2|

Figure 3.6. Isentropic efficiency curve of the turbine generators

The isentropic efficiency curves of the turbine generators are used for nonlinear models. For linear modeling of the CCHP plant, a constant isentropic efficiency is assumed for each turbine generator and given as an input to the turbine generator model in the place of Eq.3.14. The isentropic efficiency assumed for the linear modeling of the TG1 is 65% and for the TG2 is 55%. These values depend on the average isentropic efficiency between 60% to 80% of the input throttle steam load for each turbine generator based on its performance data.

In the extraction/condensing turbine (TG1), the steam exhausted at vacuum pressure is condensed to saturated liquid in the condenser using water from the cooling tower. The condenser heat rejection ($\dot{Q}_{co,TG1}$) is related to the heat transfer in the condensing exhaust steam ($\dot{Q}_{ex2,TG1}$) and energy balances on the steam side and cooling water side are given by Eqs. 3.15-3.17.

$$\dot{Q}_{co,TG1} = \dot{Q}_{ex2,TG1} \tag{3.15}$$

$$\dot{Q}_{ex2,TG1} = \left(x_{s,TG1} - x_{s,ex1,TG1}\right) * \Delta h_{ex2,co,TG1} \tag{3.16}$$

$$\dot{Q}_{co,TG1} = \dot{m}_{co}C_{p,co}(T_{co,o} - x_{T,co,i}) \tag{3.17}$$

The steam flow $\left(x_{s,TG1} - x_{s,ex1,TG1}\right)$, pressure ($P_{ex2,TG1}$) and calculated temperature ($T_{ex2,TG1}$) from the exhaust of the turbine, and condenser water inlet temperature ($x_{T,co,i}$) are given as inputs

66

to the condenser model. The condenser water flow ($\dot{m}_{co}$) is calculated as a function of condenser heat rejection ($\dot{Q}_{co,TG1}$) from the plant operational data. From these inputs, condenser water leaving temperature ($T_{co,o}$) is determined. The set of mathematical expressions can be grouped and expressed in functional (input-output) form for the nonlinear model of each turbine generator as:

$$[E_{TG1}, \dot{m}_{co}, T_{co,o}]_{TG1} = TG1\big(x_{s,TG1}, x_{s,ex1,TG1}, P_{600}, x_{T,600}, P_{ex1,TG1}, P_{ex2,TG1}, x_{T,co,i}\big)_{TG1} \qquad (3.18)$$

$$[E_{TG2}] = TG2\big(x_{s,TG2}, x_{s,ex1,TG2}, P_{600}, x_{T,600}, P_{ex1,TG2}, P_{ex2,TG2}\big)_{TG2} \qquad (3.19)$$

and for the linear model as:

$$[E_{TG1}, \dot{m}_{co}, T_{co,o}]_{TG1} = TG1\big(x_{s,TG1}, x_{s,ex1,TG1}, P_{600}, T_{600}, P_{ex1,TG1}, P_{ex2,TG1}, x_{T,co,i}, \eta_{TG1}\big)_{TG1} \qquad (3.20)$$

$$[E_{TG2}] = TG2\big(x_{s,TG2}, x_{s,ex1,TG2}, P_{600}, T_{600}, P_{ex1,TG2}, P_{ex2,TG2}, \eta_{TG2}\big)_{TG2} \qquad (3.21)$$

Generally, 30%-60% of Purdue's electricity is produced from turbine generators while the rest of the electricity is purchased from the local electric utility, which includes a real-time pricing (RTP) component. The plant also has a diesel generator with a capacity of 1.8 MW that is used only for emergency purposes. The electricity generated from the CHP facility is sent directly to the grid and not used by the Wade plant to meet any electrical demand.

3.3.4   Chillers

The cooling demand of the Purdue campus is satisfied by steam and electric chillers at the Wade power plant and electric chillers at the Northwest Chiller Plant (NWCP). The Wade power plant has three steam-driven centrifugal chillers and four electric chillers. The NWCP plant provides additional cooling especially during summer with six dual compressor electric chillers. Both the plants deliver chilled water through 37 km of underground piping to meet the cooling requirements of more than 150 buildings on the campus (an average of 92.4 MMTon-hr per year). The chilled water supply temperature set-point is correlated with ambient dry-bulb temperature and varied between 40°F in the winter and 43°F in summer. Generally, a temperature differential of 15°F delta T is assumed between the chilled water supply temperature and return temperature from campus.

Electric Chillers

The Wade power plant has four and NWCP has six dual compressor electric chillers whose specifications are listed in Table 3.7. A simplified schematic of the chiller is shown in Figure 3.7.

Table 3.7. Dual centrifugal electric chillers specification at rated conditions

Electric Chillers (E-C)	Wade Chillers: 1&2 NWCP Chillers: 1, 2 & 3	Wade Chillers 3&4	NWCP Chillers 4 & 5	NWCP Chiller 6
Nominal capacity, Ton (kW)	2000 (7034)	3800 (13364)	2700 (9496)	2700 (9496)
Evaporator flow, gpm (lt/s)	3185 (201)	4150 (262)	4298 (271)	4320 (272.5)
Evaporator entering temp., °F (°C)	55 (12.78)	60.25 (15.69)	55 (12.78)	54.93 (12.74)
Evaporator leaving temp., °F (°C)	40 (4.44)	38 (3.33)	40 (4.44)	40 (4.44)
Condenser flow, gpm (lt/s)	6000 (379)	9300 (587)	7652 (483)	8101 (511)
Condenser entering temp., °F (°C)	85 (29.44)	85 (29.44)	85 (29.44)	85 (29.44)
Condenser leaving temp., °F (°C)	94.47 (34.71)	96.7 (35.94)	95 (35.00)	94.41 (34.67)
Nominal power, kW	1205	2434	1633	1540
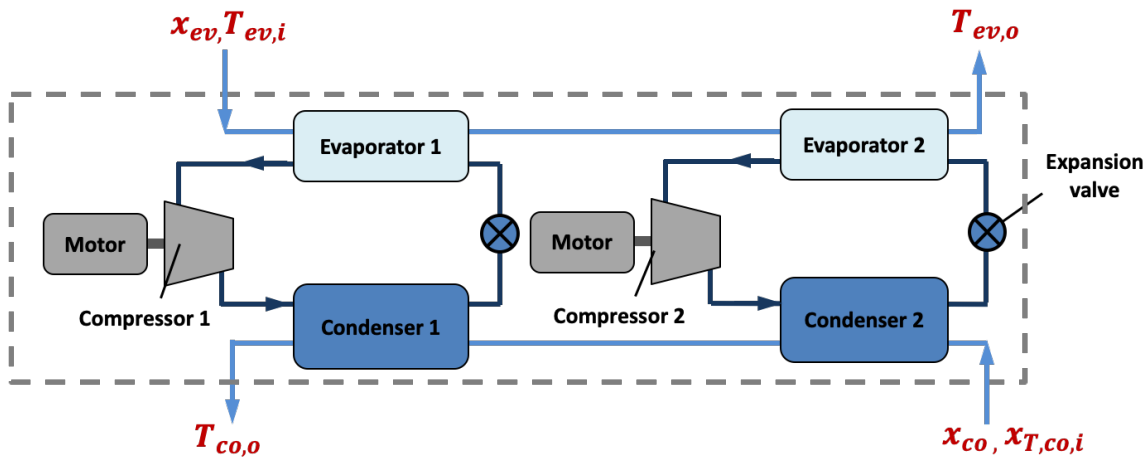
Figure 3.7. Schematic of a dual compressor chiller

Both the electricity generated from the power plant and the purchased electricity are used to run these chillers. The power consumption of an electric chiller can be represented as a quadratic function of the load and the lift (Braun, 1987):

$$Z = a_0 + a_1X + a_2X^2 + a_3Y + a_4Y^2 + a_5XY \qquad (3.22)$$

where Z is the ratio of actual power consumption (P) to the power consumed at design conditions (P_{des}):

$$Z = \frac{P}{P_{des}} \qquad (3.23)$$

X is the part load ratio, which is the actual cooling effect produced by the chiller $(\dot{Q}_{ev})$ divided by the cooling effect at design conditions $(\dot{Q}_{ev,des})$:

$$X = \frac{\dot{Q}_{ev}}{\dot{Q}_{ev,des}} \qquad (3.24)$$

Y is a dimensionless lift where lift is defined as the difference between the condenser water leaving temperature $(T_{co,o})$ and evaporator water leaving temperature $(T_{ev,o})$, such that,

$$Y = \frac{T_{co,o} - T_{ev,o}}{\left(T_{co,o} - T_{ev,o}\right)_{des}} \qquad (3.25)$$

The coefficients of Eq.3.22 are estimated for each type of chiller by regression of its performance data. Figure 3.8 shows a comparison between the power ratio obtained from performance data and the power ratio calculated with the correlation for the three types of electric chillers. It can be observed that the correlation provides a close fit of the performance data. The root mean square error for all cases was less than 0.005.
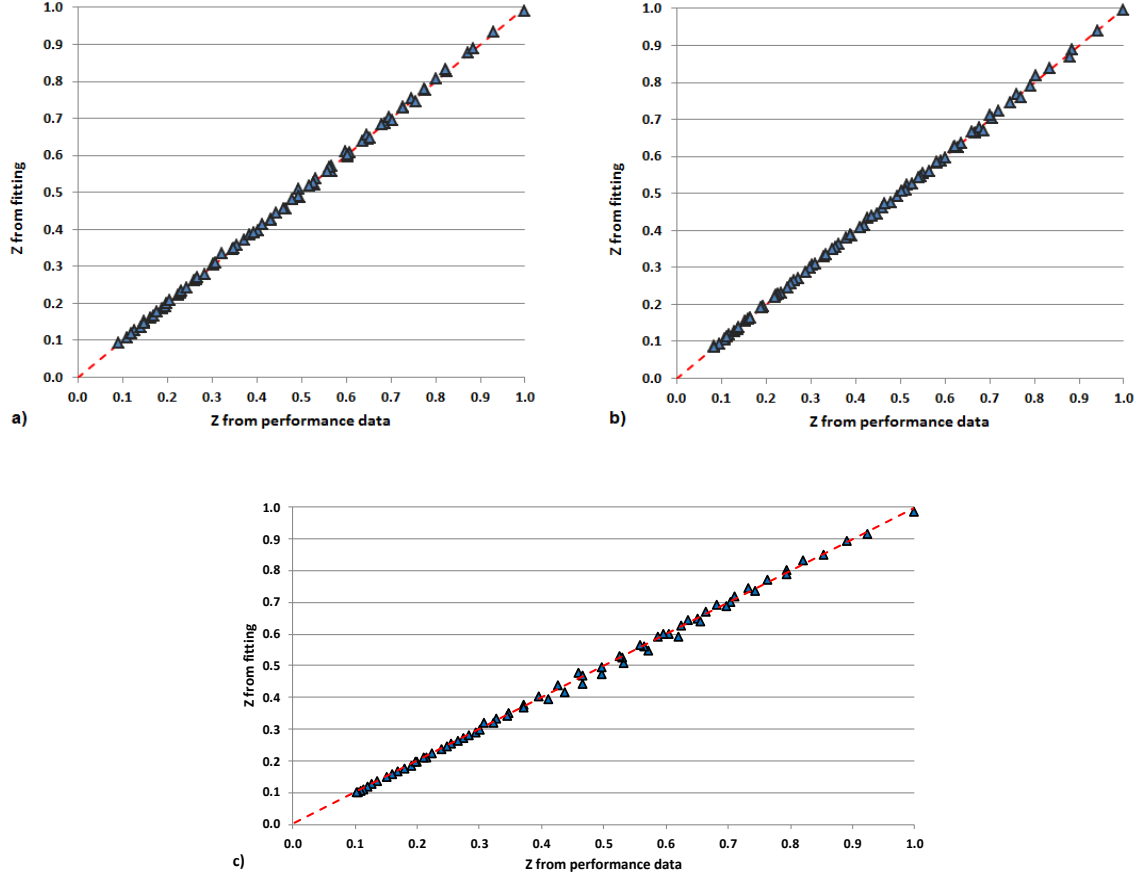
Figure 3.8. Power ratio (Z) from fitting vs performance data for a) 2000 Ton Chillers b) 2700 Ton Chillers and c) 3800 Ton Chillers

The condenser heat rejection ($\dot{Q}_{co}$) is related to the chiller load ($\dot{Q}_{ev}$) and the power consumed by the compressor (P) by Eq.3.26, where η_m is the compressor's motor efficiency. The energy balances on the chiller evaporator side and the condenser side results in Eq.3.27 and Eq.3.28, respectively.

$$\dot{Q}_{co} = \dot{Q}_{ev} + \eta_m P \tag{3.26}$$

$$\dot{Q}_{ev} = x_{ev} C_{p,ev} (T_{ev,i} - T_{ev,o}) \tag{3.27}$$

$$\dot{Q}_{co} = x_{co} C_{p,co} (T_{co,o} - x_{T,co,i}) \tag{3.28}$$

The evaporator water inlet temperature ($T_{ev,i}$) and leaving temperature ($T_{ev,o}$), condenser water inlet temperature ($x_{T,co,i}$) and condenser water flow (x_{co}) are given as inputs to the chiller model. The evaporator water flow (x_{ev}) of each chiller is dependent on the campus cooling

70

demand. From these inputs, the chiller power consumption (P), evaporator load $(\dot{Q}_{ev})$ and condenser water leaving temperature $(T_{co,o})$ are solved. The set of mathematical expressions can be grouped and expressed in functional (input-output) form for the nonlinear model of each electric chiller $(E\text{-}C)$ in the Wade plant (W) and Northwest chiller plant (NW) as Eq.3.29 and Eq.3.30 respectively.

$$\left[\dot{Q}_{ev}, P, T_{co,o}\right]_{E\text{-}C,W} = ElectricChiller, W\left(x_{ev}, T_{ev,i}, T_{ev,o}, x_{co}, x_{T,co,i}, \eta_m\right)_{E\text{-}C,W} \qquad (3.29)$$

$$\left[\dot{Q}_{ev}, P, T_{co,o}\right]_{E\text{-}C,NW} = ElectricChiller, NW\left(x_{ev}, T_{ev,i}, T_{ev,o}, x_{co}, x_{T,co,i}, \eta_m\right)_{E\text{-}C,NW} \qquad (3.30)$$

For the linear model of chillers, a constant coefficient of performance (COP) is assumed for each electric chiller depending on its performance data and the values are shown in Table 3.8. The chiller load $(\dot{Q}_{ev})$ is calculated using Eq.3.27 and the power consumed by the compressor (P) using Eq.3.31.

$$P = \frac{\dot{Q}_{ev}}{COP} \qquad (3.31)$$

The condenser water flow (x_{co}) is not considered as a decision variable for the linear model, but it $(\dot{m}_{co})$ is represented as a linear function of the evaporator water flow (x_{ev}) or chiller load $(\dot{Q}_{ev})$ from the performance data of chillers.

Table 3.8. COP values of electric chillers

Chillers	Wade Chillers: 1&2 NWCP Chillers: 1, 2 & 3	Wade Chillers 3&4	NWCP Chillers 4 & 5	NWCP Chiller 6
COP	5.84	5.5	5.82	6.17

The functional (input-output) form for the linear models for each electric chiller in the Wade plant (W) and Northwest chiller plant (NW) are represented as:

$$\left[\dot{Q}_{ev}, P, \dot{m}_{co}, T_{co,o}\right]_{E\text{-}C,W} = ElectricChiller, W\left(x_{ev}, T_{ev,i}, T_{ev,o}, COP, x_{T,co,i}, \eta_m\right)_{E\text{-}C,W} \qquad (3.32)$$

$$\left[\dot{Q}_{ev}, P, \dot{m}_{co}, T_{co,o}\right]_{E\text{-}C,NW} = ElectricChiller, NW\left(x_{ev}, T_{ev,i}, T_{ev,o}, COP, x_{T,co,i}, \eta_m\right)_{E\text{-}C,NW} \qquad (3.33)$$

Steam Chillers

The Wade power plant has three steam turbine centrifugal chillers (S-C1, S-C2, and S-C3). These chillers utilize the 125 psig steam extracted from the 125 psig steam line to run the turbines of the centrifugal chillers and the exhaust steam is condensed. The specifications of the steam chillers are listed in Table 3.9 and a simplified schematic of the steam chiller is shown in Figure 3.9.

Table 3.9. Steam turbine centrifugal chillers specification at rated conditions

Steam Chillers	Chiller #1 S-C1	Chiller #2 S-C2	Chiller #3 S-C3
Nominal capacity, Ton (kW)	3000 (10550)	4500 (15826)	5000 (17584)
Evaporator flow, gpm (lt/s)	4800 (303)	7191 (454)	8000 (505)
Evaporator entering temp., °F (°C)	55 (12.8)	55 (12.8)	55 (12.8)
Evaporator leaving temp., °F (°C)	40 (4.4)	40 (4.4)	40 (4.4)
Condenser flow, gpm (lt/s)	9000 (568)	13500 (852)	15000 (947)
Condenser entering temp., °F (°C)	85 (29.4)	85 (29.4)	85 (29.4)
Condenser leaving temp., °F (°C)	94.4 (34.7)	94.4 (34.7)	94.4 (34.7)
Compressor power, bhp (kW)	2513 (1874)	3531 (2633)	3928 (2929)
Compressor speed (RPM)	5215	5799	3585
Turbine steam inlet pressure, psig (kPa)	125 (962.2)	125 (962.2)	125 (962.2)
Turbine steam inlet temperature, °F (K)	550 (561)	550 (561)	550 (561)
Turbine steam flow, lb/h (kg/s)	25280 (3.19)	36687 (4.62)	40262 (5.07)
Exhaust steam pressure, psia (kPa)	1.47 (10.14)	1.47 (10.14)	1.47 (10.14)
Inline Condenser entering temp., °F (°C)	95 (35.0)	95 (35.0)	95 (35.0)
Condenser leaving temp., °F (°C)	100.5 (38.1)	100.5 (38.1)	100.5 (38.1)
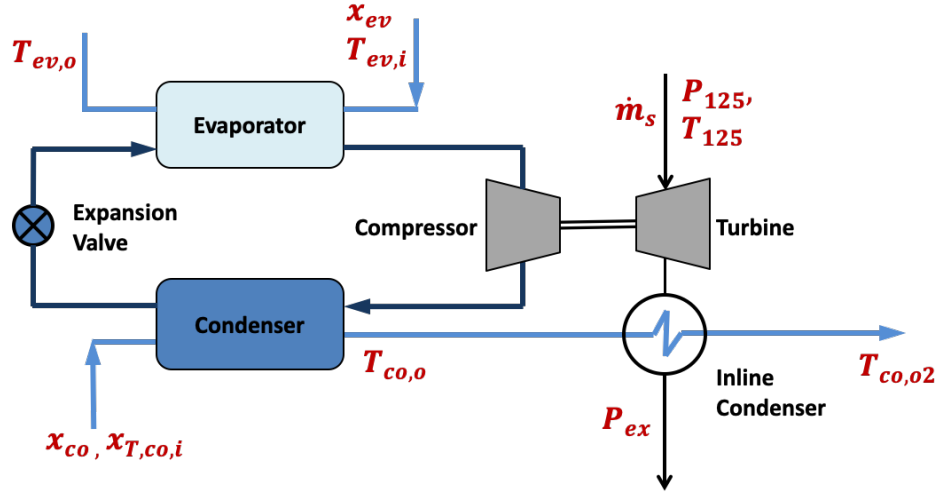
Figure 3.9. Schematic of a steam turbine centrifugal chiller

For the nonlinear model of steam chillers, the condenser heat rejection ($\dot{Q}_{co,S-C}$), the steam chiller load ($\dot{Q}_{ev,S-C}$) and the power consumed by the compressor (P_{S-C}) are calculated in a similar way as the electric chillers and given by Eqs.3.26-3.28. The power consumption of each chiller is represented as a quadratic function of the load and the lift as in Eq.3.22. The coefficients of the equation are estimated for each steam chiller by regression of its performance data and listed in Table 3.10.

Table 3.10. Coefficients of power ratio curve for steam chillers

Steam Chillers	a_0	a_1	a_2	a_3	a_4	a_5	Data points	RMSE
$S-C1$	0.008208	0.7529	-0.3355	-0.294	0.5841	0.2528	28	0.0131
$S-C2$	0.1089	0.08671	-0.208	-0.03662	0.7803	0.267	40	0.0122
$S-C3$	-0.09849	-0.3048	0.5367	0.8988	-0.4401	0.4223	21	0.0133

Figure 3.10 shows a comparison between the power ratio obtained from performance data and the power ratio calculated with the correlation for the three steam chillers. It can be observed that the correlation provides a close fit of the performance data.

73
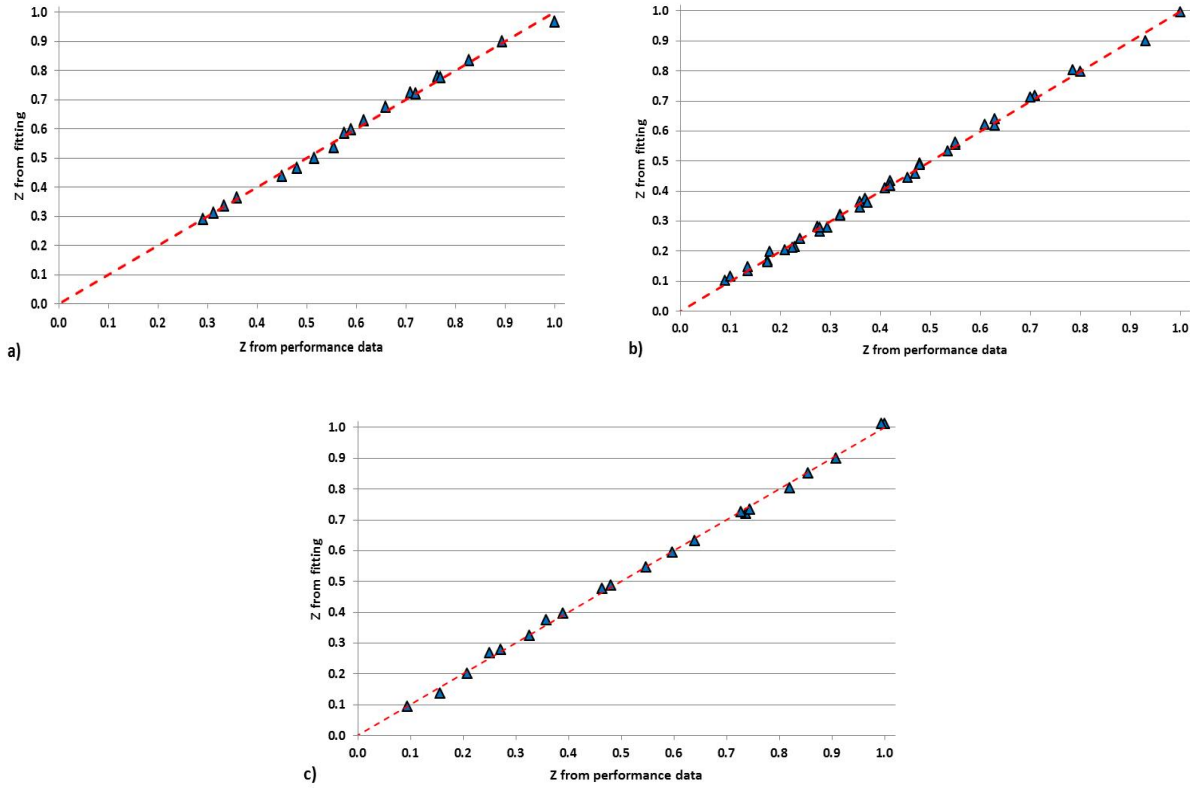
Figure 3.10. Power ratio (Z) from fitting vs performance data for steam chillers a) S-C1 b) S-C2 and c) S-C3

The power generated by the steam turbine utilizing the 125 psig steam is given as input power to the compressor of each steam chiller and is given by Eq.3.34:

$$P_{S-C} = \eta_{t,S-C} * \dot{m}_{s,S-C} * \Delta h_{is,S-C} \tag{3.34}$$

where,

$\dot{m}_{s,S-C}$ – Input steam to steam turbine of chillers [kg/s]

$\Delta h_{is,S-C}$ – Isentropic expansion work of turbine generator [kJ/kg]

$\eta_{t,S-C}$ – Isentropic turbine generator efficiency of steam chillers [-]

The isentropic efficiency of the turbine changes due to steam load in the turbine and a quadratic efficiency curve in terms of inlet steam ($\dot{m}_{s,S-C}$) is used to represent the performance of the turbine.

$$\eta_{t,S-C} = b1 * \dot{m}_{s,S-C}^2 + b2 * \dot{m}_{s,S-C} + b3 \tag{3.35}$$

The coefficients $(b1, b2, b3)$ of this equation are estimated for each turbine by regression of its actual performance data and R-squared values are listed in Table 3.11.

Table 3.11. Coefficients of turbine efficiency curve

Steam Chillers	$b1$	$b2$	$b3$	Data points	R-squared
$S - C1$	-0.1071	0.5785	0.0015	4	0.9981
$S - C2$	-0.0732	0.4971	0.0002	4	0.9981
$S - C3$	-0.0370	0.3340	0.0013	4	0.9992

The 125 psig inlet steam pressure (P_{125}) and calculated temperature (T_{125}), and exhaust pressure $(P_{ex,S-C})$ are given as inputs to the turbine model to determine the isentropic expansion work of turbine $(\Delta h_{is,S-C})$ and the inlet steam to the turbine $(\dot{m}_{s,S-C})$ is calculated from the power consumed by chiller compressor (P_{S-C}) as shown in Eq.3.34. The steam is exhausted from the turbine at vacuum pressure and is condensed to saturated liquid in the inline condenser using the water coming out of chiller condenser. The inline condenser heat rejection $(\dot{Q}_{co2,S-C})$ is related to the heat transfer in the condensing exhaust steam $(\dot{Q}_{ex,S-C})$ and the energy balances on steam side and cooling water side are calculated as described for the extraction/condensing turbine (TG1) and given by Eqs.3.15-3.17. The steam flow $(\dot{m}_{s,S-C})$, pressure $(P_{ex,S-C})$ and temperature $(T_{ex,S-C})$ from the exhaust of the turbine, and chiller condenser water leaving temperature $(T_{co,o,S-C})$ and condenser water flow $(x_{co,S-C})$ are given as inputs to the inline condenser model. From these inputs, condenser water leaving temperature $(T_{co,o2,S-C})$ from the inline condenser is determined. The functional (input-output) form for the nonlinear model of the steam chiller $(S-C)$ is represented as:

$$\left[\dot{Q}_{ev}, \dot{m}_s, T_{co,o2} \right]_{S-C} = SteamChiller(x_{ev}, T_{ev,i}, T_{ev,o}, x_{co}, x_{T,co,i}, P_{125}, T_{125}, P_{ex})_{S-C} \tag{3.36}$$

For the linear model of steam chillers, a constant coefficient of performance (COP) is assumed for each steam chiller depending on its performance data and the values are shown in Table 3.12. The steam chiller load ($\dot{Q}_{ev,S-C}$) and the power consumed by the chiller compressor (P_{S-C}) are calculated in the similar way as the linear model of electric chillers as given by Eq.3.27 and Eq.3.31 respectively. Similarly, the condenser water flow ($x_{co,S-C}$) is not considered as a decision variable for the linear model, but it ($\dot{m}_{co,S-C}$) is represented as a linear function of the evaporator water flow ($x_{ev,S-C}$) or chiller load ($\dot{Q}_{ev,S-C}$) based on the performance data of chillers. To determine the mass flow rate of inlet steam to the turbine ($\dot{m}_{s,S-C}$), a constant isentropic efficiency is assumed for the turbines of each steam chiller in the place of Eq.3.35 and the values are listed in Table 3.12.

Table 3.12. COP and isentropic efficiency values of steam chillers

Steam Chillers	Chiller #1 (S-C1)	Chiller #2 (S-C2)	Chiller #3 (S-C3)
COP [-]	5.63	6.01	6.00
$\eta_{t,S-C}$ [%]	75.0	72.0	73.0

For the linear model of the steam chiller ($S-C$), the functional (input-output) form is:

$$\left[\dot{Q}_{ev}, \dot{m}_{co}, \dot{m}_s, T_{co,o2}\right]_{S-C} = SteamChiller(x_{ev}, T_{ev,i}, T_{ev,o}, COP, x_{T,co,i}, P_{125}, T_{125}, P_{ex}, \eta_t)_{S-C} \quad (3.37)$$

3.3.5 Cooling Towers

There are five induced draft design, evaporative cooling towers installed which include one counter-flow concrete tower at Wade plant and one at Northwest Chiller Plant (NWCP); and three metal cross-flow towers at NWCP. The characteristics of both types of towers are shown in Table 3.13. A schematic of a cooling tower cell is shown in Figure 3.11. The Wade cooling tower has six cells while the NWCP cooling tower has three cells per tower each giving a total of 12 tower cells for one counter-flow concrete tower and three metal cross-flow towers. Each tower cell is operated using 2-speed and variable speed fans.

Table 3.13. Cooling towers specifications at rated conditions

Description	Wade Counter-Flow Concrete Tower	NWCP Counter-Flow Concrete Tower	NWCP Cross-Flow Metal Tower
Installed units	1	1	3
Number of cells per tower	6	3	3
Water flow per cell, gpm (lt/s)	15000 (947)	6000 (379)	2567 (162)
Hot water temperature, °F (°C)	101 (38.33)	95 (35.00)	95 (35.00)
Cold water temperature, °F (°C)	85 (29.44)	85 (29.44)	85 (29.44)
Wet bulb temperature, °F (°C)	76.8 (24.89)	78.2 (25.67)	79 (26.11)
Air flow per cell, cfm (m3/s)	1,302,231 (615)	478,740 (225.94)	250,100 (118.03)
Nominal fan power per cell, HP (kW)	200 (149)	75 (55.93)	60 (44.74)

Figure 3.11. Schematic of an evaporative cooling tower cell
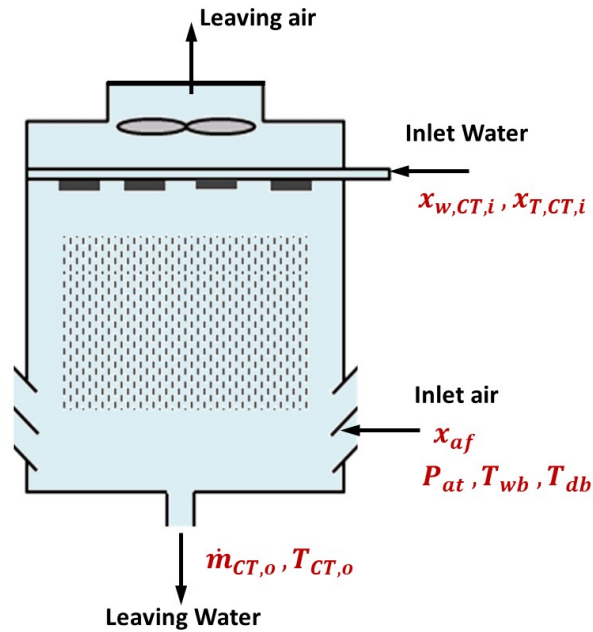
The water flowing through the cooling tower is cooled due to both sensible heat transfer due to the temperature differences between water and air and mass transfer from water evaporation to the air. The cooling tower performance is modeled based on an effectiveness-NTU approach. The total energy transfer rate between the water and air for a tower cell is given by:

$$\dot{Q}_{CT} = \varepsilon_a \dot{m}_a (h_{aswi} - h_{a,i}) \tag{3.38}$$

where,

$\dot{m}_a$ - mass flow rate of air through the cooling tower calculated from volumetric flowrate of air (x_{af}) across the tower cell [kg/s]

h_{aswi} - specific enthalpy of saturated air at inlet water temperature [kJ/kg]

$h_{a,i}$ - specific enthalpy of inlet air [kJ/kg]

ε_a - effectiveness is defined as the ratio between the actual energy transfer rate and the theoretical maximum energy transfer rate attainable, which occurs when the air that exits the tower is saturated with moisture at a temperature equal to that of inlet water.

Braun (1988) has shown that the effectiveness of a cooling tower can be determined using the relationships for sensible heat exchangers with modified definitions for NTU and the capacitance rate ratios, as shown in Eq.3.39 and Eq.3.40, which give the effectiveness for counter-flow and cross-flow cooling towers, respectively.

$$\varepsilon_a = \frac{1 - \exp\left(-NTU(1 - m^*)\right)}{1 - m^* \exp\left(-NTU(1 - m^*)\right)} \tag{3.39}$$

$$\varepsilon_a = \frac{1}{m^*}\left(1 - \exp\left(-m^*(1 - \exp(-NTU))\right)\right) \tag{3.40}$$

Here, m^* is a modified capacitance ratio given by Eq. 3.41:

$$m^* = \frac{\dot{m}_a C_s}{\dot{m}_{CT,i} C_{pw}} \tag{3.41}$$

where $\dot{m}_{CT,i}$ is the cell inlet water mass flow rate calculated from the volumetric flow rate of water $(x_{w,CT,i})$, C_{pw} is the specific heat of water, and C_s is the saturation specific heat defined as the ratio of the difference between the specific enthalpies of saturated air at inlet and leaving water temperatures to the difference between inlet $(x_{T,CT,i})$ and leaving water temperatures $(T_{CT,o})$ as shown in Eq. 3.42.

$$C_s = \frac{h_{aswi} - h_{asw0}}{x_{T,CT,i} - T_{CT,o}} \tag{3.42}$$

The previous expressions are incorporated into a mathematical model in conjunction with mass and energy balances. This model was fed with input data from performance curves of cooling towers covering the range of operating conditions to estimate NTU. Subsequently, the NTU values are correlated with the ratio of water flow to air flow through regressions to obtain the coefficients c and n of the expression, given by Eq.3.43.

$$NTU = c \left(\frac{\dot{m}_{CT}}{\dot{m}_a}\right)^n \tag{3.43}$$

To validate the model, tower heat transfer rates are calculated for each set of data using the corresponding NTU correlation and compared with the corresponding manufacturer's heat transfer rate (heat transfer rate calculated with the inlet and outlet temperatures from performance curves). The root mean square error obtained for each cooling tower was normalized by dividing it by the range (difference between the maximum and minimum value of heat transfer rate). The results are reported as NRMSE in Table 3.14.

Table 3.14. Coefficients of NTU Correlation for Cooling Towers

Cooling Tower Type	c	n	Data points	NRMSE
Counter-flow concrete tower	1.96412	0.231058	100	2.67%
Cross-flow metal tower	4.78587	-1.0684	18	6.62%

The power consumed by a variable-speed cooling tower fan can be calculated from the tower cell airflow (x_{af}). The airflow rate can be conveniently expressed as relative fan speed (f_{sp}), or ratio of current fan speed to the fan speed at rated conditions. The relative fan speed is approximately equal to the relative tower cell airflow or ratio of the airflow through the cell to the nominal airflow. The power consumed by the tower variable-speed fan can be represented as a cubic polynomial of the relative fan speed, as shown in Eq.3.44.

$$P_{CT} = P_{CT,d} * f_{sp}{}^3 \tag{3.44}$$

where $P_{CT,d}$ is the fan power consumption at a rating condition. Finally, the set of mathematical relations for the nonlinear model of a cooling tower cell (CT) can be grouped and expressed in

input-output form, which gives the power consumed by a variable-speed cooling tower fan (P_{CT}), the tower cell leaving water flow rate and temperature ($\dot{m}_{CT,o}$, $T_{CT,o}$) as a function of ambient air conditions (P_{at}, T_{wb}, T_{db}), airflow rate (x_{af}) and the tower cell inlet water flow rate and temperature ($x_{w,CT,i}, x_{T,CT,i}$). The relations for the Wade cooling tower (W) and NWCP (NW) counter-flow concrete cooling tower (Con) and cross-flow metal cooling tower (Met) are given by Eq.3.45, Eq.3.46 and Eq.3.47 respectively.

$$[\dot{m}_{CT,o},\ T_{CT,o}, P_{CT}]_W = WCT(P_{at}, T_{wb}, T_{db}, x_{af}, x_{w,CT,i}, x_{T,CT,i})_W \tag{3.45}$$

$$[\dot{m}_{CT,o},\ T_{CT,o}, P_{CT}]_{NWConCT} = NWConCT(P_{at}, T_{wb}, T_{db}, x_{af}, x_{w,CT,i}, x_{T,CT,i})_{NWConCT} \tag{3.46}$$

$$[\dot{m}_{CT,o},\ T_{CT,o}, P_{CT}]_{NWMetCT} = NWMetCT(P_{at}, T_{wb}, T_{db}, x_{af}, x_{w,CT,i}, x_{T,CT,i})_{NWMetCT} \tag{3.47}$$

For the linear model of a cooling tower cell, the airflow rate (x_{af}) is not considered as a decision variable but is directly calculated as a linear function of tower cell inlet water flow rate ($x_{w,CT,i}$), and the power consumed by the cooling tower fan (P_{CT}) is calculated as a linear function of x_{af} using the plant performance data. The tower cell leaving water mass flow rate ($\dot{m}_{CT,o}$) is assumed equal to the inlet water flowrate calculated from $x_{w,CT,i}$. The tower cell leaving water temperature ($T_{CT,o}$) is assumed to maintain a setpoint temperature determined by:

$$T_{CT,o} = Max(T_{CT,min}, (0.85T_{wb} + 14.06)) \tag{3.48}$$

where T_{wb} is the ambient wet-bulb temperature and $T_{CT,min}$ is the minimum allowable temperature to avoid cooling tower freezing (40°F). For the linear model of cooling tower cell (CT), the functional (input-output) form is:

$$[\dot{m}_{CT,o}, T_{CT,o}, P_{CT}]_W = WCT(T_{wb}, x_{w,CT,i})_W \tag{3.49}$$

$$[\dot{m}_{CT,o},\ T_{CT,o}, P_{CT}]_{NWConCT} = NWConCT(T_{wb}, x_{w,CT,i})_{NWConCT} \tag{3.50}$$

$$[\dot{m}_{CT,o},\ T_{CT,o}, P_{CT}]_{NWMetCT} = NWMetCT(T_{wb}, x_{w,CT,i})_{NWMetCT} \tag{3.51}$$

3.3.6 Pumps

The water pump is quite simply the component that drives the water flow in the power plant. The Wade power plant and NWCP have chilled water pumps (CWP) on the campus chilled-water loop and condenser water pumps ($COWP$) on the condenser-water loop. In the condenser water loop, the chillers reject heat to the water that is circulated through the cooling towers and stored in the cold well. From there, the water is pumped again to the chillers by the condenser pumps ($COWP$), whose specifications are listed in Table 3.15 for both Wade and the NWCP. All the condenser water pumps are operated by electricity. In the chilled water loop, the water from the chillers is circulated to campus through chilled water pumps (CWP), whose specifications are listed in Table 3.16. All the chilled water pumps in the NWCP are operated by electricity while four chilled water pumps in the Wade plant are operated by electricity and three are operated using 600 psig steam. Feedwater to boilers is delivered through seven boiler feedwater pumps from the condensate tank. There are four feedwater pumps driven by 600 psig steam and the rest of the pumps are operated by electricity. The specifications of feedwater pumps (FWP) are listed in Table 3.17.

Table 3.15. Condenser Water Pumps ($COWP$) Specifications at Rated Conditions

Description	Wade $COWP$	NWCP $COWP$	NWCP $COWP$
Installed units	6	3	3
Flow rate, gpm (lt/s)	15000 (946)	6000 (379)	7900 (498.4)
Total Head, ft (m)	95 (28.97)	83 (25.30)	107.5(32.77)
Efficiency, %	87	83.3	81.7
Power required, HP (kW)	400(298.3)	155 (115.6)	269 (200.6)
NPSH Required, ft (m)	27.35(8.34)	29.18 (8.89)	22.22 (6.77)
Nominal speed, rpm	1190	1785	1785

Table 3.16. Chilled Water Pumps (CWP) Specifications at Rated Conditions

Description	Wade S–CWP	Wade E–CWP	NWCP E–CWP	NWCP E–CWP
Installed units	3	4	3	3
Fuel type	600 psig steam	Electricity	Electricity	Electricity
Flow rate, gpm (lt/s)	4800 (302.8)	4800 (302.8)	3200 (201.9)	4300 (271.3)
Total Head, ft (m)	310 (94.5)	240 (73.2)	185 (56.4)	185 (56.4)
Efficiency, %	85	83	84.4	87
Power required, HP (kW)	460 (343)	500 (372.9)	200 (149.1)	250 (186.4)
NPSH Required, ft (m)	25.6 (7.8)	22.2 (6.8)	14.83 (4.5)	25.6 (7.8)
Nominal speed, rpm	1775	1780	1785	1781
Inlet steam flow, lb/h (kg/s)	30,000 (3.78)	-	-	-
Inlet steam pressure, psig (kPa)	600 (4238.2)	-	-	-
Extraction steam pressure, psig (kPa)	125 (962.2)	-	-	-

Table 3.17. Boiler Feedwater Pumps (FWP) Specifications at Rated Conditions

Description	S–FWP	S–FWP	S–FWP	E–FWP	E–FWP
Installed units	1	1	2	2	1
Fuel type	600 psig steam	600 psig steam	600 psig steam	Electricity	Electricity
Flow rate, gpm (lt/s)	1300 (82)	595 (37.5)	530 (33.4)	685 (43.2)	895 (56.5)
Total Head, ft (m)	2200 (670.5)	2070 (630.9)	2250 (685.8)	2300 (701.1)	2200 (670.6)
Efficiency, %	78	70.7	74.4	75	78.2
Power required, HP (kW)	868 (647.3)	420 (313.2)	382 (284.9)	398 (296.8)	596 (444.4)
NPSH Required, ft (m)	15 (4.6)	17 (5.2)	12.1 (3.7)	15 (4.6)	16 (4.9)
Nominal speed, rpm	3560	3560	3560	3560	3560
Inlet steam flow, lb/h (kg/s)	24,874 (3.13)	10,945 (1.38)	11,193 (1.4)	-	-
Inlet steam pressure, psig (kPa)	600 (4238.2)	600 (4238.2)	600 (4238.2)	-	-
Extraction steam pressure, psig (kPa)	125 (962.2)	125 (962.2)	125 (962.2)	-	-

For the nonlinear model of pumps, the differential head (H) and power consumption (P) of each pump can be adequately represented as cubic polynomials of the flow (Q), as shown in Eq.3.52 and Eq.3.53. The coefficients of these polynomials can be determined by fitting the pump performance data at the rotor nominal speed.

$$H = a_o + a_1 Q + a_2 Q^2 + a_3 Q^3 \tag{3.52}$$

$$P = b_o + b_1 Q + b_2 Q^2 + b_3 Q^3 \tag{3.53}$$

The power plant has pumps that operate at single-speed as well as variable frequency drives to provide the required flow. The head and power consumption curves of a pump operating at a different rotor speed can be approximated using pump affinity laws as shown in Eq.3.54-Eq.3.56.

$$\frac{Q_2}{Q_1} = \frac{\omega_2}{\omega_1} \tag{3.54}$$

$$\frac{H_2}{H_1} = \left(\frac{\omega_2}{\omega_1}\right)^2 \tag{3.55}$$

$$\frac{P_2}{P_1} = \left(\frac{\omega_2}{\omega_1}\right)^3 \tag{3.56}$$

The system head loss can be represented as a function of the square of the flow. This equation can be solved in conjunction with the correlation of head given by Eq.3.52 (where the coefficients have been recalculated for the new rotor speed) to find the pump's operating point and the corresponding power consumption. For optimization purposes, the control variable is water flow (x_w). Then, for a certain pump flow (x_w), the equation of the system gives the head loss and the pump power consumption (P). The mass flow rate of water ($\dot{m}_w$) is calculated from density and volumetric flow rate (x_w) of water through the pump. For the nonlinear model, the electric pump model ($E-P$) is expressed in the input-output form by Eq.3.57.

$$[P]_{E-P} = ElectricPump(x_w)_{E-P} \tag{3.57}$$

Four feedwater pumps and three chilled water pumps are driven by backpressure noncondensing steam turbines that utilize the 600 psig steam and they output steam at 125 psig. The power generated by each steam turbine utilizing the 600 psig steam is given as input power to a pump and is given by Eq.3.58:

$$P = \eta_{t,S-P} * \dot{m}_{s,S-P} * \Delta h_{is,S-P} \tag{3.58}$$

where,

$\dot{m}_{s,S-P}$ – Input steam to turbine driven pump [kg/s]

$\Delta h_{is,S-P}$ – Isentropic expansion work of turbine [kJ/kg]

$\eta_{t,S-P}$ – Isentropic turbine efficiency of pump [-]

The inlet steam pressure (P_{600}) and temperature (T_{600}) and outlet pressure (P_{125}) are given as inputs to the turbine model to determine $\Delta h_{is,S-P}$ and $\dot{m}_{s,S-P}$ is dependent on the power required to run the pump (P). A constant isentropic efficiency (65%) is assumed for the steam-driven pump model depending on the plant data. The nonlinear model for the steam turbine-driven pump ($S-P$) is expressed in input-output form by Eq.3.59.

$$[\dot{m}_s]_{S-P} = SteamPump(x_w, P_{600}, T_{600}, P_{125}, \eta_t)_{S-P} \tag{3.59}$$

For the linear model of the pumps, a nominal pump efficiency (η_P) and head (H) values as listed in the tables above are used and the pump power (P) is calculated as:

$$P = \frac{Q * H * SG}{3960 * \eta_P * \eta_m} \tag{3.60}$$

where,

P – pump power [bhp]

Q – flowrate of water [gpm]

H – differential head [ft]

SG – specific gravity of water [-]

η_m – motor efficiency [-]

Q is represented as the control variable for water flow (x_w). The linear model for the electric pump $(E\text{-}P)$ is expressed in input-output form by Eq.3.61.

$$[P]_{E\text{-}P} = ElectricPump(x_w, H, SG, \eta_P, \eta_m)_{E\text{-}P} \tag{3.61}$$

For the steam turbine driven pumps, the power generated by the steam turbine utilizing the 600 psig steam is given as input power to the pump as shown in Eq.3.58. The linear model for the steam turbine-driven pump $(S\text{-}P)$ is expressed in input-output form by Eq.3.62.

$$[\dot{m}_s]_{S\text{-}P} = SteamPump(x_w, H, SG, \eta_P, \eta_m, P_{600}, T_{600}, P_{125}, \eta_t)_{S\text{-}P} \tag{3.62}$$

3.3.7   Boiler Fans

Boiler systems use several types of fans to maintain airflow, recirculate air and remove exhaust gases. Based on boiler type and airflow requirement, forced draft (FD), induced draft (ID), primary air (PA) and secondary air (SA) fans are used with varied capabilities. A forced draft (FD) fan forces outside air into the heating system whereas an induced draft (ID) fan draws flue gases from the system into the atmosphere. Both primary air (PA) and secondary air (SA) fans are used in coal boilers to ensure complete combustion of coal in the furnace. The specifications of the three natural gas boiler fans are listed in Table 3.18 and the coil boiler fans are listed in Table 3.19. The boiler #1 FD and ID fans, boiler #2 FD fan and boiler #4 ID and PA fans are driven by both steam turbines and electricity while the boiler #3 FD and boiler #4 SA fans are operated by electricity.

Table 3.18. Natural Gas Boiler Fans Specifications at Rated Conditions

Description	B1 *ID* Fan	B1 *FD* Fan	B2 *FD* Fan	B3 *FD* Fan
Fuel type	125 psig steam/ Electricity	125 psig steam/ Electricity	600 psig steam/ Electricity	Electricity
Air Volume, ft^3/min (m^3/s)	220,000 (103.8)	125,574 (59.3)	150,890 (71.2)	77,128 (36.4)
Speed, rpm	878	1180	1768	1750
Static Pressure, iwc (kPa)	29 (7.2)	29 (7.2)	50 (12.4)	46.6 (11.6)
Power required, hp (kW)	1000 (745.7)	200 (149.1)	800 (596.6)	698(520.3)
Inlet steam flow, lb/h (kg/s)	31,466 (4.0)	6,543 (0.8)	11,404 (1.4)	-
Inlet steam pressure, psig (kPa)	125 (962.2)	125 (962.2)	600 (4238.2)	-
Extraction steam pressure, psig (kPa)	15 (204.7)	15 (204.7)	15 (204.7)	-

Table 3.19. Coal Boiler Fans Specifications at Rated Conditions

Description	B4 *ID* Fan	B4 *PA* Fan	B4 *SA* Fan
Fuel type	600 psig steam/ Electricity	125 psig steam/ Electricity	Electricity
Air Volume, ft^3/min (m^3/s)	145,900 (68.9)	65,612 (31.0)	23,923 (11.3)
Speed, rpm	1193	1782	1784
Static Pressure, iwc (kPa)	34.03 (8.5)	85.8 (21.4)	42.1 (10.5)
Power required, HP (kW)	900 (671.1)	1000 (745.7)	200 (149.1)
Inlet steam flow, lb/h (kg/s)	15,899 (2.0)	31,466 (4.0)	-
Inlet steam pressure, psig (kPa)	600 (4238.2)	125 (962.2)	-
Extraction steam pressure, psig (kPa)	125 (962.2)	15 (204.7)	-

For the nonlinear model of fans, the static pressure (SP) and power consumption (P) are represented as a function of air flowrate (Q_a), as shown in Eq.3.63 and Eq.3.64. Each fan operates on a single system curve that uniquely maps airflow to static pressure. The coefficients of these polynomials can be determined from the fitting of fan performance data at the nominal speed.

$$SP = a_o + a_1 Q_a + a_2 Q_a{}^2 + a_3 Q_a{}^3 \tag{3.63}$$

$$P = b_o + b_1 Q_a + b_2 Q_a{}^2 + b_3 Q_a{}^3 \tag{3.64}$$

The volumetric flow rate of air (Q_a) is calculated from density and mass flow rate of air through the fan. The mass flow rate of combustion air and flue gas is estimated by combustion calculations for the fuel being combusted (f) in the boiler. The amount of fuel consumed is calculated from the boiler steam production as in section 3.3.1. The electric fan ($E\text{-}F$) model of the boiler is expressed in input-output form by Eq.3.65.

$$[P]_{E\text{-}F} = ElectricFan(f)_{E\text{-}F} \qquad (3.65)$$

For the steam turbine-driven fans, the 125 psig steam is extracted at 15 psig by the B1 ID, B1 FD and B4 PA fans while the 600 psig steam is extracted at 15 psig by the B2 FD fan and at 125 psig by the B4 ID fan. The power generated by each steam turbine is given as input power to run each boiler fan and is given by Eq.3.66:

$$P = \eta_{t,S\text{-}F} * \dot{m}_{s,S\text{-}F} * \Delta h_{is,S\text{-}F} \qquad (3.66)$$

where,

$\dot{m}_{s,S\text{-}F}$ – Input steam to turbine driven fan [kg/s]

$\Delta h_{is,S\text{-}F}$ – Isentropic expansion work of turbine [kJ/kg]

$\eta_{t,S\text{-}F}$ – Isentropic turbine efficiency of fan [-]

The inlet steam pressure (P_{in}) and temperature (T_{in}) and outlet pressure (P_{out}) are given as inputs to the turbine model to determine the isentropic expansion work of the turbine ($\Delta h_{is,S\text{-}F}$) and input steam to the turbine of fan ($\dot{m}_{s,S\text{-}F}$) is dependent on the power required to run the fan (P). A constant isentropic efficiency (65%) is given as an input to the steam-driven fan model depending on the plant data. The nonlinear model for the steam turbine driven fan ($S\text{-}F$) is expressed in input-output form by Eq.3.67.

$$[\dot{m}_s]_{S\text{-}F} = SteamFan(f, P_{in}, T_{in}, P_{out}, \eta_t)_{S\text{-}F} \qquad (3.67)$$

For the linear model of the boiler fans, the power consumed by the boiler fan (P) is calculated as a linear function of air flowrate (Q_a) using the plant performance data. The boiler air flowrate is calculated from the mass flow rate of combustion air and flue gas estimated by combustion

calculations for the fuel being combusted (f) in the boiler. The linear model for the electric fan ($E-F$) model of the boiler is expressed in input-output form using Eq.3.65. For the steam turbine driven fans, the power generated by the steam turbine utilizing the 600 psig steam is given as input power to the pump as shown in Eq.3.66. A linear model is used to calculate the fan power. The linear model for the steam turbine-driven fan ($S-F$) is expressed in the input-output form by Eq.3.67.

3.3.8 Steam Lines to Campus

Steam to campus is distributed through a steam tunnel system for campus heating through two lines: 125 psig steam line to buildings far away from the Wade plant and 15 psig steam line to buildings close to the plant. Heating load requirements provided by the 125 psig (H_{125}) and 15 psig (H_{15}) steam lines are calculated as:

$$H_{125} = \Delta h_{125L} * \dot{m}_{s,125L} \tag{3.68}$$

$$H_{15} = \Delta h_{15L} * \dot{m}_{s,15L} \tag{3.69}$$

where,

Δh_{125L} - specific enthalpy change for 125 psig campus steam line [kJ/kg]

Δh_{15L} - specific enthalpy change for 15 psig campus steam line [kJ/kg]

$\dot{m}_{s,125L}$ - 125 psig steam output to campus [kg/s]

$\dot{m}_{s,15L}$ - 15 psig steam output to campus [kg/s]

The steam pressure (P_{125}) and temperature (T_{125}) for the 125 psig steam line, steam pressure (P_{15}) and temperature (T_{15}) for the 15 psig steam line and condensate return pressure (P_{cr}) and temperature (T_{cr}) are given as inputs to the campus steam model from the plant operational specifications. The mass flow rates of steam through the 125 psig steam line ($\dot{m}_{s,125L}$) and 15 psig steam line ($\dot{m}_{s,15L}$) are determined from the campus heating demand H_{125} and H_{15} respectively. The set of mathematical expressions can be grouped and expressed as:

$$[\dot{m}_{s,125L}] = 125CampusSteam(H_{125}, P_{125}, T_{125}, P_{cr}, T_{cr}) \tag{3.70}$$

$$[\dot{m}_{s,15L}] = 15CampusSteam(H_{15}, P_{15}, T_{15}, P_{cr}, T_{cr}) \tag{3.71}$$

88

3.3.9   Pressure Reducing Valves

There are pressure reducing valves (PRV) across the 600 to 125 psig steam line and 125 to 15 psig steam line. These valves bypass other components and are used to reduce steam pressure to meet the heating requirements when the demand is high (especially during winter periods) and when not all of the high-pressure steam can be used for other productive purposes (e.g., power production or cooling). The outlet steam temperature (T_{PRV}) for the PRV is controlled by spraying some feedwater ($\dot{m}_{fw,PRV}$). Then, the specific enthalpy of the outlet stream ($h_{out,PRV}$) can be determined for a given outlet pressure. The mass flow rate of steam across the PRV ($x_{s,PRV}$) is determined by the campus heating demand and then the amount of feedwater sprayed ($\dot{m}_{fw,PRV}$) is determined from the overall energy balance of Eq.3.72 that assumes that the valve is adiabatic and has negligible changes in kinetic and potential energy.

$$\left(x_{s,PRV} * h_{in}\right) + \left(\dot{m}_{fw,PRV} * h_{fw}\right) = \left(x_{s,PRV1} + \dot{m}_{fw,PRV}\right) * h_{out,PRV} \tag{3.72}$$

where,

$x_{s,PRV}$ – inlet steam to PRV [kg/s]

h_{in} – specific enthalpy of inlet steam to PRV [kJ/kg]

$\dot{m}_{fw,PRV}$ – amount of feedwater sprayed [kg/s]

h_{fw}– specific enthalpy of feedwater sprayed to PRV [kJ/kg]

$h_{out,PRV}$– specific enthalpy of outlet steam from PRV [kJ/kg]

$\dot{m}_{s,PRV}$ – total outlet steam from PRV $\left(x_{s,PRV1} + \dot{m}_{fw,PRV}\right)$ [kg/s]

The PRV model is expressed in input-output form by Eq.3.73 for $PRV1$ across the 600 to 125 psig steam lines and Eq.3.74 for $PRV2$ across the 125 to 15 psig steam lines.

$$[\dot{m}_{s,PRV1}] = PRV1\left(x_{s,PRV1}, P_{600}, T_{600}, P_{125}, T_{PRV1}, T_{fw}\right) \tag{3.73}$$

$$[\dot{m}_{s,PRV2}] = PRV2\left(x_{s,PRV2}, P_{125}, T_{125}, P_{15}, T_{PRV2}, T_{fw}\right) \tag{3.74}$$

3.3.10 Auxiliaries

Feedwater Heater

Feedwater from the condensate tank and deaerator is pumped into the boilers at 600 psig / 250 °F using feedwater pumps. The natural gas boiler #1 (B1) has a closed feedwater heater (FWH) that uses 125 psig steam to pre-heat water, so its inlet feedwater temperature to B1 is approximately 350°F. The mass flow rate of steam through the boiler ($x_{s,B1}$) is given as the input for feedwater assuming no losses across the boiler. The 125 psig inlet steam is used to pre-heat the feedwater and the outlet steam is condensed to saturated liquid. The feedwater pressure ($P_{fw,B1}$), inlet ($T_{i,fw,B1}$) and outlet temperatures ($T_{o,fw,B1}$), 125 psig steam pressure (P_{125}) and temperature (T_{125}) are given as inputs to the FWH to determine the inlet ($h_{i,fw}$) and outlet ($h_{o,fw}$) enthalpy of the feedwater, and inlet ($h_{i,125}$) and outlet ($h_{o,125}$) enthalpy of the 125 psig steam. The amount of 125 psig steam ($\dot{m}_{s,FWH,125}$) used to preheat the feedwater ($x_{s,B1}$) to boiler B1 is determined using Eq.3.75:

$$\dot{m}_{s,FWH,125}\left(h_{i,125} - h_{o,125}\right) = x_{s,B1} * \left(h_{o,fw} - h_{i,fw}\right) \tag{3.75}$$

The model of the FWH is expressed in input-output form by Eq.3.76:

$$[\dot{m}_{s,FWH,125}] = FWHeater\left(x_{s,B1}, P_{fw,B1}, T_{i,fw,B1}, T_{o,fw,B1}, P_{125}, T_{125}\right)_{FWH} \tag{3.76}$$

Deaerator

The condensate from campus and the various plant components is collected in the condensate tank and makeup water is added to compensate for any losses. Before feeding the water to boilers using feedwater pumps, the water is sent through a deaerator (DA) to remove oxygen and other dissolved gases. Some amount of 15 psig steam is mixed in the deaerator to bring the water to the required feedwater temperature. The total condensate mass flowrate ($\dot{m}_{cond}$) from all components and campus, condensate pressure (P_{cond}), condensate temperature (T_{cond}), and 15 psig steam pressure (P_{15}) and temperature (T_{15}) are given as inputs to the DA to determine the inlet enthalpy

of condensate (h_{cond}) and inlet enthalpy of 15 psig steam ($h_{DA,15}$). The amount of 15 psig steam ($\dot{m}_{s,DA,15}$) required for the deaerator is determined using Eq.3.77:

$$\dot{m}_{cond} * h_{cond} + \dot{m}_{s,DA,15} * h_{DA,15} = (\dot{m}_{cond} + \dot{m}_{DA,15}) * h_{DA,out} \qquad (3.77)$$

The model of the DA is expressed in input-output form by Eq.3.78:

$$[\dot{m}_{s,DA,15}] = Deaerator(\dot{m}_{cond}, P_{cond}, T_{cond}, P_{15}, T_{15})_{DA} \qquad (3.78)$$

Other Auxiliaries

Apart from all the equipment mentioned above, there are some minor auxiliary components that utilize 600 psig, 125 psig and 15 psig steam. There are also other auxiliaries that utilize some electricity. The amounts of steam used by auxiliaries at 600 psig ($S-A1$), 125 psig ($S-A2$)and 15 psig ($S-A3$) steam lines are represented as $\dot{m}_{s,S-A1}$, $\dot{m}_{s,S-A2}$ and $\dot{m}_{s,S-A3}$ respectively. The power consumed by minor electric auxiliaries ($E-A$) is represented as P_{E-A}. These are given as constant input to both linear and nonlinear models to account for some steam and electricity consumption by these auxiliaries.

3.3.11 Component Assembly

To simulate the performance of the entire plant, the model components are integrated according to their physical configuration through stream variables (i.e., flows, pressures and temperatures). The main loops where mixing occurs include steam, condensate and feedwater loops, and condenser and cooling tower water loops. For the steam loop from Figure 3.2, it can be seen that the mixing of steam happens at the 600 psig, 125 psig and 15 psig steam lines. Across the 600 psig steam line, the outlet specific enthalpy (h_{600}) and the corresponding temperature (T_{600}) are determined from the energy balance of steam from all four boilers and the CHP facility.

$$\sum_{j=1}^{4}(x_{s,B,j} * h_{s,B,j}) + (x_{s,UF} * h_{s,UF}) + (x_{s,F} * h_{s,F}) = [\sum_{j=1}^{4} x_{s,B,j} + x_{s,UF} + x_{s,F}] * h_{600} \qquad (3.79)$$

The outlet steam pressure and calculated outlet temperature of each boiler and the CHP facility are given as inputs to find the enthalpy of the outlet steam (h_s) from each equipment. The outlet

temperature (T_{600}) is determined for the 600 psig steam line from the calculated specific enthalpy (h_{600}) at pressure (P_{600}). Similarly, the outlet temperature from the mixing of steam in the 125 psig (T_{125}) and 15 psig steam lines (T_{15}) are given by Eqs.3.80 and 3.81 respectively. The 125 psig steam extracted from turbine generator #1 ($TG1$), turbine generator #2 ($TG2$), four steam-driven feedwater pumps ($S\text{--}FWP$), three steam-driven chilled water pumps ($S\text{--}CWP$), boiler #4 steam-driven ID fan ($S\text{--}F, B4_{ID}$) and pressure reducing valve #1 ($PRV1$) are mixed in the 125 psig steam line. Likewise, the 15 psig steam extracted from boiler #2 FD fan ($S\text{--}F, B2_{FD}$), boiler #1 FD fan ($S\text{--}F, B1_{FD}$) and ID fan ($S\text{--}F, B1_{ID}$), boiler #4 PA fan ($S\text{--}F, B4_{PA}$), pressure reducing valve #2 ($PRV2$) and turbine generator #2 ($TG2$) are mixed in the 15 psig steam line.

$$
\begin{aligned}
&\left(x_{s,ex1,TG1} * h_{ex1,TG1}\right) + \left(x_{s,ex1,TG2} * h_{ex1,TG2}\right) + \sum_{j=1}^{4}\left(\dot{m}_{s,S-FWP,j} * h_{S-FWP,j}\right) + \\
&\sum_{j=1}^{3}\left(\dot{m}_{s,S-CWP,j} * h_{S-CWP,j}\right) + \left(\dot{m}_{s,S-F,B4_{ID}} * h_{S-F,B4_{ID}}\right) + \left(\dot{m}_{s,PRV1} * h_{PRV1}\right) = \\
&\left[x_{s,ex1,TG1} + x_{s,ex1,TG2} + \sum_{j=1}^{4}\dot{m}_{s,S-FWP,j} + \sum_{j=1}^{3}\dot{m}_{s,S-CWP,j} + \dot{m}_{s,S-F,B4_{ID}} + \right. \\
&\left. \dot{m}_{s,PRV1}\right] * h_{125}
\end{aligned}
\tag{3.80}
$$

$$
\begin{aligned}
&\left(\dot{m}_{s,S-F,B2_{FD}} * h_{S-F,B2_{FD}}\right) + \left(\dot{m}_{s,S-F,B1_{ID}} * h_{S-F,B1_{ID}}\right) + \left(\dot{m}_{s,S-F,B1_{FD}} * h_{S-F,B1_{FD}}\right) + \\
&\left(\dot{m}_{s,S-F,B4_{PA}} * h_{S-F,B4_{PA}}\right) + \left(\dot{m}_{s,PRV2} * h_{PRV2}\right) + \left(x_{s,TG2} - x_{s,ex1,TG2}\right) * h_{ex2,TG2} = \\
&\left[\dot{m}_{s,S-F,B2_{FD}} + \dot{m}_{s,S-F,B1_{ID}} + \dot{m}_{s,S-F,B1_{FD}} + \dot{m}_{s,S-F,B4_{PA}} + \dot{m}_{s,PRV2} + \left(x_{s,TG2} - \right.\right. \\
&\left.\left. x_{s,ex1,TG2}\right)\right] * h_{15}
\end{aligned}
\tag{3.81}
$$

The condensate from campus and the various plant components is collected in the condensate tank. Across this condensate line, the specific enthalpy (h_{cond}) and temperature (T_{cond}) of the condensate are determined from the energy balance of total condensate mass flowrate ($\dot{m}_{cond}$) from all components and campus.

$$
\begin{aligned}
&\left(x_{s,TG1} - x_{s,ex1,TG1}\right) * h_{cond,TG1} + \sum_{j=1}^{3}\left(\dot{m}_{s,S-C,j} * h_{cond,S-C,j}\right) + \left(\dot{m}_{s,125L} * h_{cr}\right) + \\
&\left(\dot{m}_{s,15L} * h_{cr}\right) + \left(\dot{m}_{FWH,125} * h_{o,FWH}\right) + \sum_{j=1}^{3}\left(\dot{m}_{s,S-A,j} * h_{cond,S-A,j}\right) = \\
&\left[\left(x_{s,TG1} - x_{s,ex1,TG1}\right) + \sum_{j=1}^{3}\dot{m}_{s,S-C,j} + \dot{m}_{s,125L} + \dot{m}_{s,15L} + \dot{m}_{FWH,125} + \right. \\
&\left. \sum_{j=1}^{3}\dot{m}_{s,S-A,j}\right] * h_{cond}
\end{aligned}
\tag{3.82}
$$

From the condenser water loop as shown in Figure 3.3, it can be seen that water from all the chiller condensers is mixed and circulated through the cooling towers. After cooling, the water from all the cooling tower cells is mixed and stored in the cold well. From there, the water is pumped again to the chillers by the condenser water pumps. The stream variables of the cooling tower cells are related by an energy balance on the cold well (CW) giving the variation of temperature of water in the cold well which is the condenser water inlet temperature ($T_{co,i}$), assuming that the water in the cold well is fully mixed and neglecting thermal losses. Eq.3.83 gives the cold well energy balance in the Wade plant while Eq.3.84 gives the cold well energy balance in the NWCP plant.

$$\left[\sum_{j=1}^{6}(T_{CT,o,j} * \dot{m}_{CT,o,j}) + T_{mu}\sum_{j=1}^{6}\left(\dot{m}_{CT,i,j} - \dot{m}_{CT,o,j}\right) = T_{co,i}\sum_{j=1}^{6}\dot{m}_{CT,i,j}\right]_W \tag{3.83}$$

$$\left[\sum_{j=1}^{12}(T_{CT,o,j} * \dot{m}_{CT,o,j}) + T_{mu}\sum_{j=1}^{12}\left(\dot{m}_{CT,i,j} - \dot{m}_{CT,o,j}\right) = T_{co,i}\sum_{j=1}^{12}\dot{m}_{CT,i,j}\right]_{NW} \tag{3.84}$$

In the above expressions, $T_{CT,o,j}$ is the temperature of the water and $\dot{m}_{CT,o,j}$ is the mass flowrate of water leaving the jth tower cell of the cooling tower. T_{mu} is the make-up water temperature and the mass flowrate of water entering the jth tower cell $\left(\dot{m}_{CT,i,j}\right)$ is calculated from its inlet volumetric flowrate $\left(x_{w,CT,i,j}\right)$. The outlet temperature of the water mixing in the cold well is the inlet water temperature ($T_{co,i}$) to the condensers of each chiller calculated using the above equations. The outlet water from each condenser is mixed in the line and sent to each cell of the cooling tower. Eq.3.85 gives the energy balance for the outlet water from all the condensers (condensers of turbine generator, steam chillers, electric chillers) in the Wade plant while Eq.3.86 gives the condenser water energy balance in the NWCP plant.

$$\left[\left(T_{co,o} * \dot{m}_{co}\right)_{TG1} + \sum_{j=1}^{3}(T_{co,o2,j} * \dot{m}_{co,j})_{S-C} + \sum_{j=1}^{4}(T_{co,o,j} * \dot{m}_{co,j})_{E-C} = \right.$$
$$\left. T_{CT,i}\left((\dot{m}_{co})_{TG1} + \sum_{j=1}^{3}(\dot{m}_{co,j})_{S-C} + \sum_{j=1}^{4}(\dot{m}_{co,j})_{E-C}\right)\right]_W \tag{3.85}$$

$$\left[\sum_{j=1}^{6}(T_{co,o,j} * \dot{m}_{co,j})_{E-C} = T_{CT,i}\sum_{j=1}^{6}(\dot{m}_{co,j})_{E-C}\right]_{NW} \tag{3.86}$$

From the above expressions, the inlet temperature of the water to the cooling tower cell $(T_{CT,i})$ is calculated. $T_{co,o,j}$ is the outlet temperature from each condenser and the mass flowrate of water leaving the jth condenser $(\dot{m}_{co,j})$ is calculated from its outlet volumetric flow rate $(x_{co,j})$.

Thus, all the components in the CCHP plant are interconnected according to their physical arrangement. It can be observed that some of the inputs to the equipment model come from the plant operational specifications, some come from control heuristics, and some come from outputs of other components.

3.4 Plant Validation

The entire model was integrated into the MATLAB (R2019b) simulation environment. The model input data consists of heating (DH), campus cooling (DC) and electrical demand (DE), ambient wet-bulb (T_{wb}) and dry-bulb (T_{db}) temperatures, chilled water supply set-point $(T_{ev,o})$ and return temperature $(T_{ev,i})$ from campus, pressure of 600 (P_{600}), 125 (P_{125}), 15 (P_{15}) psig steam lines, feedwater (P_{fw}), condensate line (P_{cond}), exhaust from equipment (P_{ex}), and condensate return from campus (P_{cr}) and temperatures of feedwater (T_{fw}) and condensate return from campus (T_{cr}). In addition, some inputs specific for the equipment are defined based on the plant performance data as described under each component model. The model output consists of power consumption and steam input along with the state variables associated with each piece of equipment. All the equipment model equations are interconnected according to their physical arrangement in the plant and the integrated model predictions are compared with measurements for both the linear and nonlinear model implementations. Historical data from the Wade and NWCP power plant sampled at one-hour interval including the campus thermal and electrical demand during a 24-hour period in four different seasons [spring (20th April 2016); fall (18th October 2017); summer (27th August 2018); winter (18th February 2015)] were used as inputs to simulate the performance of the CCHP plant and validate the linear and nonlinear model implementations. Figure 3.12 represents heating, cooling and electrical demand of the Purdue campus during spring (a), fall (b), summer (c) and winter (d) for a 24-hour period that were used as inputs to the model.
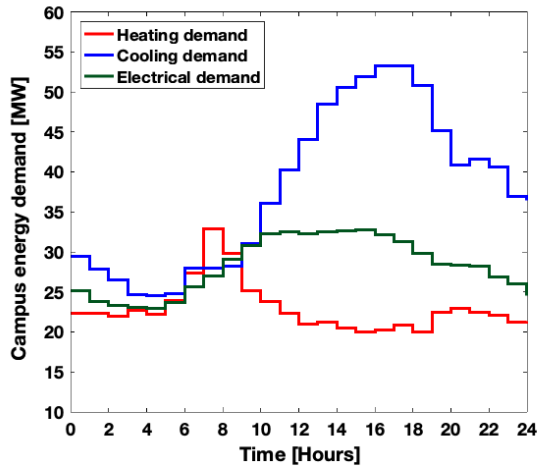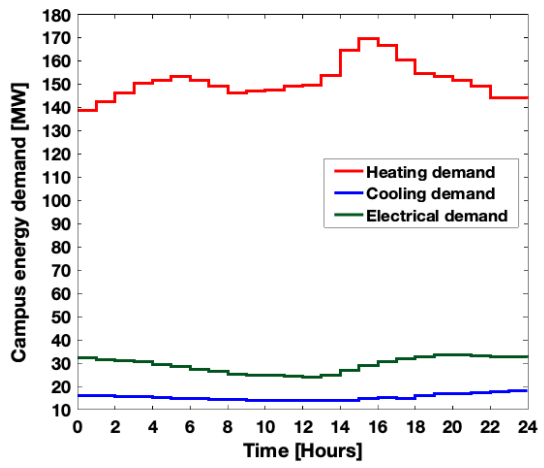
(a) Spring   (b) Fall
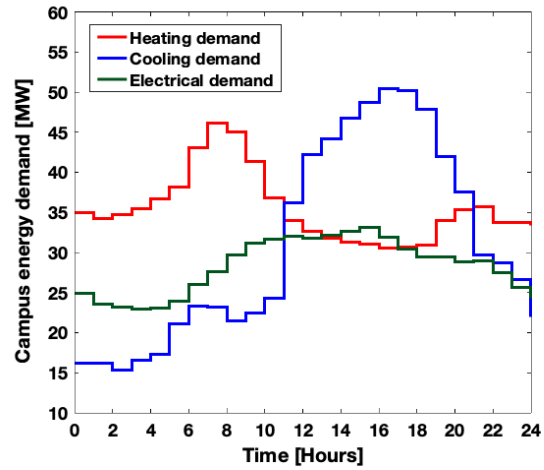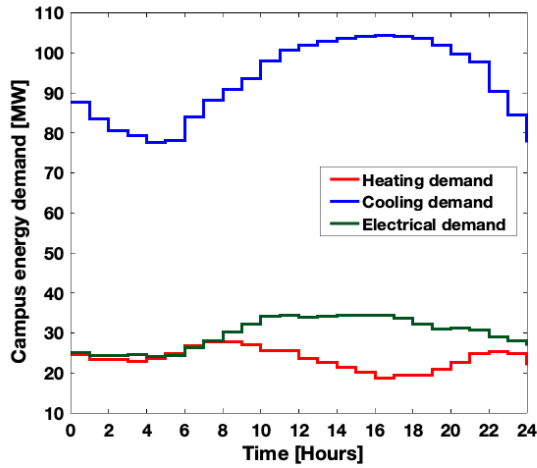
(c) Summer   (d) Winter

Figure 3.12. Energy demand of Purdue campus

Figure 3.13 shows comparisons of measured steam produced from the plant data and the total steam produced estimated with the linear and nonlinear models during a period of 24 hours corresponding to spring, fall, summer and winter seasons. The total amount of steam produced from the boilers is used to satisfy all types of steam demand which includes the total steam consumption from all steam-driven equipment in the plant and campus heating demand. Similarly, Figure 3.14 shows comparisons of measured electricity generated and purchased from the plant data and the total power (generated and purchased) estimated with the linear and nonlinear models for the same 24-hour periods in spring, fall, summer and winter seasons. The combination of the

amount of electricity produced by the two turbine generators and the amount of electricity purchased is used to meet all electrical demands which includes the total power consumption from equipment electrical usage in the plant plus campus electrical demand. In both cases, both the linear and nonlinear model predictions agree well with the actual plant performance for all the seasons. However, the nonlinear model shows better agreement especially for the power predictions. In all the four different seasonal scenarios, the maximum deviation of steam produced from the actual plant measurements was below 5% for the linear model and below 4% for the nonlinear model. For the total amount of electricity generated and purchased, the deviations from plant data were below 5% for the linear model and below 4% for the nonlinear model.

(a) Spring

(b) Fall

(c) Summer

(d) Winter
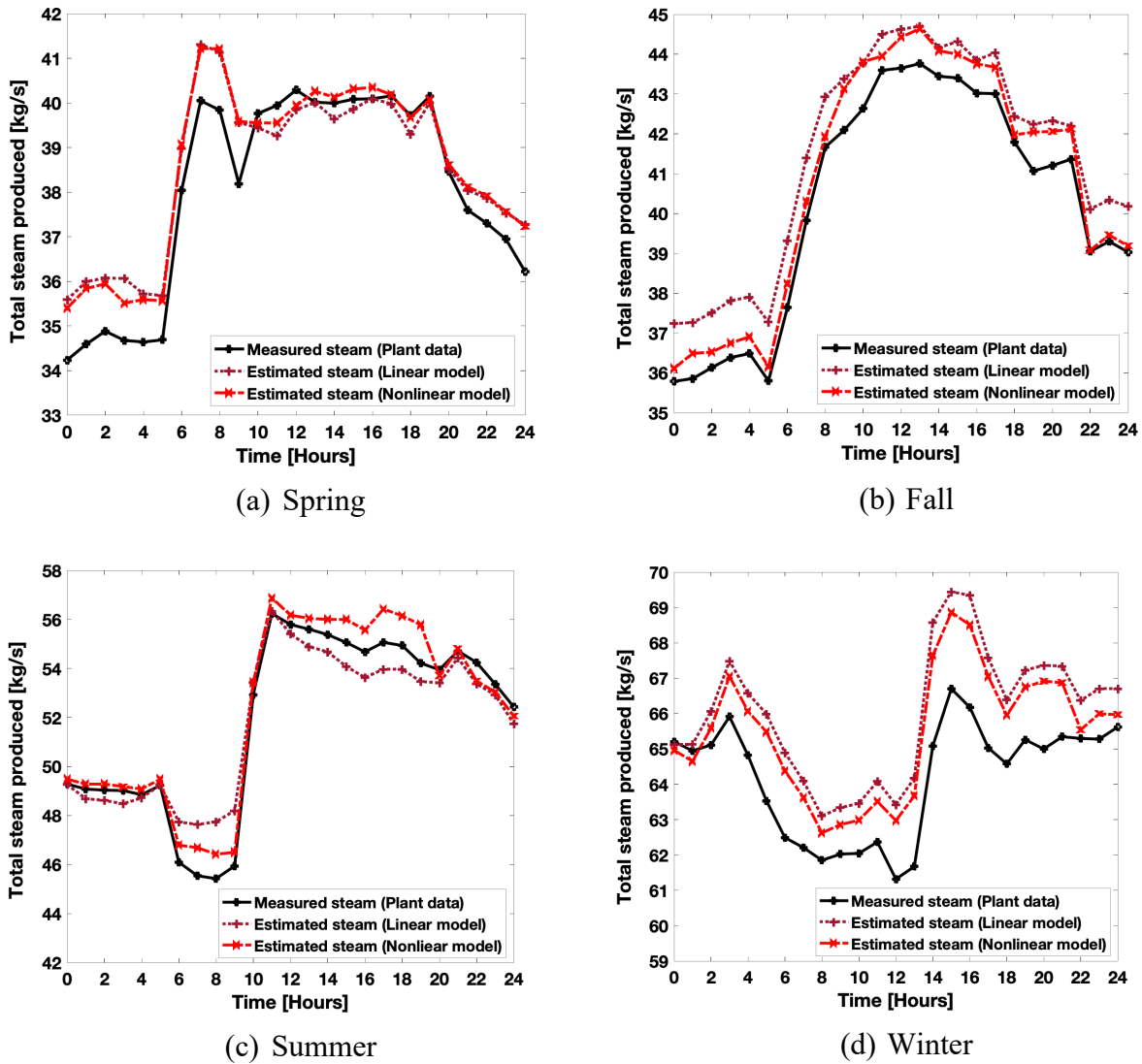
Figure 3.13. Total steam produced from the CCHP plant

(a) Spring

(b) Fall

(c) Summer

(d) Winter
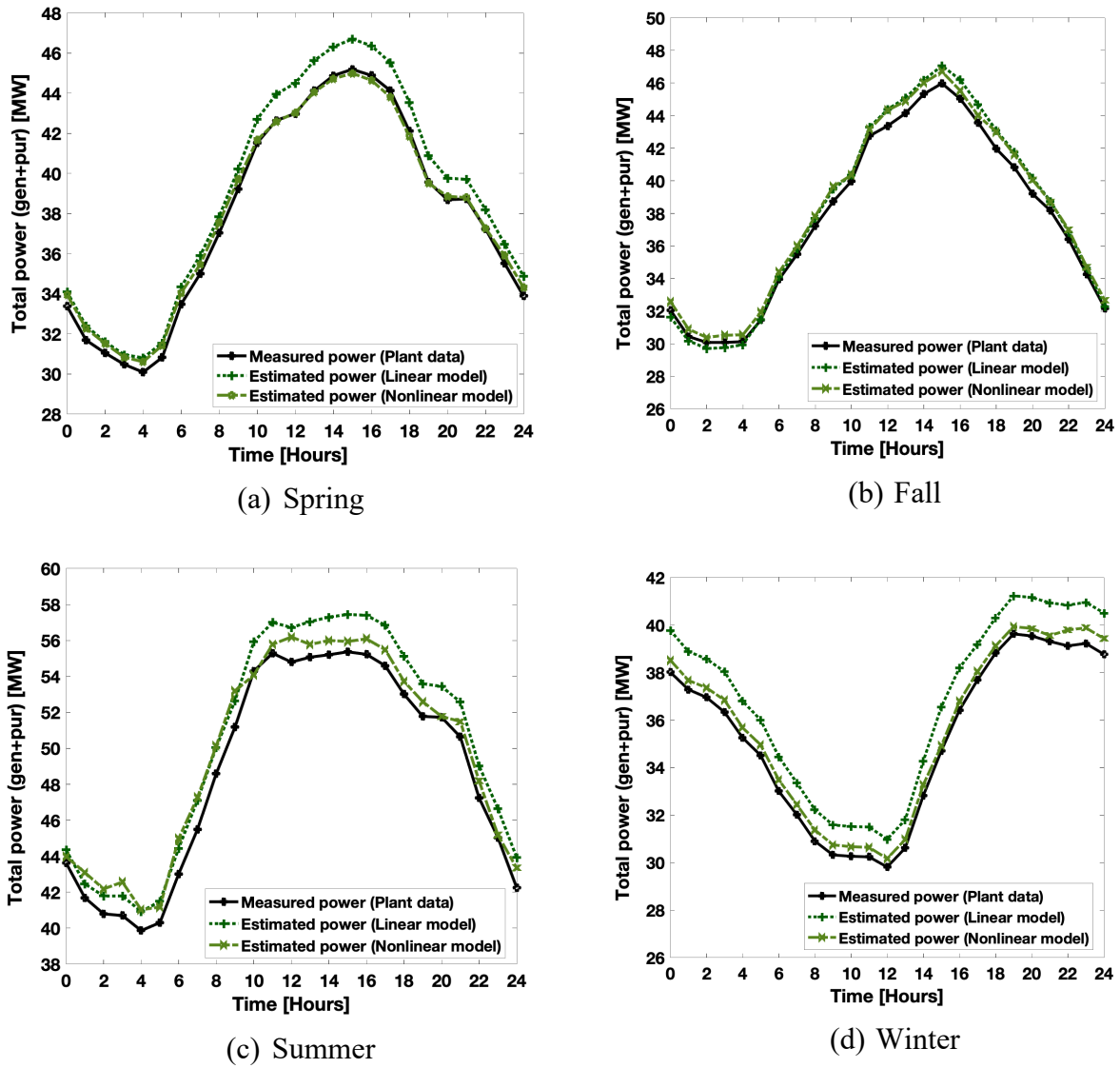
Figure 3.14. Total electricity generated and purchased from the CCHP plant.

3.5   Chapter Summary

In this chapter, mathematical models for the equipment used in the Wade Power Plant and the Northwest Chiller Plant (NWCP) were described. Each plant component model is represented as a set of mathematical expressions in terms of parameter, input and output variables with both linear and nonlinear forms. Most of the model parameters were determined from plant performance data, but a few came from the equipment manufacturer's data. The model components were integrated according to their physical configuration within MATLAB (R2019b). The integrated

linear and nonlinear model predictions were then compared with plant measurements for total steam and electricity consumption occurring within the Wade and Northwest plants and showed good agreement for 24-hour periods in different seasons. These linear and nonlinear mathematical models are used within the mixed integer linear programming (MILP) and nonlinear programming (NLP) optimization methods that are described in the next chapter for determining optimal operation.

4. OPTIMIZATION FRAMEWORK

The following section describes the formulation of an energy dispatch algorithm using a network energy flow model. The objective function and constraints are based on the electric and thermal energy flows through the CCHP equipment that depend on the campus energy demand. Two different formulations of the optimal energy dispatch problem: mixed-integer linear programming (MILP) and nonlinear programming (NLP) are presented.

4.1   Control of the CCHP System

The CCHP system has major components such as boilers, chillers, and turbine generators that are used for producing steam, chilled water, and electricity and other auxiliary components such as pumps (boiler feedwater pumps, chilled water pumps, condenser water pumps, etc.), fans (boiler fans and cooling tower fans) and other equipment that run along with the major components to meet campus energy demands. The control of the CCHP system is realized through a hierarchical paradigm. The outer supervisory control layer determines which major components should be operating (on/off states) along with their loads. The solution depends primarily on electric, cooling, and heating energy demand, energy costs, and the component performance characteristics and constraints. Depending on the results of the outer layer, the inner layer of component controllers activates other auxiliary equipment associated with the major components in the CCHP system based on control heuristics. For example, the boiler feedwater pumps are activated depending on the total steam load on the boilers and CHP facility. The fan of the respective boiler is switched on when the corresponding boiler is running to meet the steam demand. Similarly, the chilled water pumps, condensate water pumps, and the cooling tower fans are activated based on the chiller load. The operation of auxiliary equipment is a function of the load on the major components. These details were included in the mathematical models of auxiliary equipment presented in the last chapter. In this hierarchical paradigm of CCHP system control, the outer layer is supervisory while the inner layer is basically a slave to the supervisory control.

4.2   Network Flow Model

Based on the energy flows of steam, chilled water, and electricity described in section 3.2, a deterministic network flow model has been developed that connects the supply to the demand. The campus energy demand activates the operation of major components such as boilers, chillers, and turbine generators to produce steam, chilled water, and electricity. The other auxiliary components are run along with the major components to meet campus energy demands. The network flow model for the case study CCHP system is shown in Figure 4.1. The network flow model helps in visualizing the electric and thermal energy flows through the CCHP equipment. Elements in the network include nodes, hubs and connecting lines. The nodes in this network represent sources of energy and energy demand points, i.e., the nodes include components that provide as well as consume energy. The demand drives the activation of individual components throughout the network. The energy (fuel, steam, electricity, cooling, heating) flows across the components from supply to demand in order to meet the campus thermal and electrical demands. Every component has some operational limitations and energy paths have capacity constraints (e.g., energy flow through a node and path cannot exceed its capacity based on equipment performance constraints). The network flow model allows different energy paths to transfer the supply to the demand. The optimal path chosen to meet the energy demands depends on the objective. The orange lines represent steam flow within the plant, while the green lines represent electricity flow, blue lines represent cooling rates and red lines represent heating rates to campus.

Legend:
- ····▸ Electricity
- —·—▸ Cooling to campus
- ----▸ Heating to campus
- ——▸ Steam flow within plant
- ----▸ Fuel flow
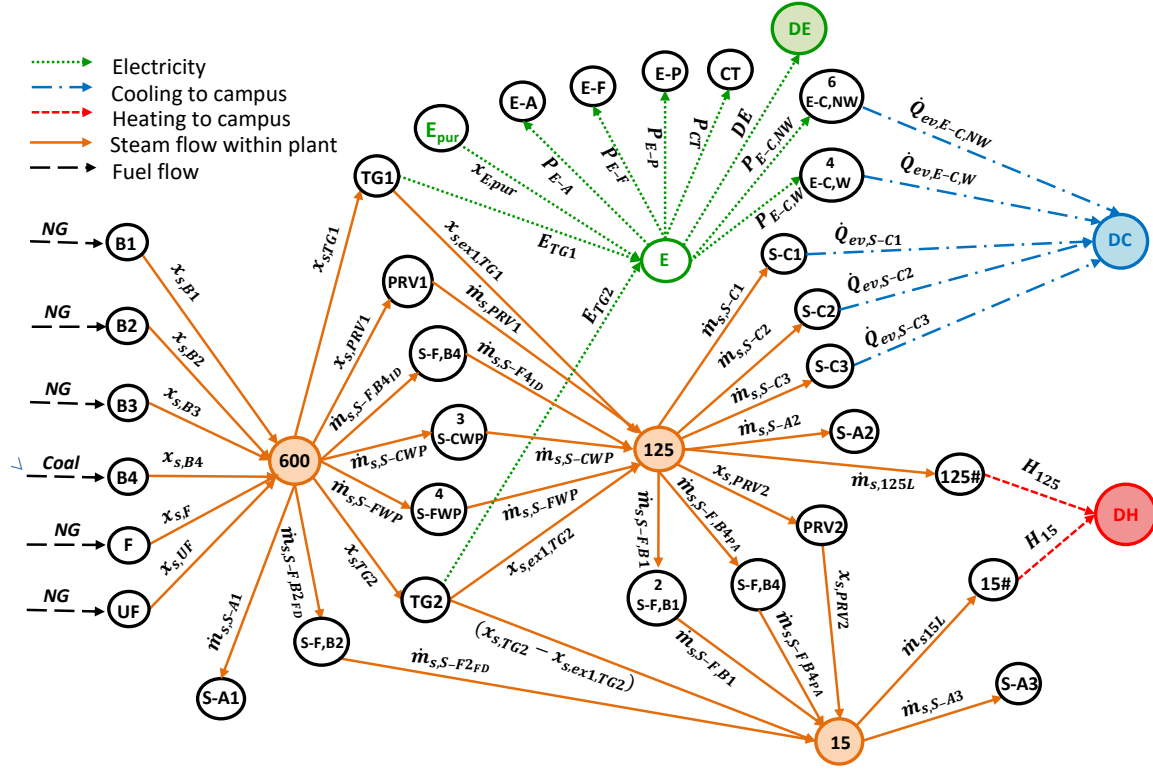
Nodes

Node B: Boilers

Node F, UF: Fired and Unfired steam of CHP

Node 600, 125, 15: 600, 125, 15 psig steam lines

Node TG: Turbine generators

Node S-FWP: Steam-driven feed water pumps

Node S-CWP: Steam-driven chilled water pumps

Node S-F,B: Steam-driven fan of the boiler

Node PRV: Pressure reducing valve

Node S-C: Steam-driven chillers

Node E-C,W: Wade Electric chillers

Node E-C,NW: NWCP Electric chillers

Node 125#, 15#: Steam line to campus

Node S-A: Steam Auxiliaries

Node Epur: Electricity purchased from utility

Node CT: Cooling tower (Wade & NWCP)

Node E-P: Electric pumps (FWP, COWP & CWP)

Node E-F: Electric fan of the boiler

Node: E-A: Electric Auxiliaries

Node E: Electricity line

Node DE, DC, DH: Electricity, Cooling, Heating demand of Purdue campus

Energy flow

$x_{s,B}$: Steam from boilers [kg/s]

$x_{s,F/UF}$: Steam from CHP facility (fired/unfired) [kg/s]

$x_{s,TG}$: Steam to turbine generators [kg/s]

$x_{s,ex1,TG}$: Steam extracted from turbine generators [kg/s]

$x_{s,PRV}$: Steam to PRV [kg/s]

$\dot{m}_{s,PRV}$: Steam from PRV [kg/s]

$\dot{m}_{s,S-C}$: Steam to steam chillers [kg/s]

$\dot{m}_{s,L}$: 125 psig & 15 psig steam to campus [kg/s]

$x_{E,pur}$: Electricity purchased [kW]

E_{TG}: Electricity generated from turbine generators [kW]

P_{E-C}: Electricity to electric chillers [kW]

$\dot{Q}_{ev,E-C}$: Cooling capacity from electric chillers [kW]

$\dot{Q}_{ev,S-C}$: Cooling capacity from steam chillers [kW]

H: Heating capacity from 125/15 psig steam line [kW]

$\dot{m}_{s,S-F,B}$: Steam from/to steam driven boiler fans [kg/s]

$\dot{m}_{s,S-FWP}$: Steam from/to steam driven FWP [kg/s]

$\dot{m}_{s,S-CWP}$: Steam from/to steam driven CWP [kg/s]

$\dot{m}_{s,S-A}$: Steam to auxiliaries [kg/s]

P_{E-A}: Electricity to electric auxiliaries [kW]

P_{E-P}: Electricity to electric pumps [kW]

P_{E-F}: Electricity to electric fans [kW]

P_{CT}: Electricity to cooling towers [kW]

DE: Electricity to meet campus electricity demand [kW]

Figure 4.1. Network energy flow model of the CCHP system

101

4.3 Energy Dispatch Algorithm

In general, the CCHP energy dispatch problem is intrinsically difficult to solve because of the non-convex, non-differentiable, multimodal (multiple local minima), and discontinuous nature of the optimization problem along with strong coupling to multiple energy components (electricity, heating, and cooling). Optimal control of CCHP systems involves the determination of the mode of operation and set points to satisfy the specific energy requirements. The problem is complicated because of a high number of decision variables, both continuous and discrete. While the energy flow (unit load) and setpoint decision variables are continuous, the availability (on/off staging) of the equipment represents discrete variables. Due to the nonlinear nature of equipment performance (typically nonlinear with respect to load and sometimes temperature, pressure, relative humidity) along with continuous and discrete variables, the resulting problem is a mixed-integer nonlinear programming (MINLP) problem. Even though there are many MINLP solution methodologies available, it is computationally expensive to solve these large-scale problems with a large number of discrete and continuous variables and numerous constraints along with the nonlinearities. Also, it is extremely challenging to implement these algorithms for the daily operation of a complex power plant. The mixed-integer linear programming (MILP) formulation is widely used for these types of problems to find a globally optimum solution, but it assumes linear approximate models for the equipment. Adopting a piecewise linear approximation with an appropriate number of intervals to account for nonlinear equipment models becomes complicated when the degrees of freedom increases to two or more. On the other hand, a nonlinear programming (NLP) optimization technique takes into account the actual nonlinear characteristics of the equipment, but the optimization solution might get trapped in a poor local minimum due to the multi modal nature of the problem without finding the global optimum solution. Sometimes, there is no guarantee for the convergence of the solution. Heuristic optimization techniques like genetic algorithms (GA), simulated annealing (SA), particle swarm optimization (PSO), etc. can be used for MINLP problems, but some control strategy or heuristic rules must be applied to reduce the number of variables when applied to large scale problems. Also, different solutions might be obtained in each trial since they are sensitive to parameter settings. Compared to heuristics, deterministic optimization techniques can obtain robust solutions due to their strong mathematical foundations.

For these reasons, a hybrid approach combining mixed-integer linear programming (MILP) and nonlinear programming (NLP) was chosen as the solution methodology for this work. In the first step, MILP is applied to a plant model that includes linear models for all components and a penalty for turning on or off the boilers and steam chillers. The on and off penalty cost is applied to only the boilers and steam-driven chillers since it requires significant time and cost to bring these components online or offline. The MILP step determines which components need to be turned on and their respective loading that is needed to meet the campus energy demand for the chosen time period (short, medium or long term). Based on the solution from the MILP solver as a starting point, the NLP solver determines the hourly state of operation of each component based on nonlinear performance characteristics of the components. A comparison of MILP solutions with and without the on/off penalty for boilers and steam chillers are examined in this study to analyze their effect on startup/shutdown behavior. The significance of the hybrid approach employed in this study is that a high-quality global solution is determined when the linear model is feasible while still taking into account the nonlinear nature of the problem.

For most optimization algorithms, the approach used to handle constraints can have a significant impact on the quality of the solutions obtained. A deterministic hierarchical network energy flow model as described in section 4.2 along with supervisory control as described in section 0 helps in tackling the constraint problem when there are a large number of decision variables, and linear and nonlinear constraints. Mass and energy conservation were applied to nodes within the network model to develop the energy dispatch algorithm. To determine the optimal operational condition of each equipment in each time step, the MILP and NLP optimization techniques were integrated with the equipment models (including linear and nonlinear characteristics). Plant primary energy use and operational cost depend on decisions regarding generation and/or purchasing of electricity and usage of steam-driven and/or electric equipment in response to time varying factors while meeting the campus electricity, heating and cooling demands. Optimal control of the CCHP plant involves determining the values of the decision variables that minimize the objective function at any time in response to uncontrolled parameters while satisfying all constraints including the campus demands for heating, cooling, and electricity. Given the electrical and thermal (heating and cooling) load behavior of the Purdue campus, the tariff structure for grid-supplied electricity, the price of primary fuel (e.g., natural gas & coal), and the characteristics of the CCHP components and systems, the hybrid optimization

algorithms determine operation of the CCHP plant that minimizes the overall economic objective within the bounds of the constraints (e.g., installed capacities).

4.4   Implementation of MILP-NLP Approach

The solution for minimizing the operating cost while satisfying the heating, cooling, and electrical demand of the Purdue campus was implemented in two steps. In the first step, MILP is used to determine which components are on/off along with the operative variables (load) of each unit needed to meet the campus energy demand for the chosen time horizon (daily, weekly, monthly) with one-hour resolution. In the second step, the solution from MILP is used as a starting point for the NLP solver to determine the hourly state of operation of each component using their nonlinear performance characteristics. For the MILP implementation, two optimization cases are considered for analysis: MILP [no on/off switch penalty (SP)] and MILP [including on/off switch penalty (SP)]. A comparison of the MILP with and without the on/off penalty cost is included to understand the importance of the startup/shutdown operations. However, only the output from MILP that includes the on/off switch penalty (SP) was used in combination with the NLP optimization. The MILP on/off signals are provided as inputs to the NLP approach, since the NLP implementation does not include any switch penalty costs. The entire model was coded in MATLAB (R2019b) and the optimization was carried out using the MATLAB optimization toolbox: branch and bound mixed integer linear program algorithm for the MILP optimization and constrained nonlinear multivariable solver using the interior-point algorithm for the NLP optimization. Both algorithms can handle large-scale problems.

4.4.1   Data required for the model

Time range and resolution play an important role in the planning of CCHP control. The time range can be short, medium or long-term which is daily, weekly, monthly or yearly. The time range can be chosen depending on the planning strategy for the operation of the plant. As for resolution, hourly data is used to meet the demand in this study. Since there is no storage in the model, hourly static optimization is applied for all the cases. For the MILP step, T represents the chosen time range for optimization and t represents the t-th hour of the sample range T ($t \in T$). For the NLP

step, each t-th hour is optimized individually based on the outputs from MILP for every t-th hour.

Data required for the CCHP cost optimization and performance evaluation were obtained from Purdue physical facilities for this study and were inputs to the model. Some of these inputs depend on time such as ambient conditions, demand, market or other factors and they have a different value for each hour (t), such as:

- Hourly energy demand data of Purdue campus for electricity (DE^t), heating (DH^t), and cooling (DC^t)
    - End-use loads vary by application type, building size, location, season, work week, and hour of the day
    - The heating demand (DH^t), includes both high temperature 125 psig steam and low temperature 15 psig steam
- Cost of purchased electricity for every hour (c_E^t)
    - Real-time pricing (RTP) is obtained from the utility 24 hours ahead
- Ambient conditions for every hour
    - Wet-bulb (T_{wb}^t) and dry-bulb (T_{db}^t) temperatures, relative humidity(RH^t)

Other input data are constant over time during the analysis period:

- Price of on-site fuel from the plant operational data
    - Cost of natural gas (c_{NG})
    - Cost of coal (c_C), which includes the cost of limestone, ash handling and so on
- Switch penalty (SP) cost for turning on/off the equipment (c_{SP})
    - Included only in MILP optimization
- Range of "effective" operation of CCHP components for a given installed capacity
    - Minimum and maximum capacity of the equipment

The system model input data consists of chilled water supply set-point $(T_{ev,o})$ and return temperature $(T_{ev,i})$ from campus, pressure of 600 (P_{600}), 125 (P_{125}), 15 (P_{15}) psig steam lines, feedwater (P_{fw}), condensate line (P_{cond}), exhaust from equipment (P_{ex}), condensate return from campus (P_{cr}), and atmosphere (P_{atm}), and temperature of feedwater (T_{fw}) and condensate return

from campus (T_{cr}). In addition, some inputs that are specific for the equipment are defined based on the plant performance data as mentioned in the modeling of the equipment. All the equipment model equations were interconnected according to their physical arrangement in the plant.

The model incorporates some heuristic rules for some of the variations associated with the operation of the power plant as listed below.

- Chillers are controlled to provide identical chilled-water supply temperatures $(T_{ev,o})$. The chilled water supply temperature set-point is 40°F during winter and 43°F during other times of the year.
- A temperature differential of 15°F delta T is assumed between the chilled water supply temperature $(T_{ev,o})$ and return temperature from campus $(T_{ev,i})$.
- Only boilers are operated for the generation of steam. The CHP facility is incorporated in the model for future use, but the values were set to zero because it is currently not in operation.
- Similarly, the steam chiller #1 (S-C1) is currently not in operation. So, the values were set to zero.
- Turbine generators are operated continuously unless they are taken offline for maintenance. So, on/off settings for the turbine generators were disabled in the optimization and they were always operated between their minimum and maximum capacity.

For every hour (t), x^t represents the continuous decision variables and y^t and z^t represent binary variables. $y^t, z^t \in \{0,1\}$ and is applied only in the MILP optimization.

4.5   Mixed Integer Linear Programming (MILP) Formulation

The general formulation of the MILP problem is:

$$min_{x,y} f(x,y) \tag{4.1}$$

$$g_i(x,y) \leq 0; \quad \forall \ i = 1,2,\dots,n_{ieq}$$

$$h_j(x,y) = 0; \quad \forall \ j = 1,2,\dots,n_{eq}$$

$$LB \ \leq \ x,y \ \leq UB \text{ where } x \in \mathbb{R}, y \in \{0,1\}$$

where,

x- vector of real continuous decision variables

y- vector of discrete integer decision variables

$f(x, y)$ - objective function to be minimized over vector x, y

$g_i(x, y)$ - inequality constraints

$h_j(x, y)$ - equality constraints

LB/UB - lower bounds / upper bounds

The main objective function is to minimize the operational cost of running the CCHP system for the total time period (T), while satisfying the total energy demand for every hour (t).

$$
\begin{aligned}
\text{Minimize} \quad Cost(x^t, y^t, z^t) = \sum_{t=1}^{T} \Big[\sum_{i=1}^{3} c_{NG} \, f_{NG,B,i}^t + c_C \, f_{C,B4}^t + c_{NG} \Big(f_{NG,UF}^t + \\
f_{NG,F}^t \Big) + c_E^t \, x_{E,pur}^t + \sum_{i=1}^{4} c_{SP,B,i} \, y_{B,i}^t + \sum_{i=1}^{3} c_{SP,S-C,i} \, y_{S-C,i}^t \Big]
\end{aligned}
$$

(4.2)

where,

c_{NG}- fuel cost of natural gas [\$/DTH]

c_C- fuel cost of coal [\$/ST]

c_E^t- RTP of electricity purchased from utility for time t [\$/kWh]

c_{SP}- switch penalty (SP) cost for both turning on and switching off the boilers and steam chillers [\$]

f_{NG}^t- amount of natural gas consumed by three NG boilers (B), unfired (UF) and fired (F) steam from the CHP facility for time t (DT)

$f_{C,B4}^t$- amount of coal consumed by coal boiler $(B4)$ for time t (ST)

$x_{E,pur}^t$- electricity purchased from utility for time t [kW]

$y_i^t \in \{0,1\}$ - binary variable to indicate the change of state from "on" at time $(t-1)$ to "off" at time t or vice-versa for the i-th boiler (B) and steam chiller $(S-C)$. The current state/availability of the equipment, whether it is on or off is given by binary variable z_i^t.

For the economic objective, only the primary energy costs, purchased electricity cost from grid and penalty cost for turning on/off boilers and steam chillers are considered. Maintenance and life cycle costs of the equipment, labor costs and other auxiliary costs for operation are not considered in the operational cost. Penalties for the startup and shutdown operations are included only for

boilers and steam chillers since it is very difficult to ramp-up and down these units. It takes almost 5 hours to bring a boiler online and 2 hours to shut it down while the steam chiller takes 3 hours for starting and 1 hour for shutting down. Electric chillers and other steam-driven or electric equipment do not take much time for startup and shutdown compared to boilers and steam chillers. No penalty is included for turbine generators since they are never turned on or off under regular operation. The total penalty cost for startup or shutdown was calculated based on the total time for startup or shutdown, total labor cost, total maintenance cost, life cycle cost and reliability cost of the equipment. The penalty costs for on/off operation were estimated to be $700 for natural gas boilers, $4000 for coal boilers and $500 for steam chillers. Even though the CHP facility is not currently operating, unfired and fired steam from the CHP facility is included in the optimization model in order to allow future analyses.

Two types of constraints are considered in this problem, i.e., equality and inequality constraints. The former are mass and energy balance constraints while the latter constraints reflect the limits on heating, cooling and power capacities of each unit. The combinations of continuous control variables of equipment, x_i^t along with discrete control variables, z_i^t indicating the availability of equipment and y_i^t indicating the change of state were implemented within inequality constraints as part of the MILP optimization. The binary variable $z_i^t \in [0,1]$ is used to indicate the current state (on/off - availability) of the i-th equipment (major components like boilers, steam chillers and electric chillers) at time t as they cannot operate continually from 0% partial load. Operating below a minimum capacity of these components might lead to a significant penalty and degradation of equipment performance over time. For these reasons, the availability of the equipment is set to 0 i.e., off when the decision variable goes below a minimum value. This constraint is implemented using disjunctive inequalities (on/off – availability) in the MILP optimization and the availability constraints for the boilers, steam chillers and electric chillers are given by Eq.4.3- Eq.4.5 respectively.

$$z_{B,i}^t \, S_{B,i}^{min} \leq x_{s,B,i}^t \leq z_{B,i}^t \, S_{B,i}^{max} \quad \forall \ i = 1,\dots,4 \tag{4.3}$$

$$z_{S-C,i}^t \, W_{S-C,i}^{min} \leq x_{ev,S-C,i}^t \leq z_{S-C,i}^t \, W_{S-C,i}^{max} \quad \forall \ i = 1,\dots,3 \tag{4.4}$$

$$z_{E-C,i}^t \, W_{E-C,i}^{min} \leq x_{ev,E-C,i}^t \leq z_{E-C,i}^t \, W_{E-C,i}^{max} \quad \forall \ i = 1,\dots,10 \tag{4.5}$$

Here, z_i^t represents state of the i-th equipment at time t (0 when off and 1 when on). Decision variable $x_{s,B,i}^t$ is the mass flow rate of steam produced in the i-th boiler at time t and the availability of boiler is set to 1, i.e., on only when $x_{s,B,i}^t$ is between the minimum $\left(S_{B,i}^{min}\right)$ and maximum $\left(S_{B,i}^{max}\right)$ allowable amount of steam that can be produced in the respective boiler. The minimum $\left(S_{B,i}^{min}\right)$ and maximum $\left(S_{B,i}^{max}\right)$ amount of steam for each boiler is listed as the operating range in Table 3.2. Similarly, $x_{ev,C,i}^t$ is the volumetric flowrate of chilled water produced from the evaporator of the i-th each chiller (steam, $S-C$ or electric, $E-C$) to meet the cooling demand. $W_{C,i}^{min}$ and $W_{C,i}^{max}$ represent the minimum and maximum limits on the water flow across each chiller, respectively. The maximum amount of evaporator water flow $\left(W_{C,i}^{max}\right)$ is listed in Table 3.7 for electric chillers and in Table 3.9 for steam chillers. A 40% minimum flowrate is assumed for all chillers. The on/off availability variable is not added for turbine generators since they are considered to be operating under all circumstances. Even though other auxiliary components like pumps, fans, cooling tower and other equipment have minimum operating capacities, on/off characteristics depending on minimum load were not considered to avoid addition of more variables and constraints, and computational complexity. These components were assumed to operate from 0% to their maximum capacity within the MILP solution. However, the minimum operating range for these components were considered in the NLP optimization.

To combine the binary variable y_i^t indicating the change of state along with z_i^t indicating the availability of equipment, XOR constraints representing the flip of the on/off state [0->1 | 1->0] were implemented for boilers (Eq.4.6- Eq.4.9) and steam chillers (Eq.4.10- Eq.4.13).

$$-z_{B,i}^{t-1} - z_{B,i}^t + y_{B,i}^t \leq 0 \quad \forall \; i = 1, \ldots, 4 \tag{4.6}$$

$$z_{B,i}^{t-1} - z_{B,i}^t - y_{B,i}^t \leq 0 \quad \forall \; i = 1, \ldots, 4 \tag{4.7}$$

$$-z_{B,i}^{t-1} + z_{B,i}^t - y_{B,i}^t \leq 0 \quad \forall \; i = 1, \ldots, 4 \tag{4.8}$$

$$z_{B,i}^{t-1} + z_{B,i}^t + y_{B,i}^t \leq 2 \quad \forall \; i = 1, \ldots, 4 \tag{4.9}$$

$$-z_{S-C,i}^{t-1} - z_{S-C,i}^t + y_{S-C,i}^t \leq 0 \quad \forall \; i = 1, \ldots, 3 \tag{4.10}$$

$$z_{S-C,i}^{t-1} - z_{S-C,i}^t - y_{S-C,i}^t \leq 0 \quad \forall \; i = 1, \ldots, 3 \tag{4.11}$$

$$-z_{S-C,i}^{t-1} + z_{S-C,i}^t - y_{S-C,i}^t \leq 0 \quad \forall \; i = 1, \ldots, 3 \tag{4.12}$$

$$z_{S-C,i}^{t-1} + z_{S-C,i}^t + y_{S-C,i}^t \leq 2 \quad \forall \; i = 1, \ldots, 3 \tag{4.13}$$

$\mathcal{y}_i^t$ of i-th equipment (boiler, B or steam chiller, $S - C$) at time t is set to 0 when z_i^{t-1} and z_i^t have the same values indicating there is no change of state. If z_i^{t-1} and z_i^t have different values [0->1 | 1->0], the $\mathcal{y}_i^t$ is set to 1 indicating a flip of the on/off states. The constraints are applied only to boilers and steam chillers because of their penalty cost for startup and shutdown.

Additional inequality constraints deal with peak capacity limitations of the components and are represented in Eq.4.14 for 10 electric chillers, Eq.4.15 for 3 steam chillers and Eq.4.16- Eq.4.17 for 2 turbine generators. Even though the minimum capacity for chillers is set to 0, the constraints given by Eq.4.4 and Eq.4.5 takes into account the minimum capacity when the chillers are on. The minimum and maximum capacity of the components are listed in the plant component modeling section 3.3.

$$0 \le \dot{Q}_{ev,E-C,i}^t \le \dot{Q}_{ev,E-C,i}^{max} \quad \forall \ i = 1, \dots, 10 \tag{4.14}$$

$$0 \le \dot{Q}_{ev,S-C,i}^t \le \dot{Q}_{ev,S-C,i}^{max} \quad \forall \ i = 1, \dots, 3 \tag{4.15}$$

$$E_{TG1}^{min} \le E_{TG1}^t \le E_{TG1}^{max} \tag{4.16}$$

$$E_{TG2}^{min} \le E_{TG2}^t \le E_{TG2}^{max} \tag{4.17}$$

Some additional constraints on the amount of steam extracted from turbine generators are included so that they don't exceed the inlet throttle steam as shown in Eq.4.18. Also, the maximum amount of steam that can be exhausted from turbine generator #2 cannot exceed 55 klb/h (6.93 kg/s) as shown in Eq.4.19.

$$x_{s,ex1,TG,i}^t \le x_{s,TG,i}^t \quad \forall \ i = 1,2 \tag{4.18}$$

$$x_{s,TG2}^t - x_{s,ex1,TG2}^t \le 6.93 \tag{4.19}$$

The network energy flow model as shown in Figure 4.1, the steam flow described in Figure 3.2 and chilled water flow as depicted in Figure 3.3 are useful in formulating the steady-state equality constraints. The constraints are computed for every hour (t). Eqs.4.20-4.33 represent mass balances across each node in Figure 4.1, assuming no losses and the impacts of those decisions on the supply of energy to meet the campus energy demands. Mass balances for the 600 psig, 125 psig and 15 psig steam line nodes in Figure 4.1 that were described in section 3.2 are

enforced by driving Eqs. 4.20, 4.21 and 4.22 respectively. Eq. 4.23 represent the closure of the steam cycle.

$$\sum_{i=1}^{4} x_{S,B,i}^{t} + x_{S,UF}^{t} + x_{S,F}^{t} - x_{S,TG1}^{t} - x_{S,TG2}^{t} - \sum_{i=1}^{4} \dot{m}_{S,S-FWP,i}^{t} - \sum_{i=1}^{3} \dot{m}_{S,S-CWP,i}^{t} - \\ \dot{m}_{S,S-F,B2_{FD}}^{t} - \dot{m}_{S,S-F,B4_{ID}}^{t} - x_{S,PRV1}^{t} - \dot{m}_{S,S-A1}^{t} = 0 \tag{4.20}$$

$$x_{S,ex1,TG1}^{t} + x_{S,ex1,TG2}^{t} + \sum_{i=1}^{4} \dot{m}_{S,S-FWP,i}^{t} + \sum_{i=1}^{3} \dot{m}_{S,S-CWP,i}^{t} + \dot{m}_{S,S-F,B4_{ID}}^{t} + \\ \dot{m}_{S,PRV1}^{t} - \sum_{i=1}^{3} \dot{m}_{S,S-C,i}^{t} - \dot{m}_{S,S-F,B1_{ID}}^{t} - \dot{m}_{S,S-F,B1_{FD}}^{t} - \dot{m}_{S,S-F,B4_{PA}}^{t} - \dot{m}_{S,125L}^{t} - \\ x_{S,PRV2}^{t} - \dot{m}_{S,FWH,125}^{t} - \dot{m}_{S,S-A2}^{t} = 0 \tag{4.21}$$

$$\left(x_{S,TG2}^{t} - x_{S,ex1,TG2}^{t}\right) + \dot{m}_{S,S-F,B2_{FD}}^{t} + \dot{m}_{S,S-F,B1_{ID}}^{t} + \dot{m}_{S,S-F,B1_{FD}}^{t} + \dot{m}_{S,S-F,B4_{PA}}^{t} + \\ \dot{m}_{S,PRV2}^{t} - \dot{m}_{S,15L}^{t} - \dot{m}_{S,DA,15}^{t} - \dot{m}_{S,S-A3}^{t} = 0 \tag{4.22}$$

$$\dot{m}_{S,DA_{out}}^{t} - \left(\sum_{i=1}^{4} x_{w,S-FWP,i}^{t} + \sum_{i=1}^{3} x_{w,E-FWP,i}^{t}\right)\rho_w = 0 \tag{4.23}$$

In Eq.4.23, $\dot{m}_{S,DA_{out}}^{t}$ is the mass flowrate of feedwater that goes into the steam cycle and is the sum of condensate $(\dot{m}_{cond})$ collected back from campus and various components in the plant, along with the amount of 15 psig steam mixed in the deaerator $(\dot{m}_{DA,15})$ to bring the water to the required feedwater temperature and any makeup water added to compensate for any losses. This is equal to the mass flowrate of feedwater that goes into the steam cycle. Note that ρ_w is the density of water to convert volumetric flow rate to mass flow rate.

The amount of steam generated by the boiler and CHP facility is equal to the mass flowrate of feedwater pumped into them by feedwater pumps, assuming no losses. Some feedwater is sprayed to control the outlet steam temperature of PRV.

$$\left(\sum_{i=1}^{4} x_{w,S-FWP,i}^{t} + \sum_{i=1}^{3} x_{w,E-FWP,i}^{t}\right)\rho_w - \sum_{i=1}^{4} x_{S,B,i}^{t} - x_{S,UF}^{t} - x_{S,F}^{t} - \\ \sum_{i=1}^{2} \dot{m}_{fw,PRV,i}^{t} = 0 \tag{4.24}$$

The total evaporator water flow from all the chillers is equal to the volumetric flow rate of chilled water sent to campus by chilled water pumps. Mass balances across the Wade plant and NWCP are considered separately.

$$\sum_{i=1}^{3} x_{ev,S-C,W,i}^{t} + \sum_{i=1}^{4} x_{ev,E-C,W,i}^{t} - \sum_{i=1}^{3} x_{w,S-CWP,W,i}^{t} - \sum_{i=1}^{4} x_{w,E-CWP,W,i}^{t} = 0 \tag{4.25}$$

$$\sum_{i=1}^{6} x_{ev,E-C,NW,i}^{t} - \sum_{i=1}^{6} x_{w,E-CWP,NW,i}^{t} = 0 \tag{4.26}$$

The total volume flow rate of condenser water pumps is equal to the condenser water flow to all chillers and TG1 in the Wade plant as shown in Eq.4.27 and the chillers in the NWCP as shown in Eq.4.28.

$$\sum_{i=1}^{3} x_{co,S-C,W,i}^t + \sum_{i=1}^{4} x_{co,E-C,W,i}^t + \left(\dot{m}_{co,TG1}^t / \rho_w\right) - \sum_{i=1}^{6} x_{w,E-COWP,W,i}^t = 0 \qquad (4.27)$$

$$\sum_{i=1}^{6} x_{co,E-C,NW,i}^t - \sum_{i=1}^{6} x_{w,E-COWP,NW,i}^t = 0 \qquad (4.28)$$

The water from all the condensers is equal to the sum of tower cell inlet water flow rates.

$$\sum_{i=1}^{3} x_{co,S-C,W,i}^t + \sum_{i=1}^{4} x_{co,E-C,W,i}^t + \left(\dot{m}_{co,TG1}^t / \rho_w\right) - \sum_{j=1}^{6} x_{w,CT,i,W,j}^t = 0 \qquad (4.29)$$

$$\sum_{i=1}^{6} x_{co,E-C,NW,i}^t - \sum_{j=1}^{3} x_{w,CT,i,NWCon,j}^t - \sum_{j=1}^{9} x_{w,CT,i,NWMet,j}^t = 0 \qquad (4.30)$$

Energy balances on the heating, cooling and electricity demand nodes in Figure 4.1 are also treated as constraints so that the differences in supply and demand for campus heating (DH^t), cooling (DC^t) and electricity (DE) are driven to zero using Eqs.4.31-4.33.

$$DH^t - H_{125}^t - H_{15}^t = 0 \qquad (4.31)$$

$$DC^t - \sum_{i=1}^{3} \dot{Q}_{ev,S-C,W,i}^t - \sum_{i=1}^{4} \dot{Q}_{ev,E-C,W,i}^t - \sum_{i=1}^{6} \dot{Q}_{ev,E-C,NW,i}^t = 0 \qquad (4.32)$$

$$
\begin{aligned}
& DE^t + \sum_{i=1}^{4} P_{E-C,W,i}^t + \sum_{i=1}^{6} P_{E-C,NW,i}^t + \sum_{i=1}^{6} P_{CT,W,i}^t + \sum_{i=1}^{12} P_{CT,NW,i}^t + \\
& \sum_{i=1}^{3} P_{E-FWP,i}^t + \sum_{i=1}^{4} P_{E-CWP,W,i}^t + \sum_{i=1}^{6} P_{E-CWP,NW,i}^t + \sum_{i=1}^{6} P_{E-COWP,W,i}^t + \\
& \sum_{i=1}^{6} P_{E-COWP,NW,i}^t + P_{E-F,B1_{ID}}^t + P_{E-F,B1_{FD}}^t + P_{E-F,B2_{FD}}^t + P_{E-F,B3_{FD}}^t + P_{E-F,B4_{ID}}^t + \\
& P_{E-F,B4_{PA}}^t + P_{E-F,B4_{SA}}^t + P_{E-A}^t - x_{E,pur}^t - \sum_{i=1}^{2} E_{TG,i}^t = 0
\end{aligned}
\qquad (4.33)
$$

The heating demand (DH^t) of the campus at every hour is satisfied by heating provided by steam from 125 psig and 15 psig steam lines. The cooling demand (DC^t) of campus is met by Wade steam chillers and electric chillers at Wade and NWCP. The purchased electricity ($x_{E,pur}^t$) and electricity generated by the two turbine generators provide electricity to meet campus electrical demand (DE^t) and demand from all electric components in the plant.

    The main goal of the MILP optimization is to determine which components must be operated along with load to meet the campus energy demand. For the sake of simplicity, operating temperatures are given as constant inputs to the MILP optimization to avoid nonlinearities in the

model. The temperatures of the steam lines: T_{600}, T_{125}, T_{15} and T_{cond} were specified from plant performance data. The condenser water inlet temperature $(T_{co,i})$ is the tower cell leaving water temperature and is determined using Eq.3.48. The inlet temperature of water to the cooling tower cell $(T_{CT,i})$ is the water outlet temperature from condensers and is determined by assuming a constant ΔT to inlet and outlet temperature to the condenser.

The MILP framework of the CCHP model is complex and involves 100 design variables out of which 76 are continuous variables and 24 are binary variables. There are 14 equality constraints and 75 inequality constraints. The minimum and maximum limitations of decision variables are included as lower and upper bounds in the model. The minimum is set as 0 for all decision variables for the MILP model to indicate its availability. Realistic limitations on minimum capacity are included in the NILP step of the optimization. The objective function and equality and inequality constraints includes the linear mathematical model of each component in the plant along with the thermodynamic system model. The optimal energy dispatch algorithm provides operational signals associated with resource allocation and minimizes the total operational cost for time period (T), while satisfying the total energy demand for every hour (t). The results from the MILP optimization are given as a starting point for NLP optimization.

4.6 Nonlinear Programming (NLP) Formulation

The general formulation of the NLP problem is very similar to MILP problem as shown in Eq.4.1 except that it does not include any discrete integer decision variables (y). So, the objective function to minimize the operational cost of running the CCHP system is reduced to:

$$\text{Min} \quad Cost(x^t) = \sum_{i=1}^{3} c_{NG} f_{NG,B,i}^t + c_C f_{C,B4}^t + c_{NG} \left(f_{NG,UF}^t + f_{NG,F}^t \right) + c_E^t x_{E,pur}^t \qquad (4.34)$$

The outputs from the MILP step for every t-th hour are given as inputs to NLP optimization and the economic dispatch is determined for that particular hour. From the MILP output, if the output values of decision variables are 0, the equipment is set to OFF for that hour by setting the lower and upper bounds of the decision variables to 0 in the NLP framework. If the output decision variables have values greater than 0 from the MILP optimization, then the equipment is considered ON in the NLP framework and the lower bounds are set to the minimum and maximum capacities

at which the equipment can be operated without any disruption. In this way, the equipment to meet the campus demand is selected from the MILP optimization and every equipment is operated under the best possible efficiency within its upper and lower limits using the NLP optimization. The constraints on disjunctive inequalities (on/off – availability) and XOR constraints representing flip of the on/off state are not included in the NLP optimization framework. All 14 equality constraints from Eq.4.20-Eq.4.33 are included in NLP framework similar to MILP problem.

For the NLP optimization, inlet temperature of water to the cooling tower cell $(T_{CT,i})$ is determined using Eq.3.85-Eq.3.86 and condenser water inlet temperature $(T_{co,i})$ is determined using Eq.3.83-Eq.3.84 for Wade and NWCP. The constraints for calculating these temperatures are:

$$x_{T,co,i}^t - T_{co,i}^t = 0 \tag{4.35}$$

$$x_{T,CT,i}^t - T_{CT,i}^t = 0 \tag{4.36}$$

$$x_{T,co,i}^t \leq x_{T,CT,i}^t \tag{4.37}$$

The temperatures for the steam lines: T_{600}, T_{125}, T_{15} and T_{cond} are calculated using Eq.3.79-Eq.3.82.

In the NLP formulation, additional variables and constraints are included beyond those considered for the MILP due to the nonlinearities of the components. Overall, there are 111 decision variables, 30 nonlinear inequality constraints, 18 nonlinear equality constraints and 7 linear inequality constraints. The minimum and maximum limitations of decision variables are included as lower and upper bounds in the model. The NLP optimization algorithm provides operational signals to each component to meet the total energy demand for every hour (t).

4.7   Chapter Summary

This chapter described the implementation of the MILP-NLP approach along with the network energy flow model, objective function, and constraints. The models were coded in MATLAB (R2019b) and solved using the MATLAB optimization toolbox. There are some differences in the framework of MILP and NLP optimization based on how they are formulated.

5. RESULTS AND DISCUSSION

This chapter presents results obtained using the proposed hybrid mixed-integer linear programming (MILP) and nonlinear programming (NLP) approach for cost optimal control of the Purdue CCHP system. Typical four-season weather data for 24-hour periods was chosen for analysis. Since there is no thermal storage in the plant model, hourly static optimization was applied for all the cases. As discussed in the previous sections, the objective function and constraints along with the mathematical model of the components in the CCHP plant are included within the hybrid MILP and NLP optimization framework. Figure 5.1 shows a schematic of the implementation of the hybrid MILP-NLP algorithm in a two-step process. In the first step, the MILP solver is applied to the plant model that includes linear models for all components, constraints, and cost penalties for turning on and off the boilers and steam chillers. The MILP step determines which components need to be turned on and their respective loading needed to meet the campus energy demand for the chosen time horizon with one-hour resolution. In the second step, the solution from the MILP solver is used as a starting point for NLP optimization to determine the hourly state of operation of components including their nonlinear performance characteristic curves. To validate the effectiveness of the hybrid network flow algorithm for large-scale CCHP systems, different time ranges (daily, weekly, monthly) are simulated with hourly resolution.

For the MILP step, T represents the chosen time range for optimization and t represents the t-th hour of the sample range T $(t \in T)$. For the NLP step, each t-th hour is optimized individually based on the outputs from MILP for every t-th hour. For MILP implementation in the first step, two optimization cases are considered for analysis: MILP with no on/off switch penalties (SP) and MILP including on/off switch penalties (SP). A comparison of MILP with and without the on/off penalty costs for units is examined to analyze the effects of considering these penalties on the startup/shutdown operations and overall performance. Without the on/off penalty costs, the MILP solver allows boilers and steam-driven chillers to turn on or off frequently depending on the current energy demand, which is impossible for practical operation of any CCHP plant. The on/off states of these components from the MILP step are provided along with other

outputs as inputs to the NLP optimization model. The NLP step does not include on/off equipment determination in its control optimization.

The optimal energy dispatch algorithm provides operational signals associated with resource allocation ensuring that the systems meet campus electricity, heating, and cooling demands. The entire model is coded in MATLAB (R2019b) and is optimized using the MATLAB optimization toolbox: branch and bound mixed integer linear program algorithm for MILP optimization and constrained nonlinear multivariable solver using the interior-point algorithm for NLP optimization. The optimal results from the MILP and NLP approach are compared with the conventional operational strategy (plant data) on a daily basis for different seasons in order to understand the optimal control characteristics and its economic benefits.
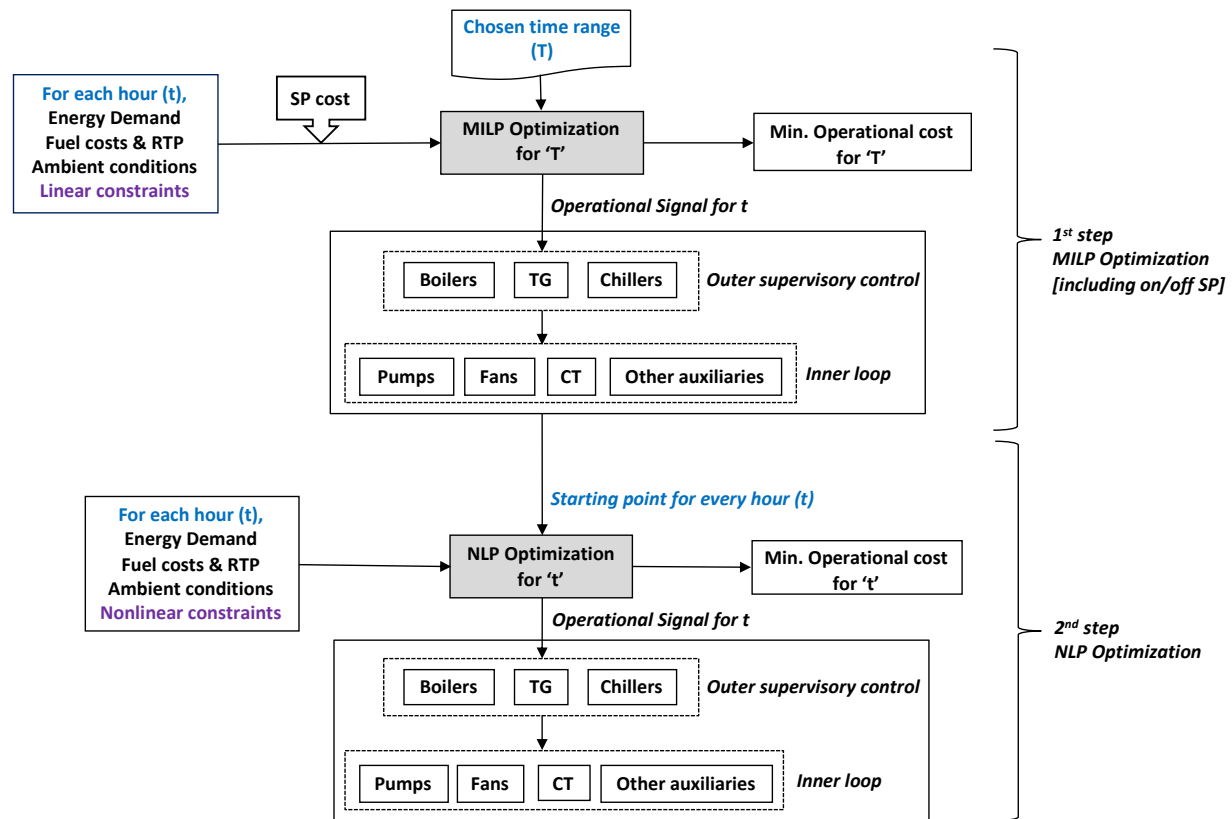
Figure 5.1. Schematic of the two-step hybrid MILP-NLP approach

5.1 Integrated Hourly Model

Example optimizations were performed for 24-hour (one day) periods with known cooling, heating, electricity demand, and real-time pricing (RTP) of electricity for the Purdue campus. The one-day simulations were performed with hourly intervals for each season to understand differences in control behavior with different campus load requirements. Variations in the energy loads are primarily due to seasonal variations which depend on ambient temperature and work schedules based on the day and school session type (e.g., weekends, weekdays, holidays, semester, semester break, summer school, Maymester, etc).

The different seasonal case studies are described as Case (a): Spring and Case; (b): Fall (moderate heating and cooling demand); Case (c): Summer (high cooling demand); Case (d): Winter (high heating demand)] as shown in Table 5.1. Weekdays were considered for all four scenarios with the school fully in session. The same scenarios were used as representative days for plant validation in section 3.4. Figure 3.12 showed the hourly heating, cooling, and electrical demand of the Purdue campus for each 24-hour period given as input data to the optimization model for the four different scenarios. In all four cases, the average electrical demand of the Purdue campus did not differ much compared to the variations of heating and cooling demand for the different seasons. Figure 5.2 shows the corresponding real-time price (RTP) of purchased electricity from the utility, also given as input data for each 24-hour time period in the four different scenarios. The RTP of purchased electricity typically increases with demand during the day. In Figure 5.2(d), it can be observed that the RTP of purchased electricity is extremely high during that particular day in winter because of severely low outdoor air temperature (OAT). The price of natural gas and coal from the plant operational data are listed in Table 5.1 for different seasons. The cost of coal includes the cost of limestone, ash handling, and so on. The penalty costs for turning on and off the boilers and steam chillers are given as inputs to the MILP optimization with the following values used for this case study: $700 for natural gas boilers; $4000 for coal boilers; $500 for steam chillers. The hourly ambient conditions are also provided as inputs to the hybrid MILP-NLP model.

Table 5.1. Purdue campus energy demand scenarios for various seasons

Season	Date	Avg. OAT °F (°C)	Avg. Cooling Load, MW (Tons)	Avg. Heating Load, MW (MMBtu/h)	Avg. Electrical Load, MW	Cost of coal ($/ST)	Cost of NG ($/DTH)
(a) Spring	04/20/2016	63 (17.2)	37.7 (10724)	22.9 (78.3)	28.2	70.8	3.0
(b) Fall	10/18/2017	57 (13.9)	30.8 (8758)	35.4 (120.8)	28.2	72.0	3.5
(c) Summer	08/27/2018	84 (28.9)	93 (26444)	24 (81.9)	30	72.0	3.5
(d) Winter	02/18/2015	2.4 (-16.4)	15 (4265)	151(515)	29	87.0	4.6
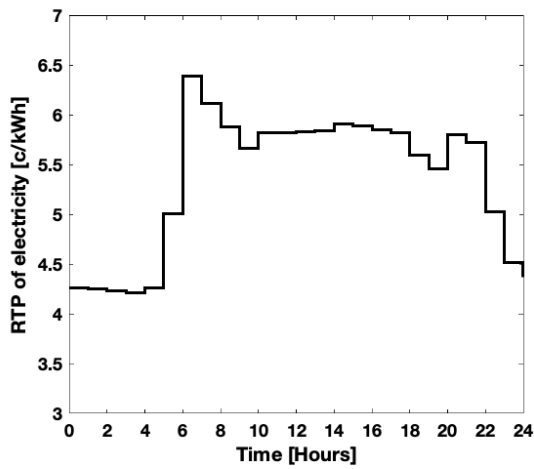
(a) Spring
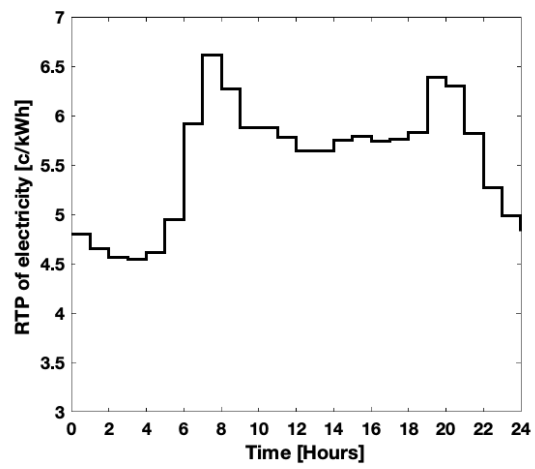
(b) Fall
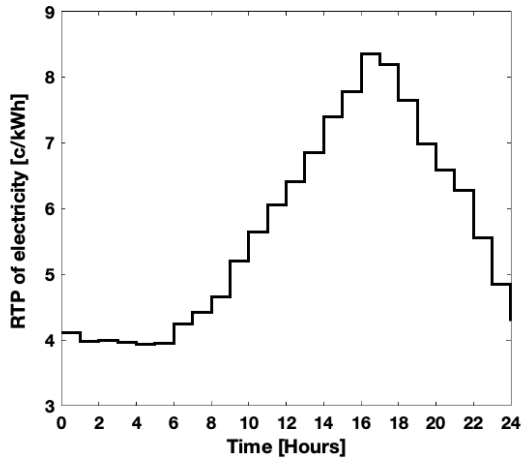
(c) Summer
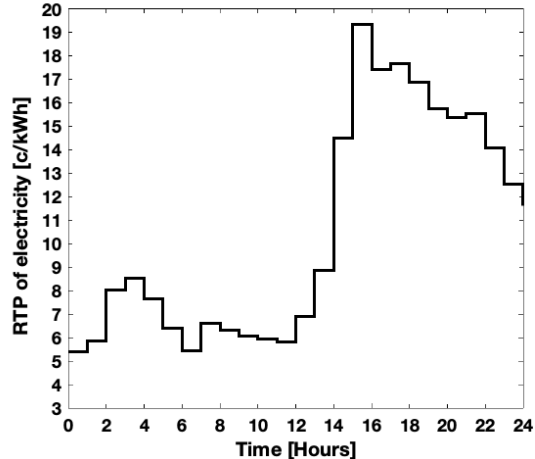
(d) Winter

Figure 5.2. Real-time price (RTP) of purchased electricity from utility

Figure 5.3 shows both inputs to and outputs from the MILP [without on/off switch penalty (SP)]; MILP [including on/off switch penalty (SP)] and the NLP solvers for the 24-hour period in spring. The optimization results are also compared with plant model predictions associated with the control decisions that were actually implemented for the 24-hour period. The input data in Figure 5.3(a) is the heating (DH), cooling (DC) and electrical demand (DE) of the Purdue campus and the outdoor air temperature (OAT) for April 20, 2016. It can be observed that the cooling demand tracks the variation in OAT. Figure 5.3(b) shows the hourly real-time pricing (RTP) of purchased electricity from utility. The input demand and RTP plots are repeated here for easy correlation with the output results.

The end-use decisions from the actual plant data that are shown in Figure 5.3 (e.g., steam produced in each boiler, electricity produced, electricity purchased, chilled water from electric chiller, chilled water from steam chillers) were provided as inputs to the cost function to estimate total operational cost for the current control in the plant. This "actual" plant operational data is used as the baseline for comparison with optimization results. Three optimization cases were considered for analysis: MILP [no on/off switch penalty (SP)]; MILP [including on/off switch penalty (SP)] and NLP optimization.

From Figure 5.3(c), it can be noticed that the total operational cost for cost optimized control is always less than the cost for current practice. Also, the NLP typically results in significantly lower hourly costs than the MILP except at low loads. Not surprisingly, the operational cost of the MILP without on/off switching penalties is lower than the MILP that includes on/off penalties. This is because the lack of a switching penalty allows the equipment to cycle on/off as needed to better optimize the use of the more efficient equipment. However, the differences between the costs are small. It is interesting to note that the cost calculated for both MILP cases are comparatively less than the NLP optimization results at lower energy demand periods (hours 1-4). This is because the MILP doesn't account for the reduction in efficiency at lower loads, whereas the NLP optimization accounts for the reduction of efficiency at lower loads leading to higher costs compared to MILP during these low-load time periods.

Figure 5.3(d) shows the total amount of steam produced in the boilers for the actual plant data and optimization results. It can be observed that more steam would have been produced for

the cost optimized operation at higher electricity demand with the additional steam being primarily used for operation of turbine generators to generate more electricity and for steam chillers to meet the cooling demand with less loading on electrical chillers. In the actual operation of power plant, the amount of steam produced from the boilers did not vary much throughout the day. For the MILP and NLP results, the amount of steam generated by the boilers increases or decreases in response to changes in heating demand and RTP signals.

Figure 5.3(e) and Figure 5.3(f) show comparisons of actual operation with the cost optimum results for the electricity produced from turbine generators and electricity purchased from utility respectively. The optimum results predict that more electricity should have been generated compared to the actual operation to meet the total electrical demand (campus electricity demand and demand from electric components) especially when the RTP goes above 5 ¢/kWh. However, the optimization still leads to purchasing of some electricity at higher RTP due to the constraint on the extraction steam from turbines for the campus heating demand. Apart from meeting campus electrical demand, the combination of produced and purchased electricity is used to meet the demand from all electric equipment in the plant. When the demand is high, it can be observed from the NLP optimization results that the turbine generators are operated at a higher load where its efficiency is maximum resulting in the increase in power generation. The mutual dependency of electricity production and steam requirements for the turbine generator limits the electricity generation due to requirement of meeting the campus heating demand. In this case, the rest of the electricity is purchased to meet additional electrical demand.

Figure 5.3(g) and Figure 5.3(h) show comparisons of cooling provided by the steam and electric chillers. For the actual operation, all the campus cooling demand was satisfied using only the electric chillers. The cost optimum results suggest the usage of both electric and steam chillers, with a greater portion of the campus load allocated to the steam chillers. It can be observed that with the MILP having no switching penalties, the steam and electric chillers are turned off and then on for short periods of time, which would not occur in practice. On the other hand, the MILP with switching penalties does not allow this behavior and would only allow these chillers to turn off for longer periods of time when it is profitable to do so. For these results, the MILP with switching penalties maintains operation of the chillers even at low loads. For the NLP optimization, the chillers are operated at their optimum load maximizing their efficiency when the

cooling demand is high. From these plots, it can be noticed that at hour-6 when the RTP increases sharply, there is a dramatic in decrease in purchased electricity and electric chiller operation and an increase in electricity being generated at the plant and use of steam chillers. As a result, more steam is generated from the boilers to serve these steam-driven components. Similarly, a reverse trend is observed at hour-19. The NLP solutions have greater fluctuations in the results compared to the MILP solutions. The non-smooth nature of the NLP optimization curves is mainly due to the combination of nonlinearities of all the equipment included in the model.

Since the on/off switch penalty cost is included only for boilers and steam chillers, the operation of these units is analyzed further. Figure 5.4 shows outputs of individual boilers and steam-driven chillers for the MILP (without on/off switch penalty); MILP (including on/off switch penalty) and NLP optimization compared with the baseline plant performance for the 24-hour period in spring. From these plots, it can be observed that the MILP with no switching penalties allows the components (both boilers and steam chillers) to turn off and on for relatively short periods depending on the changes in demand and RTP signals. However, MILP with switching penalties maintains the on or off status for all of the equipment throughout the 24-hour period since it is not profitable to turn off and bring the equipment online during such a short time horizon. A longer time period would be necessary for the system to recoup the costs of bringing any of this equipment offline or online. Instead, the components are operated at low load instead of turning off when the demand goes low. Since the output from MILP with the switching penalties is given as an input to NLP optimization for every hour, the trends for both solutions are very similar. When the equipment load increases with energy demand, the NLP optimization finds an optimum load at which the equipment can be operated at its maximum possible efficiency while still meeting the demand. For this 24-hour period in spring, the coal boiler does not operate due to high operational cost compared to that of the natural gas boilers, and all the demand was met using the natural gas boilers. For the actual plant operation, only two natural gas boilers were used, whereas the optimized results include the usage of an additional natural gas boiler due to a need for more steam production. The selection between coal and natural gas boilers depends on fuel cost, boiler efficiencies, their operating conditions, associated auxiliaries with the boilers and total steam demand which play a major role in assessing the economic benefits. Similar factors are important for selection between steam and electric chillers to meet the campus cooing demand.
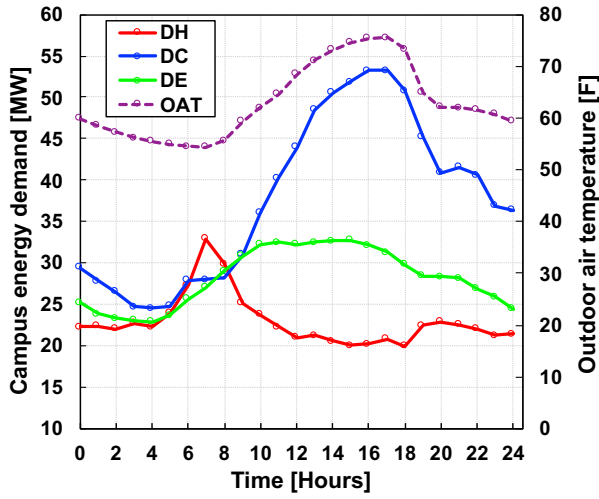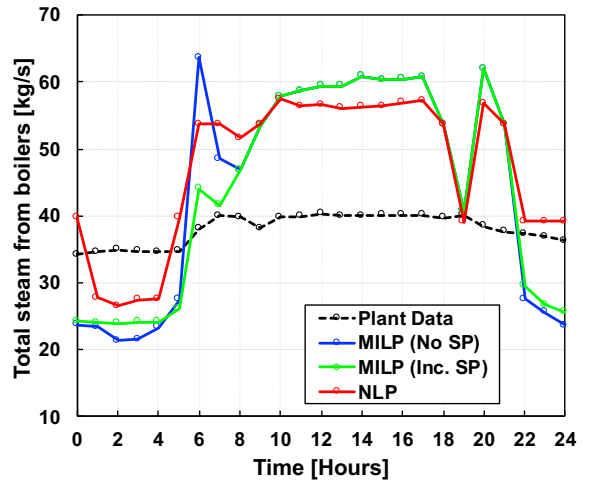
(a) Energy demand of Purdue campus and outdoor air temperature
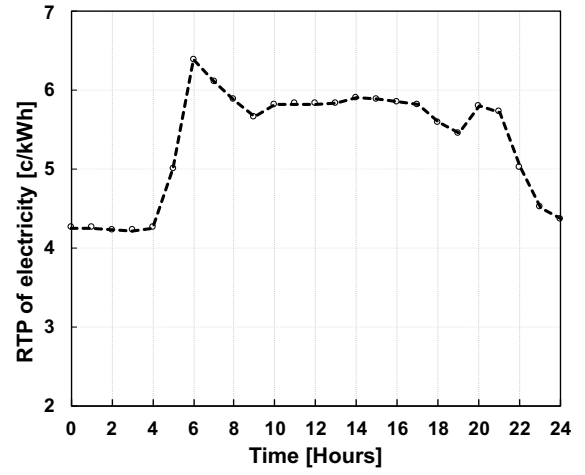
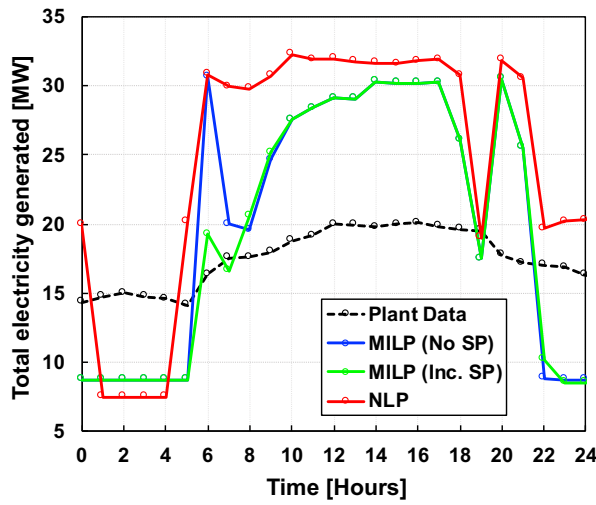(b) Real-time price of purchased electricity from utility
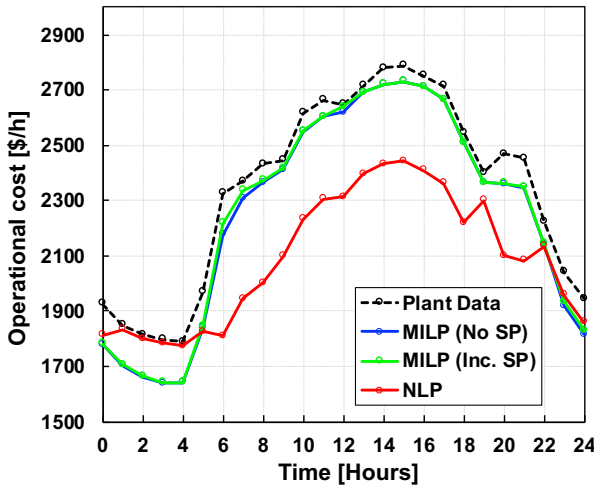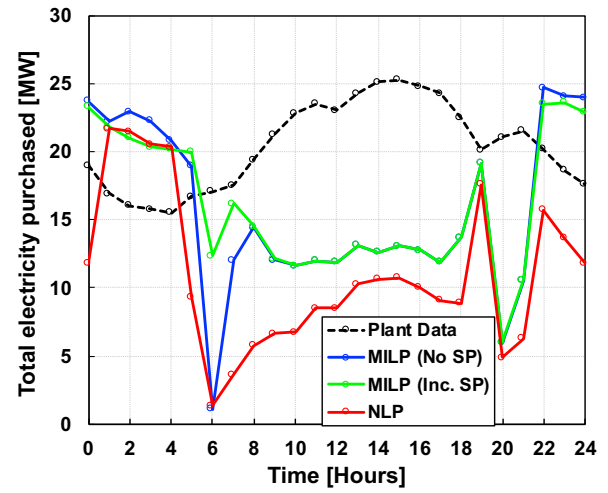
(c) Total operational cost

(d) Total steam produced from boilers

Figure 5.3. Input to the optimization model and Output from MILP (without on/off switch penalty); MILP (including on/off switch penalty) and NLP optimization compared with the actual plant data for 24-hour period [Case (a): Spring]
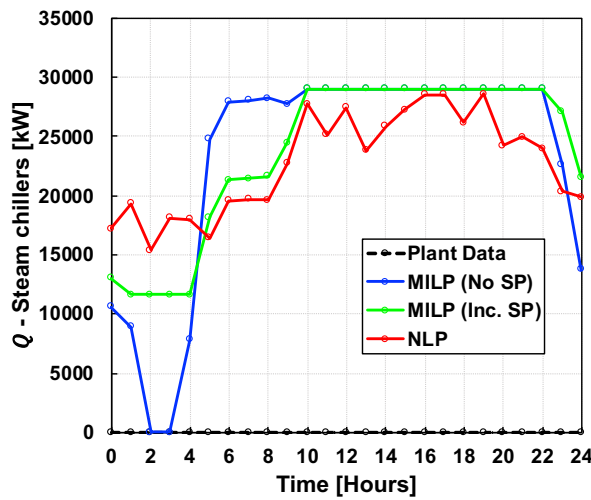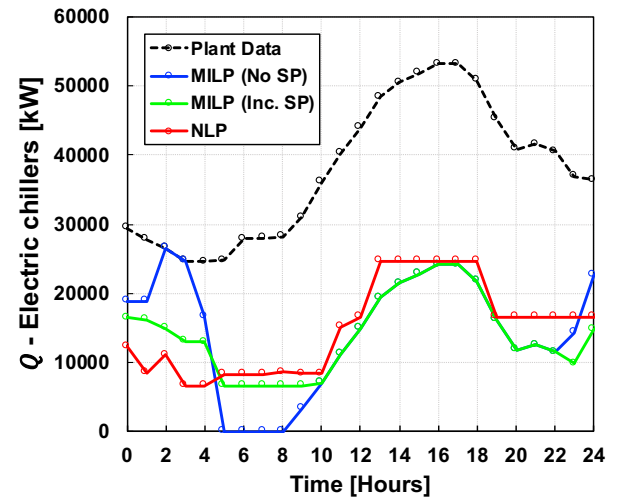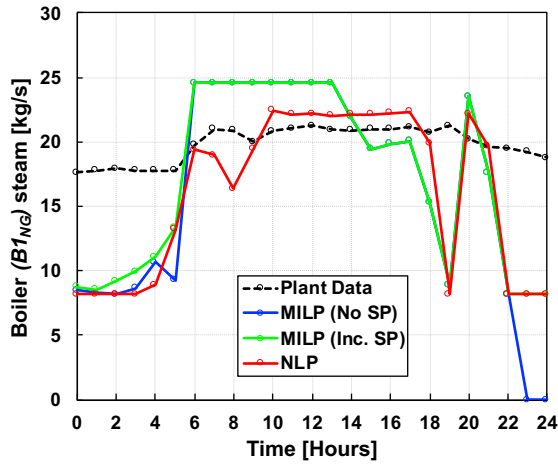
122

Figure 5.3 continued

(e) Amount of electricity generated

(f) Amount of electricity purchased

(g) Cooling capacity from steam chillers

(h) Cooling capacity from electric chillers

(a) Steam from Boiler #1 (B1)
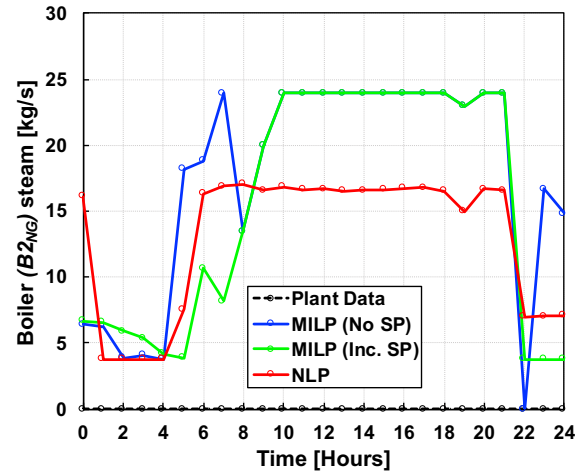
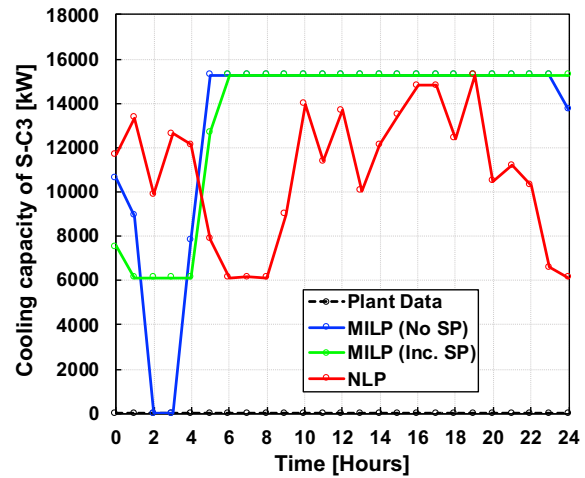(b) Steam from Boiler #2 (B2)
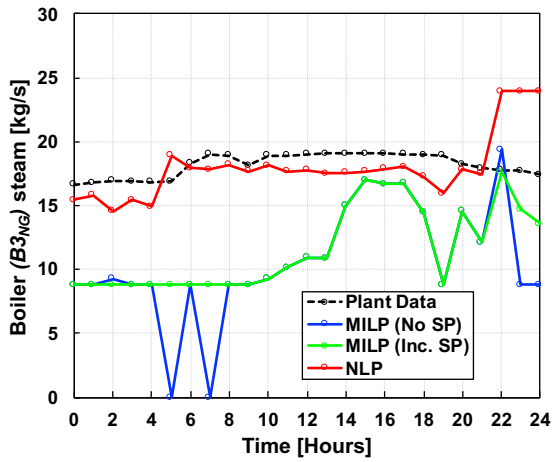
(c) Steam from Boiler #3 (B3)
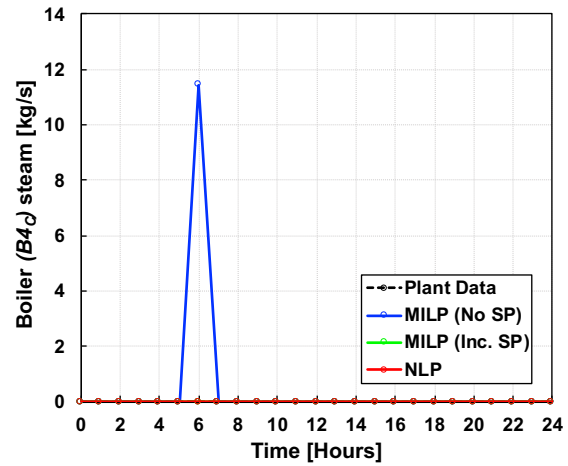
(d) Steam from Boiler #4 (B4)

Figure 5.4. Output of individual boilers and steam chillers for MILP (without on/off switch penalty); MILP (including on/off switch penalty) and NLP optimization compared with the actual plant data for 24-hour period [Case (a): Spring]

Figure 5.4 continued
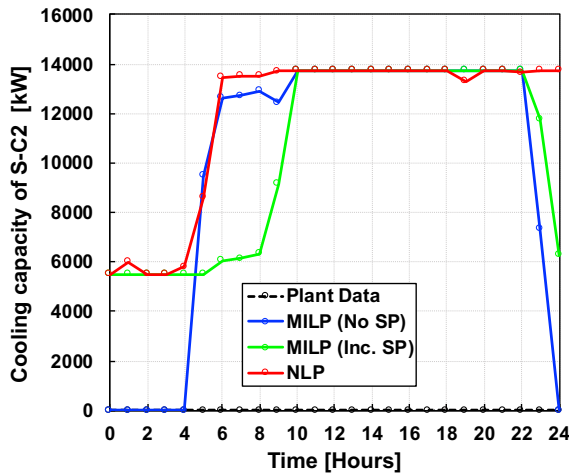
(e) Cooling capacity of steam chiller #2 (S-C2)

(f) Cooling capacity of steam chiller #3 (SC3)

Table 5.2 gives a summary of comparisons between baseline plant performance and optimized results for this integrated 24-hour period in spring. As shown previously, both the MILP and NLP optimizations result in production of more steam from boilers, more electricity generation from turbine generators, less purchasing of electricity especially when the RTP costs are high and more chilled water production from steam chillers. Natural gas boilers are preferred compared to coal boilers due to lower fuel cost of natural gas than coal. Cost optimization using the MILP with no switching penalties resulted in about 3.7% cost savings, MILP switching penalties gave about 3.5% cost savings while the NLP optimization led to almost 10.7% cost savings compared to the baseline plant costs for the current control approach. The opportunities for cost savings through optimal control are very significant with over $6200 in savings for a single day in spring.

Daily results for Case (b): Fall; Case (c): Summer; and Case (d): Winter are given in Table 5.3, Table 5.4, and Table 5.5 respectively. The savings are significant for all four seasons but depend strongly on the how different equipment in the power plant was operated under the baseline controls, which varies over time. The decisions on the amount of steam produced, electricity

generated and/or purchased, use of steam chillers or electric chillers depend on many time-varying factors such as energy demand, RTP costs, fuel prices, OAT, and equipment capacity constraints. For the fall day, even though the RTP costs and energy demand trend are similar to those for spring with moderate heating and cooling demand, the fuel costs for coal and natural gas are higher as shown in Table 5.1. It can be observed from Table 5.3 that more electricity was purchased compared to the baseline plant performance because of higher costs for coal and natural gas compared to spring. For the same reasons, the optimization results suggest purchasing more electricity and generating less steam compared to the baseline behavior for the summer day. From Table 5.5 for winter, it can be noted that there is not much savings from the optimization results compared to the baseline plant. For both baseline operation and optimization cases, PRVs were operated to meet the high heating demand. The opportunities for optimization are minimal since all the components are operated at their maximum capacity to meet the high demand.

Table 5.2. Comparison between current operation and optimized results [Case (a): Spring]

For 24 Hours	Plant data	MILP (w/o on/off penalty)	MILP (w/ on/off penalty)	NLP
Steam produced [klb]	7544	8871	8746	9331
Total electricity generated [MWh]	439	508	496	619
Total electricity purchased [MWh]	510	392	400	276
Total cooling capacity of steam chillers [MWh]	0	578	592	568
Total cooling capacity of electric chillers [MWh]	943	365	350	375
Total operational cost [$]	58,466	56,277	56,437	52,229
Total cost savings [$]		**2189 [3.7%]**	**2029 [3.5%]**	**6237 [10.7%]**

Table 5.3. Comparison between current operation and optimized results [Case (b): Fall]

For 24 Hours	Plant data	MILP (w/o on/off penalty)	MILP (w/ on/off penalty)	NLP
Steam produced [klb]	7994	5849	6177	6797
Total electricity generated [MWh]	500	260	275	343
Total electricity purchased [MWh]	443	605	588	518
Total cooling capacity from steam chillers [MWh]	0	460	523	470
Total cooling capacity from electric chillers [MWh]	771	310	247	300
Total operational cost [$]	62,537	61,490	62,027	61,655
Total cost savings [$]		**1047 1.7%**	**510 0.8%**	**882 1.4%**

Table 5.4. Comparison between current operation and optimized results [Case (c): Summer]

For 24 Hours	Plant data	MILP (w/o on/off penalty)	MILP (w/ on/off penalty)	NLP
Steam produced [klb]	10292	7484	7671	9142
Total electricity generated [MWh]	589	409	405	523
Total electricity purchased [MWh]	627	822	813	639
Total cooling capacity from steam chillers [MWh]	760	548	665	703
Total cooling capacity from electric chillers [MWh]	1558	1770	1653	1496
Total operational cost [$]	85,066	80,493	80,846	78,898
Total cost savings [$]		**4573 5.4%**	**4220 5.0%**	**6168 7.3%**

Table 5.5. Comparison between current operation and optimized results [Case (d): Winter]

For 24 Hours	Plant data	MILP (w/o on/off penalty)	MILP (w/ on/off penalty)	NLP
Steam produced [klb]	12733	13983	14349	14526
Total electricity generated [MWh]	455	476	485	497
Total electricity purchased [MWh]	427	406	383	395
Total cooling capacity from steam chillers [MWh]	0	239	337	346
Total cooling capacity from electric chillers [MWh]	385	146	48	39
Total operational cost [$]	125,004	123,664	124,372	122,857
Total cost savings [$]		**1340 1.1%**	**632.88 0.5%**	**2147 1.7%**

From the above-mentioned simulation results, a few observations have been made from the baseline behavior and optimization results that could improve the performance of the plant and increase cost savings.

- Limited use of steam chillers is observed from the actual plant data. Cost benefits can be achieved by utilizing the steam chillers to generate chilled water when the RTP costs are higher during the daytime.

- More electricity can be purchased when the RTP costs are lower during the nighttime and early morning hours to meet the electrical demand. During these times, boilers, steam chillers and turbine generators can be operated at minimum loads to maximize the purchased electricity and electrically driven equipment.

- When the energy demand is high, the equipment loads can be balanced to maximum efficiency.

- Coal boilers should only be operated during winter months when the steam demand is really high. It is not profitable to run the coal boiler during other seasons when the cost of natural gas is below $3.3/DTH due to higher cost of coal and cost of running all the associated fans of the coal boiler.

The advantage of using this hybrid algorithm is that it provides a more realistic and viable control of the operation of all equipment in the CCHP plant with lower operational cost compared to the actual plant data. The binary on/off capability of MILP optimization allows the selection of

necessary components from the pool of available components in the CCHP plant to meet the campus energy demand while minimizing the total operational cost for the chosen time horizon. By including the penalty cost for startup and shutdown, it ensures the component is not turned on or off immediately within a short time period which is similar to the practical operation of the power plant. Instead, the components are operated at low load when the demand decreases instead of turning off and turning on when the demand increases. Even though the decisions on the change of state of the equipment depends on the increase or decrease in demand, total operational cost play a major role in determining whether it is profitable to turn off and bring the equipment online during that time range. The approximate solutions for the operative variables (load) of each component for every hour from MILP [including on/off SP] optimization serves as a good initial point for optimizing the performance of selected components using NLP solver. The nonlinear characteristics curves of the components included in the NLP framework provides the actual state of operation of the selected components optimized for the lowest possible operational cost for the current hour while still meeting the demand and other operational constraints. The NLP optimization is very sensitive to the components selected and initial values provided by the MILP optimization.

5.2 Simulations for Different Time Ranges

The time period for the optimization plays a critical role in the optimization solution for a CCHP. It could be daily, weekly, monthly or longer depending on when short, medium or long-term scheduling decisions are made. Depending on the penalties associated with turning equipment on or off, different optimization periods could lead to different choices of equipment or on/off timing for equipment. Weekly and monthly optimization periods were chosen to analyze the sensitivity of optimization results. In order to study this issue, the MILP with and without switching penalties was employed. Three different time periods were considered for this study [1 week, 1 month, 3 months] starting from September (early Fall), moving into October/November (Fall) and extending till December (into Winter). The input to the cost optimization model includes time-varying energy demand of the Purdue campus, OAT and RTP costs of purchased electricity. The price of natural gas was set as 3.00 $/DTH and the cost of coal as 70.80 $/ST from plant operational specifications. The time-varying inputs to the optimization model are shown in Figure 5.5.
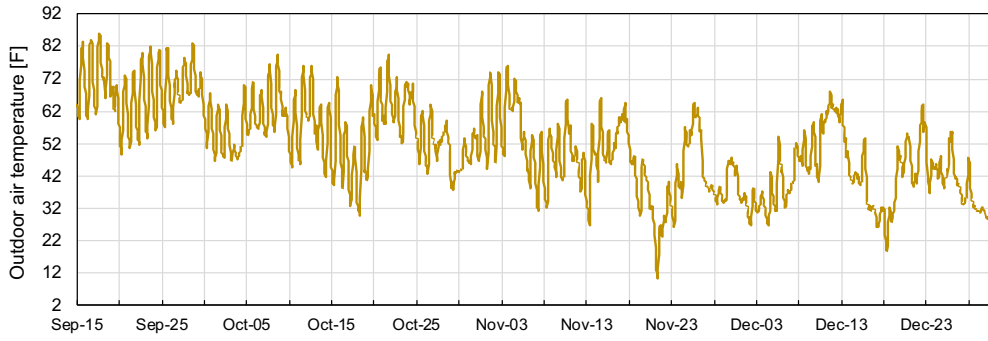
(a) Outdoor air temperature
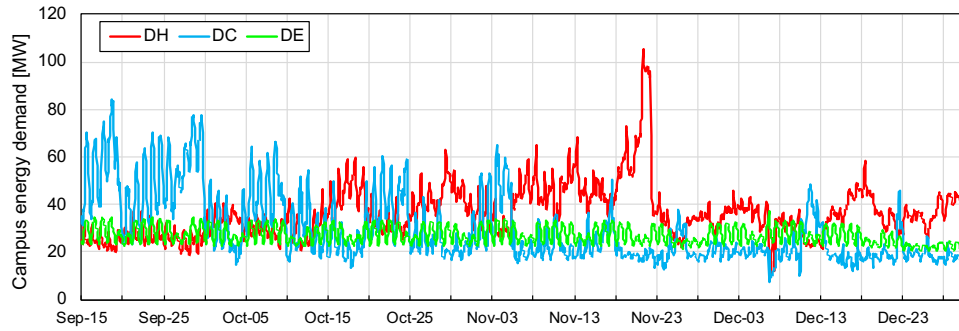
(b) Energy demand of Purdue campus
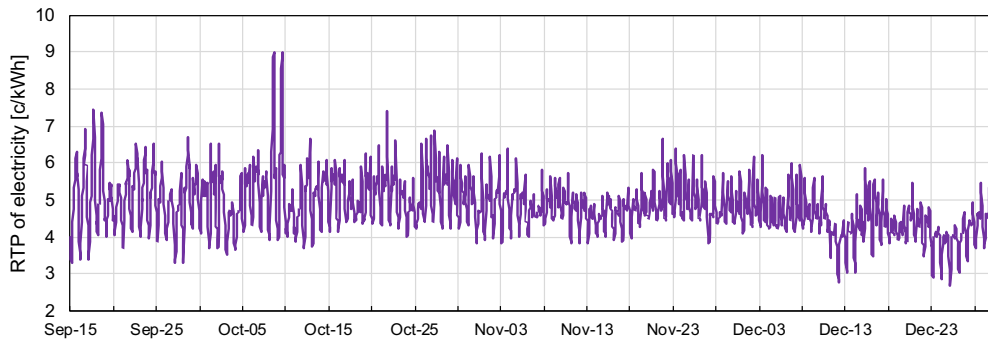
(c) Real-time electricity price of purchased electricity from utility

Figure 5.5. Time varying inputs to the MILP optimization framework

A summary of results for the three optimization periods are given in Table 5.6, Table 5.7, and

Table 5.8 respectively, comparing the baseline plant performance and the MILP optimized results (with and without on/off penalties). Cost saving opportunities are identified with MILP optimization for all three time periods. For the 3-month optimization periods, the cost optimization using MILP with no switching penalties resulted in about 9.4% cost savings whereas MILP

including penalties resulted in about 8.9% cost savings. The cost savings for a 1-week optimization were 2.7% and 2.1% for MILP without and with the penalties, respectively, and for the 1-month optimization period, the savings from MILP optimization without and with SP were 4.5 % and 3.5%, respectively.

Table 5.6. Comparison between plant data and MILP optimized results [Case (b): 1-Week]

1 week [Oct-1 to Oct-7]	Plant data	MILP (w/o on/off penalty)	MILP (w/ on/off penalty)
Steam produced [klb]	56,513	55,777	56,132
Total electricity generated [MWh]	3,608	3,136	3,075
Total electricity purchased [MWh]	2,660	2,809	2,767
Total cooling capacity from steam chillers [MWh]	0	3,210	3,812
Total cooling capacity from electric chillers [MWh]	5,809	2,577	1,975
Total operational cost [$]	367,268	357,295	359,636
Total cost savings [$]		9,974 2.7%	7,632 2.1%

Table 5.7. Comparison between plant data and MILP optimized results [Case (c): 1-Month]

| 1 month (Sep-15 to Oct-15)	Plant data	MILP (w/o on/off penalty)	MILP (w/ on/off penalty)
Steam produced [klb]	227,890	252,488	251,311
Total electricity generated [MWh]	13,427	14,550	14,281
Total electricity purchased [MWh]	14,980	17,907	18,055
Total cooling capacity from steam chillers [MWh]	3,564	15,000	16,141
Total cooling capacity from electric chillers [MWh]	27,930	16,461	15,321
Total operational cost [$]	1,720,001	1,643,150	1,659,241
Total cost savings [$]		76,851 4.5%	60,760 3.5%

Table 5.8. Comparison between plant data and MILP optimized results [3 months]

3 months (Sep-15 to Dec-31)	Plant data	MILP (w/o on/off penalty)	MILP (w/ on/off penalty)
Steam produced [klb]	886,190	800,452	821,710
Total electricity generated [MWh]	47,359	42,782	43,978
Total electricity purchased [MWh]	43,291	44,023	42,490
Total cooling capacity from steam chillers [MWh]	7,438	22,622	46,182
Total cooling capacity from electric chillers [MWh]	68,073	52,480	28,920
Total operational cost [$]	5,835,976	5,289,853	5,316,503
Total cost savings [$]		546,124 9.4%	519,473 8.9%

The penalty factors are included for boilers and steam chillers to enforce the dependencies in the adjacent hours. Since the local hourly decision variables and entire plant optimization over the horizon are closely intertwined, influence of the local decisions on the global objective function for minimizing the total operating cost of the plant can be observed clearly in our results. Unlike in MILP [w/o on/off SP], the sudden change of states (on/off of components) are reduced in MILP [w on/off SP] and allows for an efficient resource allocation (equipment on/off depending on the demand) as we increase the time horizon.

When on/off switching penalties are considered, the optimization period determines the influence of local hourly decision variables on the scheduling decisions for equipment. When the optimization period is too short (say a day or a week), turning on or off a boiler could significantly impact the short-term cost to the point where the operational savings cannot accumulate over a sufficient period of time to make up for the switching cost penalties. Employing a longer optimization period can allow for more appropriate consideration of the tradeoffs between switching penalties and operating cost savings. There is more information on the weather and demand with longer time horizon to look ahead and look back which influences the on/off characteristics of the equipment. However, longer time horizons for optimization lead to a larger optimization problem with more decision variables, which is computationally very expensive to solve.

As an example, the sensitivity of the operation of boilers over the three different optimization periods (1 week, 1 month, 3 months) is considered. Figure 5.6 shows the operation of the boilers for 3-month MILP optimization when including the penalties for startup and shutdown. It can be observed that the natural gas boiler $B1_{NG}$ always operated to meet the heating demand of campus and the other steam-driven plant equipment. The two steam-driven fans (induced draft and forced draft) of $B1_{NG}$ exhausts steam at 15 psig, which is used to meet the steam demand from 15 psig campus steam line. Boiler #2 $B2_{NG}$ was turned off after Dec-21 and never brought online during this time period. $B2_{NG}$ has one FD fan that uses 600 psig steam and exhaust steam at 15 psig. These fans are operated using steam depending on the demand of steam. Otherwise, they operate using electricity. This decision depends on the cost of electricity and other factors. Boiler #3 $B3_{NG}$ was turned on and off a couple of times during the optimization period when there was a significant change in steam demand. $B3_{NG}$ has one electric FD fan which provides some flexibility in the operation of $B3_{NG}$ since the fan is not tied to meeting steam demand. Coal boiler #4 $B4_C$ was turned on only when the heating demand was very high due to higher cost of coal and associated cost with operating its three steam/electric fans (ID, FD and PA). When the steam demand is really high, both the boilers along with the steam-driven fans help to meet steam demand. It was observed that there was no change of state (on/off) in the operation of the boilers before Nov-18.
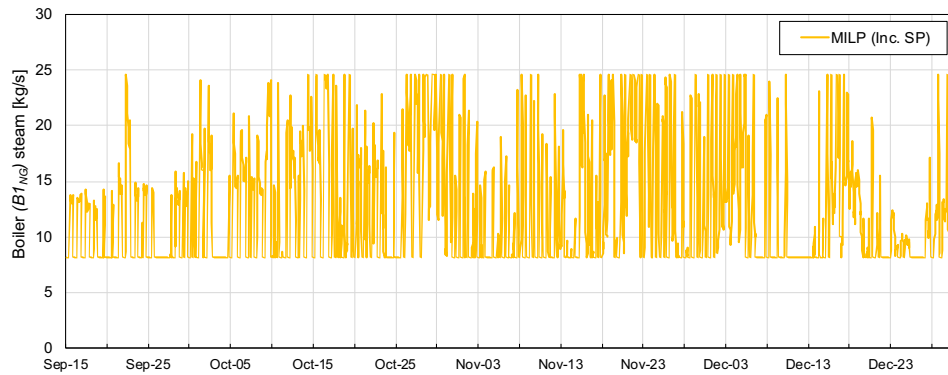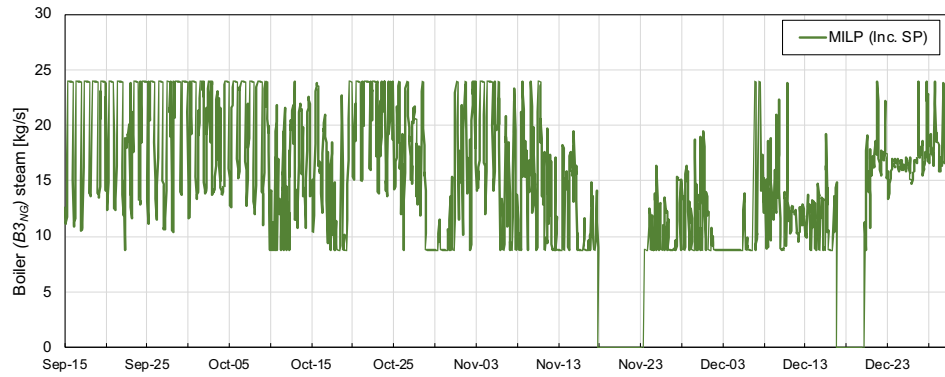

(a) Natural gas boiler #1 ($B1_{NG}$)

Figure 5.6. Operation of boilers using MILP [including on/off SP] optimization for 3-months' time range
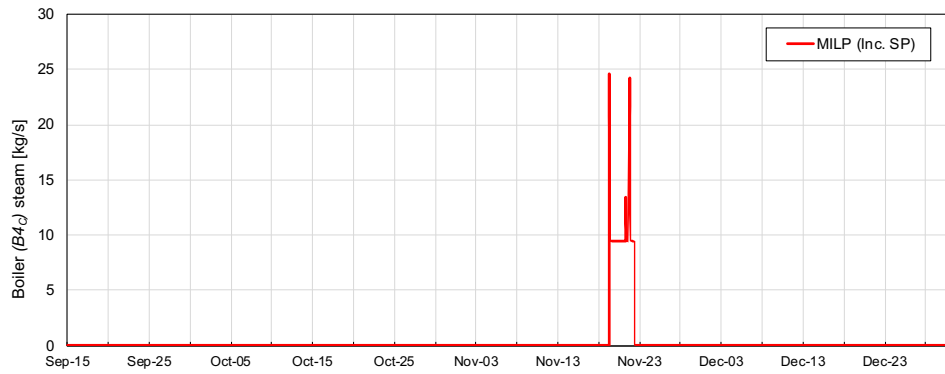
133

Figure 5.6 continued
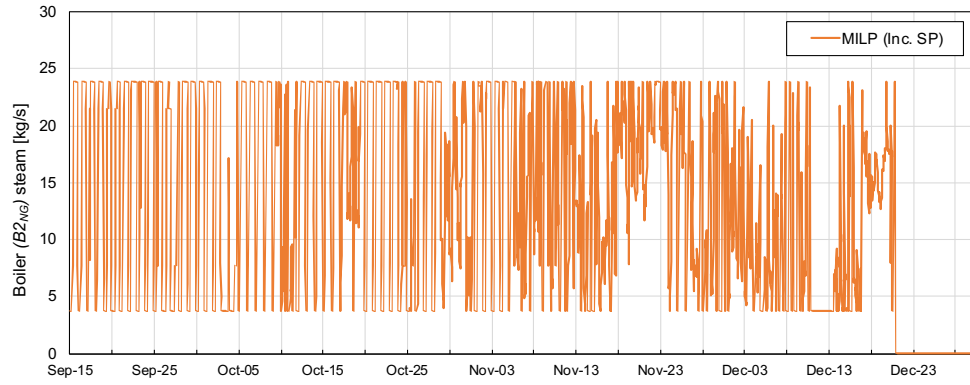
(b) Natural gas boiler #2 ($B2_{NG}$)

(c) Natural gas boiler #3 ($B3_{NG}$)

(d) Coal boiler #4 ($B4_C$)

Figure 5.7 and Figure 5.8 show the operation of the boilers for 1-week and 1-month optimizations period determined using the MILP with penalties for startup and shutdown. Similar to the 3-month optimization, it can be observed that the natural gas boilers $B1_{NG}$ and $B2_{NG}$ were always operated to meet steam demand and steam requirements of other components for both the 1-week and 1-month time ranges. However, $B3_{NG}$ was turned off and brought online between Oct-02 and Oct-04 for the 1-week time horizon. This 1-week period was sufficient to recoup the costs of brining the boiler offline and online. During the 1-month time horizon, $B3_{NG}$ was turned off and brought online a couple of times and $B4_C$ was switched on and off between Oct-09 and Oct-10 depending on the changes in demand. This behavior of the boilers was not observed during the MILP optimization for the 3-month horizon. Instead, the load between the three natural gas boilers were balanced depending on the demand and electricity price during that time period within the 3-month horizon. The on/off switching becomes less as the time horizon for optimization increases allowing for more efficient resource allocation.
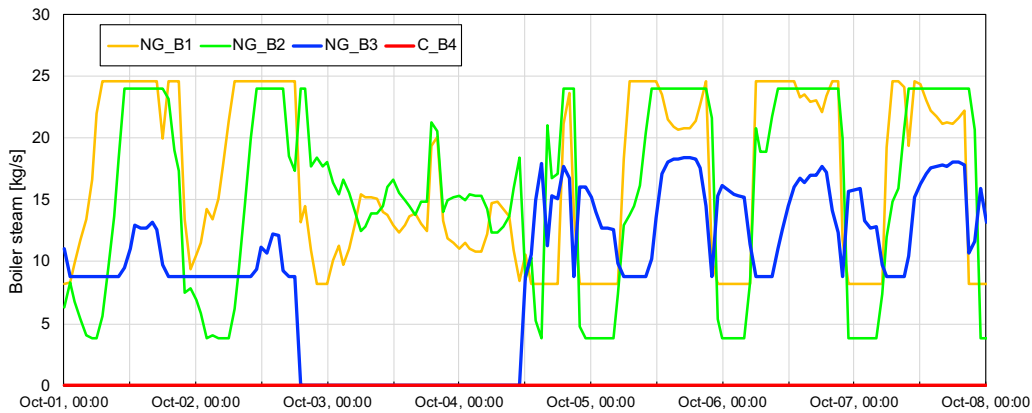

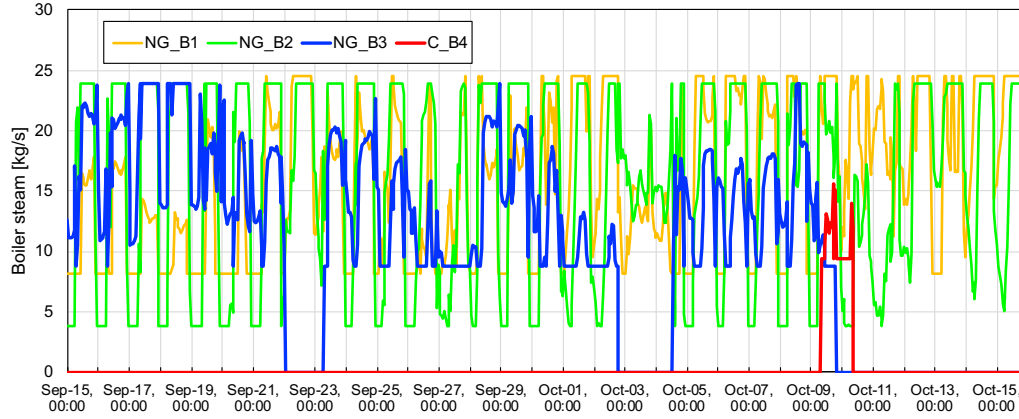Figure 5.7. Operation of boilers using MILP [including on/off SP] optimization for 1-week time range

Figure 5.8. Operation of boilers using MILP [including on/off SP] optimization for 1-month time range

## 5.3   Sensitivity to Purchased Electricity and Natural Gas Price

The primary energy usage of the CCHP plant depends on the decisions regarding generation and/or purchasing of electricity, usage of steam-driven and/or electric equipment and usage of coal or natural gas boilers in response to minimizing operational costs while meeting the time-varying campus electricity, heating and cooling demands.

The cost of purchased electricity plays an important role in determining whether to generate and/or purchase electricity or operate steam-driven or electric equipment. Since the MILP algorithm provides operational signals associated with resource allocation ensuring that the systems meet campus electricity, heating, and cooling demands, only this algorithm was considered for the analysis in this section. The sensitivity of the predicted results to the cost of purchased electricity (c_E) were studied and typical results are presented in this section. The campus energy demand for a particular hour of a summer day was used for the sensitivity analysis, where the heating demand (DH) was 95 MMBtu/h (27.7 MW), cooling demand (DC) was 25,046 Tons (88 MW) and the electrical demand (DE) was 28 MW. The outdoor air temperature was 76°F (24.4°C). This particular demand scenario was chosen because of the high cooling demand which requires the operation of both steam and electric chillers. So, the switch between steam-driven and electric equipment could be analyzed. The cost of coal was set as 70.80($/ST) and the

cost of natural gas was set as 3.00 ($/DTH) for the analysis. For studying the effect of electricity purchased from the local electric utility which includes a real-time pricing component that varies with time, the cost of purchased electricity was varied from 0 to 10 ¢/kWh.

Figure 5.9 shows individual hourly optimization results as a function of the cost of purchased electricity for these summer conditions. Figure 5.9(a) shows that the total hourly operational cost of the plant increases monotonically when the price of the purchased electricity increases. This is because some amount of electricity must be purchased apart in addition to being generated in order to meet the total electrical demand. From Figure 5.9(b), we can see that as the price of electricity increases, more steam is produced to meet a growing steam demand of the turbine generators, steam chillers and other steam-driven components in order to reduce the purchased electricity. At lower electricity prices, some amount of steam is still produced to meet the campus heating demand. In Figure 5.9(e), Boilers 1, 2 and 3 are natural gas boilers while boiler 4 is a coal boiler. The boilers are brought online depending upon the cost of coal and natural gas, their efficiency, operating conditions and fans to be operated along with the boiler. It can be noticed that the coal boiler was never turned on for this particular demand case due to its high operational cost compared to natural gas boilers. Figure 5.9(c) shows comparisons of electricity generated and purchased for the varying cost of electricity. It can be seen that a higher quantity of electricity is purchased at lower costs of electricity. As the price of electricity increases above 4.70¢/kWh, there is a reduction in the purchase of electricity and an increase in the generation of electricity from the turbine generators. However, some amount of electricity must be purchased during the day to satisfy the electrical demand of campus. All electricity cannot be generated because of the limited availability of steam from turbine generators due to a campus heating demand and the capacity limitations of the turbine generators. Figure 5.9(d) shows comparisons of cooling capacity produced by steam chillers and electric chillers over the range of electricity rates. The control switches from maximizing electric chiller operation at low rates, to using steam chillers when rates are above 3.80 ¢/kWh in order to meet the campus cooling demand. However, the electric chillers are still operated at higher electricity prices on this summer day due to high cooling demand. It can be noticed that the switch between electric chillers to steam chillers happens at 3.80 ¢/kWh and at 4.70 ¢/kWh because of the difference in efficiencies and minimum operating capacity between the chillers. As the cost of purchased electricity increases, the lower efficiency electric chillers are operated at reduced load and then turned off while the loads on steam chillers are increased and

then they are operated at full load. More specifically, at 3.80 ¢/kWh, one electric chiller at Wade plant $(E-C3)_W$ was turned off, steam chiller $(S-C3)$ was operated at full load and the load on $(S-C2)$ was increased. At 4.70 ¢/kWh, $(S-C2)$ was operated at full load and the load on electric chiller $(E-C4)_W$ was decreased while meeting the cooling demand. The switch from electric components to steam-driven components and purchased to generated electricity happens between 3.80¢/kWh and 5.30¢/kWh depending on efficiencies and operational limitations of individual components operated to meet the demand. Also, the change in the load of the major components affects the auxiliary components connected to it and vice-versa. This trend is observed from the increase in the amount of steam produced and electricity generated in stages as the steam-driven components are increased in load or brought online when the cost of purchased electricity keeps increasing.
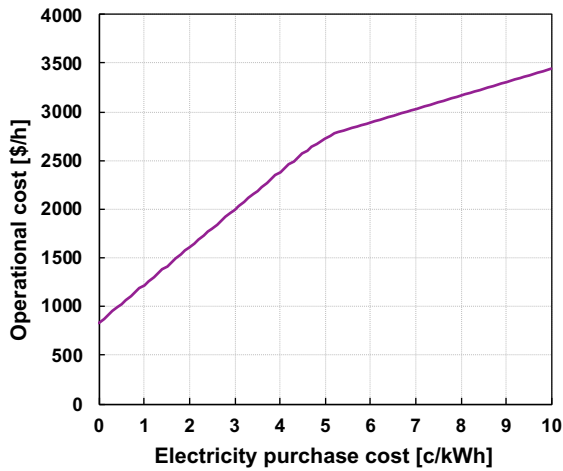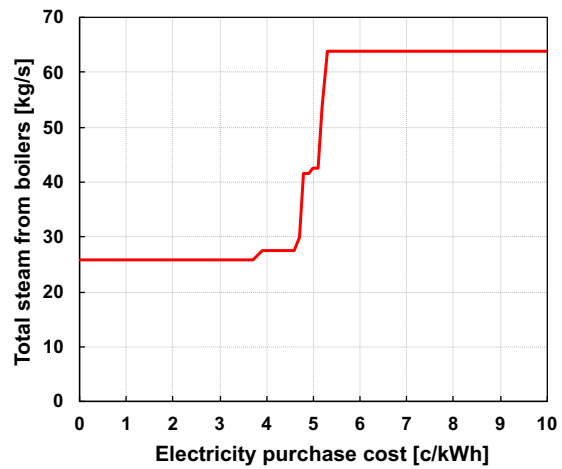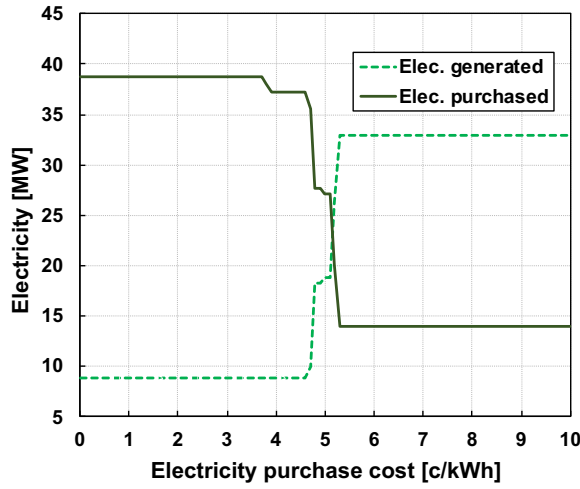

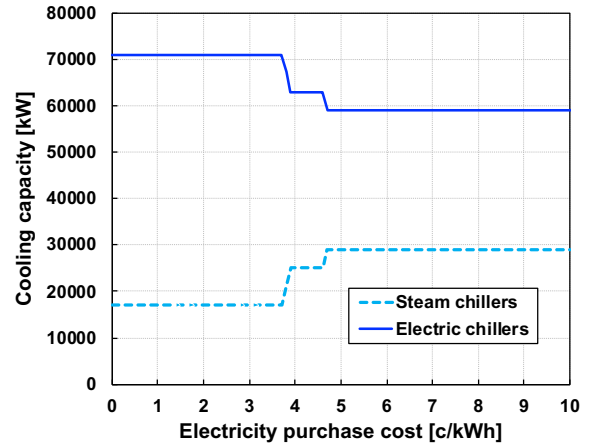(a) Total operational cost   (b) Total steam produced in boilers

Figure 5.9. MILP cost optimization results for varied electricity purchase cost (RTP)
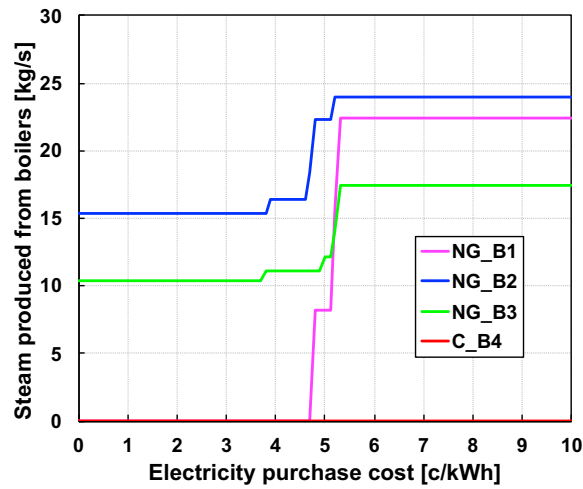
Figure 5.9 continued
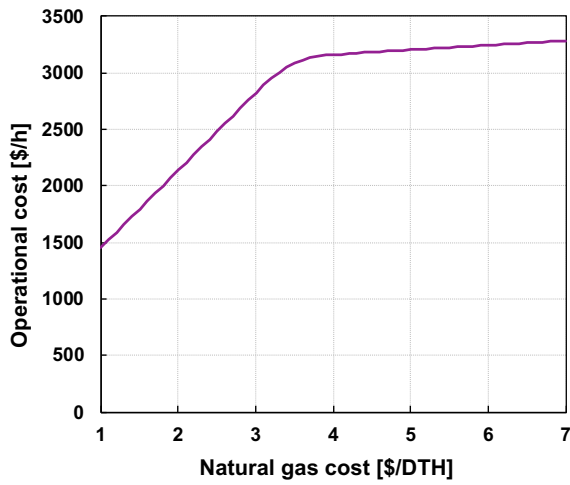

(c) Amount of electricity generated & purchased

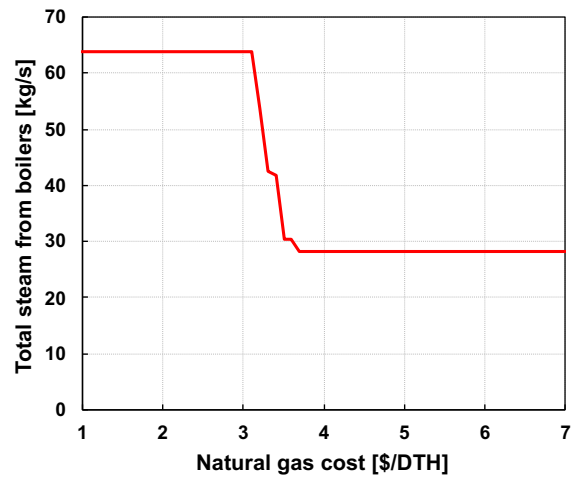(d) Cooling capacity of steam and electric chillers

(e) Amount of steam produced in individual boilers

A similar analysis was done to study the influence of the cost of natural gas (c_{NG}) on operational decisions using the MILP optimization and the same demand scenario considered for the effect of purchased electricity price. Generally, the cost of coal doesn't vary much within a year, so no sensitivity analysis was done for coal. The cost of coal was set as 70.80($/ST) and the cost of purchased electricity was set as 5.50 (¢/kWh) for this analysis. The cost of natural gas was varied from 1$/DTH to 7 $/DTH.
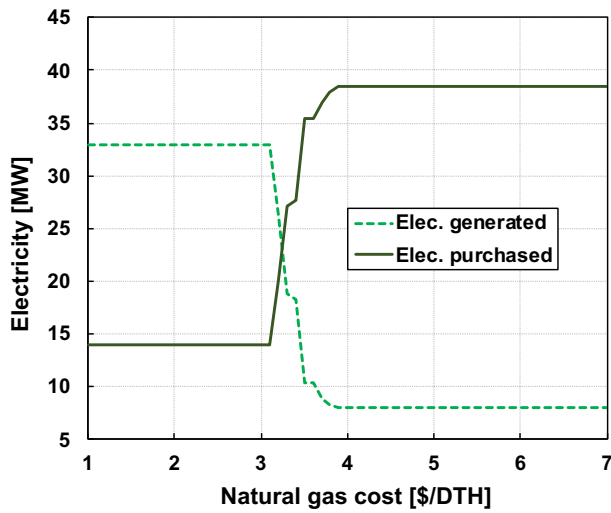
Figure 5.10 shows MILP cost optimization results as a function of the cost of natural gas. Figure 5.10(a) shows that the total operational cost of the plant increases with the price of the natural gas depending upon the amount of steam produced in the natural gas boilers. From Figure 5.10(b), it can be observed that more steam was generated from the boilers when the natural gas price was below 3.20 $/DTH. Above 3.20 $/DTH, some amount of steam is still produced from the boilers to meet campus steam demand and demand from other auxiliary steam-driven equipment. As the cost of natural gas increases, the coal boiler B4 is turned on at 3.50 $/DTH as shown in Figure 5.10(e). Some amount of steam is still generated from natural gas boiler B2 to meet the campus heating demand even when the natural gas price increases. The natural gas boilers are brought offline in stages depending on their efficiencies and minimum operational capacities. Figure 5.10(c) shows comparisons of electricity generated and purchased. It can be observed that a higher quantity of electricity is generated using the steam from natural gas boilers at lower costs of natural gas. As the price of natural gas increases above 3.20 $/DTH, there is an increase in the purchase of electricity even when the cost of purchased electricity is relatively higher. However, some amount of electricity is generated as a byproduct from meeting campus heating demand. From Figure 5.10(d), it can be noticed that there is no change in the operation of steam and electric chillers in this case where the cooling demand is high during summer. From Figure 5.9(d), it was found that the switch from electric to steam chillers happened when the RTP price was above 3.80 ¢/kWh. Since the cost of purchased electricity assumption for this analysis is 5.50 ¢/kWh, the steam chillers were always operated at full load and the rest of the cooling demand was satisfied using electric chillers. The switching from natural gas boilers to a coal boiler, electricity generated to purchasing electricity, and some steam-driven components to electric components happens in stages between 3.20 $/DTH and 3.80 $/DTH depending on efficiencies and operational limitations of different components operated to meet the demand.
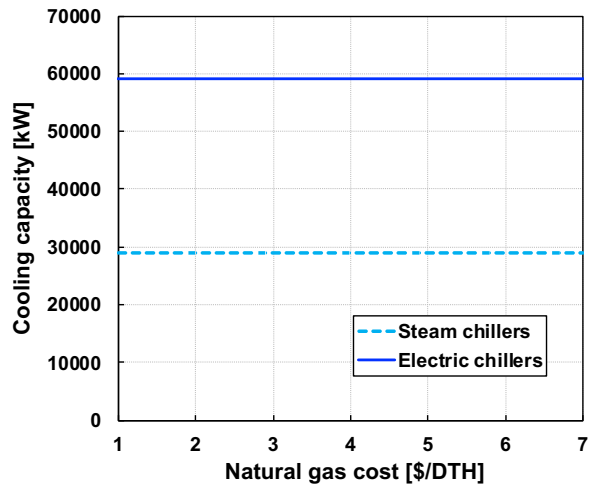
(a) Total operational cost
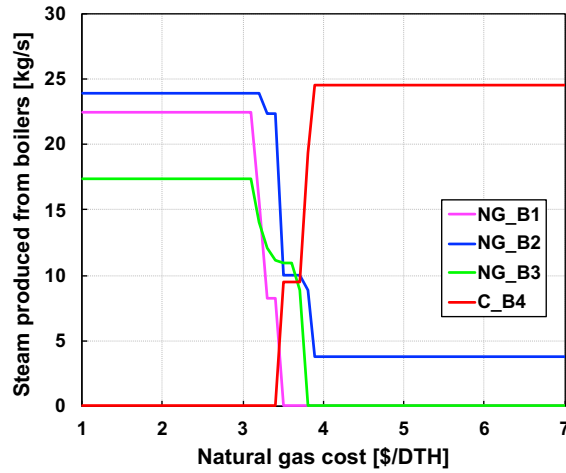
(b) Total steam produced in boilers

(c) Amount of electricity generated & purchased

(d) Cooling capacity of steam and electric chillers

Figure 5.10. MILP cost optimization results for varied natural gas price

Figure 5.10 continued

(e) Amount of steam produced in individual boilers

From both the sensitivity studies, it can be observed that the cost of purchased electricity and cost of natural gas plays an important role in the decisions regarding the generation and/or purchasing of electricity, usage of steam-driven and/or electric equipment and usage of coal or natural gas boilers to minimize the operating cost. The transition from electric to steam-driven components and vice-versa happens in stages depending on efficiencies and operational limitations of different components operated to meet the demand.

5.4   Chapter Summary

A hybrid mixed-integer linear programming (MILP) and nonlinear programming (NLP) approach was applied for the cost optimal control of CCHP systems. In this two-step approach, MILP optimization was applied in the first step to the plant model with linear component models and the penalty for turning on and off the boilers and steam chillers. The MILP step determines which components need to be turned on and their respective loading needed to meet the campus energy demand for the chosen time horizon with one-hour resolution. The solution from MILP optimization was given as a starting point for NLP optimization in the second step to determine the hourly state of operation of selected components including their nonlinear performance characteristic curves. Additionally, two cases were considered for MILP optimization: MILP with no on/off switching penalties and MILP with switching penalties. Optimal results from the MILP

and NLP approaches were compared with the baseline plant performance for current control on a daily basis for different seasons in order to understand the effectiveness of each algorithm. In all the four scenarios, there were cost savings using the MILP optimization and NLP optimization. The cost savings were generally higher for the hybrid MILP-NLP approach compared to only MILP optimization. The decisions on the amount of steam produced, electricity generated and/or purchased, using steam chillers or electric chillers, using natural gas or coal boilers depend on time-varying factors such as energy demand, RTP costs, fuel prices, OAT, and limitations on the equipment capacities. Since the output from MILP with switching penalties is provided as an input to the NLP hourly optimization, this approach was used to study the impact of optimization period on on/off operation of the boilers and steam chillers. Three different optimization time periods were considered: 1 week, 1 month and 3 months. The results showed that on/off cycling of the equipment was reduced with increasing length of the optimization period. In addition, the sensitivity of the operational decisions to the cost of purchased electricity and natural gas were studied and it was demonstrated that optimal operation of boilers, steam generators, and chillers depends strongly on these costs.

6. CONCLUSIONS AND FUTURE WORK

6.1 Conclusions

This dissertation presented a solution methodology for optimizing the operation of a large-scale CCHP system using a detailed network energy flow model solved by a hybrid approach combining mixed-integer linear programming (MILP) and nonlinear programming (NLP) optimization. The tools were then used to evaluate the cost savings potential associated with applying optimal control for this case study. In the first step, MILP is applied to the optimization model which includes a linear model of all components and the penalty for turning on or off a few major units. The MILP determines which components need to be turned on and their respective load needed to meet the campus energy demand for the chosen time period (short, medium, or long term). Based on the solution from the MILP step as a starting point, NLP determines the hourly state of operation of components including their nonlinear performance characteristics curves. Plant primary energy use and costs depend on decisions regarding generation and/or purchase of electricity and usage of steam-driven and/or electric equipment in response to time-varying prices, loads, and environmental conditions. The optimal energy dispatch algorithm provides operational signals associated with resource allocation ensuring that the systems meet campus electricity, heating, and cooling demands.

The methodology incorporates the following elements:

- a detailed thermodynamic model that considers the linear and nonlinear characteristics of all components integrated into a multi-physical CCHP system
- a deterministic network energy flow model that relates the capacity and operation of the CCHP system to the building energy demands
- an optimization algorithm capable of handling non-convex, non-differentiable, multimodal (multiple local minima) and discontinuous functions which includes strong coupling to multiple energy components (electricity, heating, and cooling)
- an energy dispatch algorithm that employs a hybrid MILP and NLP approach to provide control signals to the primary energy consuming and producing components (boilers, turbine generators, chillers, etc.) using an outer supervisory control loop based on the energy (thermal

and electric) demand and to an inner layer of auxiliary components (pumps, fans, cooling tower and other auxiliaries)

The chief benefits of this formulation are its ability to determine the optimal mix of equipment with on/off capabilities and penalties for startup and shutdown, consideration of cost from all auxiliary equipment, and applicability to large-scale energy systems with multiple heating, cooling, and power generation units resulting in improved performance.

The combined cooling, heating, and power (CCHP) plant that serves the Purdue campus was chosen as the case study to conduct an extensive computational simulation. The entire model was coded in MATLAB (R2019b) and optimized using MATLAB's MILP and NLP optimization toolbox. The models were validated with plant measurements and then used with the assumption of perfect load forecasts to evaluate the economic benefits of optimal control subjected to different operational conditions and fuel prices. Example cost optimizations were performed for 24-hour periods in different seasons with known cooling, heating, and electricity demand for Purdue's main campus, and based on actual real-time prices (RTP) for purchasing electricity. Three optimization cases were considered for analysis: MILP with no on/off switching penalties; MILP including switching penalties and NLP optimization. The outputs from the MILP with switching penalties are provided as inputs for the NLP optimization model. Almost 10% cost savings was achieved using the hybrid MILP-NLP approach compared to baseline performance associated with current controls at the plant. The optimization results suggest there are opportunities for cost savings across all seasons compared to the current operation of the power plant. For a large CCHP plant, this could mean huge savings for a year.

The impact of choosing different time periods for the optimization was studied using MILP with on/off switching penalties. For a 3-month time horizon, the cost optimization resulted in about 8.9% cost savings. Compared to shorter optimization periods, the 3-month period had fewer on/off cycles. The sensitivity of the optimized results to the cost of purchased electricity and natural gas was also performed to illustrate operational switches between steam and electric driven components, and coal and natural gas boilers that occur as costs of energy change.

Ultimately, the optimization tool could be implemented for recommending the daily operation of the power plant and provide real-time estimates of cost and energy savings as

feedback to operators and plant managers for operational planning. This framework is modular and generalizable to different types of systems so that it can be easily modified for different architectures or configurations and could be implemented for any large-scale distributed energy systems in the future.

6.2 Future Work

The work presented in this dissertation can be extended in order to make this hybrid MILP-NLP approach a general tool applicable to any centralized/distributed energy system. In the future, the following specific work could be carried to further the development and application of this technology.

- The proposed control strategy should be implemented for the real-time operation of the power plant to assess its effectiveness and limitations.
- Few heuristics can be developed based on the results from extensive-simulation and sensitivity analysis using the hybrid MILP-NLP approach for different seasons, demand scenarios, operational conditions, and fuel prices. This could be easily implemented for the daily operation of the power plant instead of running the optimization tool.
- Different MILP and NLP optimization solvers could be compared and evaluated with respect to finding global optimal solutions and minimizing computational time.
- Attempts could be made to improve the computational time of the respective mathematical programming solvers with formulation-specific heuristics.
- Storage options could be considered using dynamic optimization over a time horizon.
- The optimal time horizon should be determined for planning and scheduling the operation of the power plant.
- Accurate energy forecast models should be developed for integration with the optimization tool.
- Carbon tax can be implemented along with the objective cost function as applicable.

APPENDIX A. INPUTS TO THE OPTIMIZATION FRAMEWORK

The user inputs to the optimization framework mainly includes parameters that have a different value for each hour (t), parameters that have a constant value over the chosen time range (T), equipment specific inputs and bounds to the decision variables. MILP optimization does not require any initial point whereas NLP optimization requires initial point for every hour which is the output from MILP optimization. Data required for the CCHP cost optimization and performance evaluation are collected from Purdue physical facilities for this study and are given as an input to the model. Few parameters that have a different value for each hour (t) are:

- Hourly energy demand data of Purdue campus for electricity (DE^t), heating (DH^t), and cooling (DC^t)
- Cost of purchased electricity for every hour (c_E^t) including real-time pricing (RTP)
- Ambient conditions for every hour: wet-bulb (T_{wb}^t) and dry-bulb (T_{db}^t) temperatures, relative humidity (RH^t)

Apart from this, the other input data that are constant includes:
- Price of on-site fuel: cost of natural gas (c_{NG}) and cost of coal (c_C)
- Switch penalty (SP) cost for turning on/off the equipment (c_{SP}) : Included only in MILP optimization
- Range of effective operation of CCHP components for a given installed capacity: minimum and maximum capacity of the equipment

Other than the input data mentioned above, the list of constant input parameters to the system model are listed in Table A.1. All the equipment specific inputs are defined based on the plant performance data and are included in section 3.3. Any other input values to the optimization framework are explained in section 0.

Table A.1. Input parameters to the system model

Input parameters	Values	Description
P_{600}	600 psig (4238.2 kPa)	Pressure across 600 psig steam line
P_{125}	125 psig (963.2 kPa)	Pressure across 125 psig steam line
P_{15}	15 psig (204.77 kPa)	Pressure across 15 psig steam line
P_{fw}	925 psig (6479.0)	Pressure of feedwater
P_{cond}	15 psig (204.77 kPa)	Pressure across condensate line
P_{ex}	-13.2 psig (10.2 kPa)	Exhaust pressure from equipment
P_{cr}	0 psig (101.4 kPa)	Pressure of condensate return from campus
P_{atm}	1 atm (101.3 kPa)	Atmospheric pressure
T_{fw}	250 °F (121.1 °C)	Temperature of feedwater
T_{cr}	140 °F (60 °C)	Temperature of condensate return from campus

REFERENCES

Ahmadi, P. and Dincer, I. (2010). Exergoenvironmental analysis and optimization of a cogeneration plant system using Multimodal Genetic Algorithm (MGA). *Energy*, 35(12), 5161–5172.

Al Moussawi, H., Fardoun, F., & Louahlia-Gualous, H. (2016). Review of tri-generation technologies: Design evaluation, optimization, decision-making, and selection approach. *Energy Conversion and Management*, *120*, 157–196.

Almasi, A., Avval, H.B., Ahmadi, P. and Najafi, A.F. (2011). Thermodynamic modeling, energy and exergoeconomic analysis and optimization of Masher gas turbine power plant. *Proceedings of the Global Conference on Global Warming*, Lisbon, Portugal.

Bischi, A., Taccari, L., Martelli, E., Amaldi, E., Manzolini, G., Silva, P., ... & Macchi, E. (2014). A detailed MILP optimization model for combined cooling, heat and power system operation planning. *Energy, 74*, 12-26.

Bracco, S., Dentici, G. and Siri, S. (2013). Economic and environmental optimization model for the design and the operation of a combined heat and power distributed generation system in an urban area. *Energy*, 55, 1014–1024.

Braun, J.E. (1987). Performance and control characteristics of large central cooling systems. *ASHRAE Transactions, 93*(1), 1830–52.

Braun, J. E. (1988). *Methodologies for the design and control of central cooling plants* (Doctoral dissertation). University of Wisconsin - Madison.

Chandan, V., Do, A.T., Jin, B., Jabbari, F., Brouwer, J., Akrotirianakis, I., Chakraborty, A. and Alleyne, A. (2012). Modeling and optimization of a combined cooling, heating and power plant system. *Proceedings of the American Control Conference.* Montréal, Canada.

Chapa, M.A.G. and Galaz, J.R.V. (2004). An economic dispatch algorithm for cogeneration systems. *IEEE Power Engineering Society General Meeting*, 1, 989–994.

Cho, H., Eksioglu, S.D., Luck, R. and Chamra, L.M. (2008). Operation of a CCHP system using an optimal energy dispatch algorithm. *Proceedings of Energy Sustainability*, Jacksonville, Florida, USA.

Cho, H., Mago, P.J., Luck, R. and Chamra, L.M. (2009). Evaluation of CCHP systems performance based on operational cost, primary energy consumption, and carbon dioxide emission by utilizing an optimal operation scheme. *Applied Energy*, 86 (12), 2540–2549.

Cho, H., Luck, R. and Chamra, L.M. (2010). Supervisory feed-forward control for real-time topping cycle CHP operation. *Journal of Energy Resources Technology,* 132(1), 012401-12. doi:10.1115/1.4000920.

Cho, H., Smith, A.D. and Mago, P. (2014). Combined cooling, heating and power: A review of performance improvement and optimization. *Applied Energy*, 136, 168–185.

Deb, K. (2001). Multi-Objective Optimization using Evolutionary Algorithms. Wiley-Interscience Series in Systems and Optimization. Wiley, Chichester.

Dieu, V.N. and Ongsakul, W. (2009). Augmented Lagrange—Hopfield network for economic load dispatch with combined heat and power. *Electric Power Components and Systems*, 37(12), 1289-1304.

Drud, A. S. (1994). CONOPT-a large-scale GRG code. *ORSA Journal on computing, 6*(2), 207-216. Retrieved Nov 23, 2020, from https://pubsonline.informs.org/doi/abs/10.1287/ijoc.6.2.207.

Ebrahimi, M., Keshavarz, A. and Jamali, A. (2012). Energy and exergy analyses of a microsteam CCHP cycle for a residential building. *Energy and Buildings*, 45, 202–210.

Elsido, C., Bischi, A., Silva, P., & Martelli, E. (2017). Two-stage MINLP algorithm for the optimal synthesis and design of networks of CHP units. *Energy, 121,* 403-426.

Forrest, J., Ralphs, T., Vigerske, S., LouHafer, Kristjansson, B., jpfasano, et al. (2018). coin-or/ Cbc: version 2.9.9 Retrieved Nov 23, 2020, from https://doi.org/10.5281/ZENODO.1317566.

Fuentes-Cortés, L. F., Ponce-Ortega, J. M., Nápoles-Rivera, F., Serna-González, M., & El-Halwagi, M. M. (2015). Optimal design of integrated CHP systems for housing complexes. *Energy Conversion and Management, 99*, 252-263.

Fumo, N., Mago, P.J., & Chamra, L.M. (2009). Emission operational strategy for combined cooling, heating, and power systems. *Applied Energy*, *86*(11), 2344–2350.

Gao, Y., Liu, Q., Wang, S., & Ruan, Y. (2018). Impact of typical demand day selection on CCHP operational optimization. Energy Procedia, 152, 39-44.

Gao, L., Hwang, Y., & Cao, T. (2019). An overview of optimization technologies applied in combined cooling, heating and power systems. *Renewable and Sustainable Energy Reviews, 114,* 109344.

Gill, P. E., Murray, W., & Saunders, M. A. (2005). SNOPT: An SQP algorithm for large-scale constrained optimization. *SIAM review, 47*(1), 99-131.

Goldberg, D.E. (1989). Genetic algorithms in search, optimization, and machine learning. Addison-Wiley Publishing Company, Inc.

Guo, L., Liu, W., Cai, J., Hong, B. and Wang, C. (2013). A two-stage optimal planning and design method for combined cooling, heat and power microgrid system. *Energy Conversion and Management*, 74, 433–445.

Gurobi optimization. (2019). Retrieved Nov 23, 2020, from http://www.gurobi.com.

Gustafsson, S. and Karlsson, B. (1991). Linear programming optimization in CHP networks. *Heat Recovery Systems & CHP,* 11(4), 231-238.

Hu, M. and Cho, H. (2014). A probability constrained multi-objective optimization model for CCHP system operation decision support. *Applied Energy*, 116(1), 230–242.

Hashemi, R. (2009). A developed offline model for optimal operation of combined heating and cooling and power systems. *IEEE Transactions on Energy Conversion,* 24 (1), 222–229.

IBM ILOG CPLEX optimization studio. (2019). IBM. Retrieved Nov 23, 2020, from https://www.ibm.com/products/ilog-cplex-optimization-studio/resources.

Kerr, T. (2008). Combined heat and power: evaluating the benefits of greater global investment. *IEA, International Energy Agency.* Retrieved from https://webstore.iea.org/combined-heat-and-power.

IEA. (2012). *World Energy Outlook 2012*. IEA, Paris, France. Retrieved from https://www.iea.org/reports/world-energy-outlook-2012.

IEA. (2018). *Global Energy & CO$_2$ Status Report 2017*. IEA, Paris, France. Retrieved from https://www.iea.org/reports/global-energy-co2-status-report-2017.

Jradi, M., & Riffat, S. (2014). Tri-generation systems: Energy policies, prime movers, cooling technologies, configurations and operation strategies. *Renewable and sustainable energy reviews*, *32*, 396-415.

Kavvadias, K. C. and Maroulis, Z. B. (2010). Multi-objective optimization of a trigeneration plant. *Energy Policy*, 38, 945–954.

Lahdelma, R. and Hakonen, H. (2003). An efficient linear programming algorithm for combined heat and power production. *European Journal of Operational Research,* 148 (1), 141–151.

Li, C.Z., Shi, Y.M. and Huang, X.H. (2008). Sensitivity analysis of energy demands on performance of CCHP system. *Energy Conversion and Management*, 49, 3491–3497.

Liu, M., Shi, Y., & Fang, F. (2012). A new operation strategy for CCHP systems with hybrid chillers. *Applied Energy,* 95, 164–73.

Liu, M., Shi, Y., & Fang, F. (2014). Combined cooling, heating and power systems: A survey. *Renewable and sustainable energy reviews*, *35*, 1–22.

Lozano, M. A., Carvalho, M. and Serra, L. M. (2008). Operational strategy and marginal costs in simple trigeneration systems. *Energy,* 34(11), 2001-2008.

Lozano, M. A., Ramos, J. C. and Serra, L. M. (2010). Cost optimization of the design of CHCP (combined heat, cooling and power) systems under legal constraints. *Energy,* 35, 794–805.

Luo, Z., Wu, Z., Li, Z., Cai, H., Li, B., & Gu, W. (2017). A two-stage optimization and control for CCHP microgrid energy management. *Applied Thermal Engineering, 125*, 513-522.

Mago, P. J., Fumo, N., & Chamra, L. M. (2009). Performance analysis of CCHP and CHP systems operating following the thermal and electric load. *International Journal of Energy Research, 33*(9), 852-864.

MATLAB and Optimization Toolbox R2019b. The MathWorks, Inc., Natick, Massachusetts, United States of America. Retrieved Nov 23, 2020, from https://www.mathworks.com/products/optimization.html

Pan, S., Jian, J., & Yang, L. (2018). A hybrid MILP and IPM approach for dynamic economic dispatch with valve-point effects. *International Journal of Electrical Power & Energy Systems, 97*, 290-298.

Parameshwaran, R., Kalaiselvam, S., Harikrishnan, S., & Elayaperumala, A. (2012). Sustainable thermal energy storage technologies for buildings: a review. *Renewable and Sustainable Energy Reviews*, *16*(5), 2394–2433.

Piacentino, A. and Cardona, F. (2008). EABOT – energetic analysis as a basis for robust optimization of trigeneration systems by linear programming. *Energy Conversion and Management*, 49(11), 3006–3016.

Powell, K. M., Kim, J. S., Cole, W. J., Kapoor, K., Mojica, J. L., Hedengren, J. D., & Edgar, T. F. (2016). Thermal energy storage to minimize cost and improve efficiency of a polygeneration district energy system in a real-time electricity market. *Energy, 113*, 52-63.

Rong, A. and Lahdelma, R. (2005). An efficient linear programming model and optimization algorithm for trigeneration. *Applied Energy,* 82(1), 40–63.

Rong, A., Hakonen, H. and Lahdelma, R. (2006). An efficient linear model and optimization algorithm for multi-site combined heat and power production. *European Journal of Operational Research*, 168(2), 612–632.

Rosenthal, R.E. (2008). GAMS – a user′s guide. *GAMS Development Corporation, Washington, DC, USA.* Licensed to Antonio Valero.

Rubio-Maya, C., Uche, J. and Martínez, A. (2011). Sequential optimization of a polygeneration plant. *Energy Conversion Management,* 52, 2861–2869.

Salgado, F. and Pedrero, P. (2008). Short-term operation planning on cogeneration systems: A survey. *Electric Power Systems Research*, 78 (5), 835–848.

Safari, A., Berezkin, V., & Assadi, M. (2018, June). An Integrated Simulation Tool Proposed for Modeling and Optimization of CCHP Units. In *Turbo Expo: Power for Land, Sea, and Air* (Vol. 51043, p. V003T23A001). American Society of Mechanical Engineers.

Shi, B., Yan, L-X. and Wu, W. (2013). Multi-objective optimization for combined heat and power economic dispatch with power transmission loss and emission reduction. *Energy*, 56, 135–143.

Thorin, E., Brand, H. and Weber, C. (2005). Long-term optimization of cogeneration systems in a competitive market environment. *Applied Energy,* 81(2), 152–169.

Tichi, S.G., Ardehali, M.M. and Nazari, M.E. (2010). Examination of energy price policies in Iran for optimal configuration of CHP and CCHP systems based on particle swarm optimization algorithm. *Energy Policy*, 38, 6240–6250.

Urbanucci, L. (2018). Limits and potentials of Mixed Integer Linear Programming methods for optimization of polygeneration energy systems. *Energy Procedia, 148*, 1199-1205.

U.S. Department of Energy (DOE). (2016). *Combined heat and power (CHP) technical potential in the United States*, March 2016. Retrieved from http://www.energy.gov/sites/prod/files/2016/04/f30/CHP%20Technical%20Potential%20Study%203-31-2016%20Final.pdf.

U.S. Energy Information Administration (EIA). (2019). *International Energy Outlook 2019*, Washington, DC: Sep 24, 2019. Retrieved from https://www.eia.gov/outlooks/ieo/.

U.S. EIA. (2018). *State Electricity Profiles*. Retrieved from https://www.eia.gov/electricity/state/.

U.S. Environmental Protection Agency (EPA). (2015). *Energy and Environment Guide to Action - State Policies and Best Practices for Advancing Energy Efficiency, Renewable Energy, and Combined Heat and Power*. Retrieved from https://www.epa.gov/sites/production/files/2015-08/documents/guide_action_full.pdf.

U.S. EPA. (2015). *Combined Heat and Power Partnership - Catalog of CHP Technologies*. Retrieved from https://www.epa.gov/chp/catalog-chp-technologies.

U.S. EPA. (2015). *Emission Factors for Greenhouse Gas Inventories*. Retrieved from https://www.epa.gov/sites/production/files/2015-12/documents/emission-factors_nov_2015.pdf.

U.S. White House. (2012). *Executive Order: Accelerating Investment in Industrial Energy Efficiency.* Retrieved from https://obamawhitehouse.archives.gov/the-press-office/2012/08/30/executive-order-accelerating-investment-industrial-energy-efficiency.

Wächter, A., & Biegler, L. T. (2006). On the implementation of an interior-point filter line-search algorithm for large-scale nonlinear programming. *Mathematical programming, 106*(1), 25-57. Retrieved Nov 23, 2020, from https://coin-or.github.io/Ipopt/.

Wang, J., Jing, Y. and Zhang, C. (2010). Optimization of capacity and operation for CCHP system by genetic algorithm. *Applied Energy*, *87*(4), 1325–1335.

Wang, J., Zhai, Z., Jing, Y. and Zhang, C. (2010). Particle swarm optimization for redundant building cooling heating and power system. *Applied Energy*, *87*(12), 3668–3679.

Wang, J., Yang, K., Zhang, X., Shi, G. and Fu, C. (2014). An illustration of the optimization of combined cooling heating and power systems using genetic algorithm. *Building Serv. Eng. Res. Technol.*, *35*(3), 296–320.

Weber, C., Maréchal, F., Favrat, D. and Kraines, S. (2006). Optimization of an SOFC-based decentralized polygeneration system for providing energy services in an office-building in Tokyo. *Applied Thermal Engineering*, 26(13), 1409–1419.

Wu, D., & Wang, R. (2006). Combined cooling, heating and power: A review. *Progress in energy and combustion science, 32*(5-6), 459–495.

Wu, J. Y., Wang J. L. and Li, S. (2012). Multi-objective optimal operation strategy study of micro-CCHP system. *Energy, 48*, 472–483.

Xpress, F. I. C. O. (2014). FICO Xpress Optimization Suite.

Zhu, G., & Chow, T. T. (2019). Design optimization and two-stage control strategy on combined cooling, heating and power system. *Energy Conversion and Management, 199*, 111869.